

MECHANICAL AND DURABILITY STUDIES ON CEMENT MORTAR CONTAINING KOTA-STONE (DIMENSIONAL LIMESTONE) WASTE

Ph.D. Thesis

HARSHWARDHAN SINGH CHOUHAN

ID No. 2015RCE9518



DEPARTMENT OF CIVIL ENGINEERING
MALAVIYA NATIONAL INSTITUTE OF TECHNOLOGY JAIPUR
NOVEMBER 2019

Mechanical and Durability Studies on Cement Mortar Containing Kota-Stone (Dimensional Limestone) Waste

Submitted in

fulfillment of the requirements for the degree of

Doctor of Philosophy

by

Harshwardhan Singh Chouhan

ID: 2015RCE9518

Under the Supervision of

Dr. Pawan Kalla

Prof. Ravindra Nagar



DEPARTMENT OF CIVIL ENGINEERING
MALAVIYA NATIONAL INSTITUTE OF TECHNOLOGY JAIPUR

November 2019

Dedicated

To

My Beloved Parents, Wife and Son

Krishnaraj Singh

© Malaviya National Institute of Technology Jaipur-2019.

All rights reserved.



**MALAVIYA NATIONAL INSTITUTE OF TECHNOLOGY
JAIPUR**

DECLARATION

I, Harshwardhan Singh Chouhan, declare that this thesis titled, “**Mechanical and Durability Studies on Cement Mortar containing Kota-Stone (Dimensional Limestone) Waste**” and the work presented in it, are my own. I confirm that:

This work was done wholly or mainly while in candidature for a research degree at this university.

Where any part of this thesis has previously been submitted for a degree or any other qualification at this university or any other institution, this has been clearly stated.

Where I have consulted the published work of others, this is always clearly attributed.

Where I have quoted from the work of others, the source is always given. With the exception of such quotations, this thesis is entirely my own work.

I have acknowledged all main sources of help.

Where the thesis is based on work done by myself, jointly with others, I have made clear exactly what was done by others and what I have contributed myself.

Date:

Harshwardhan Singh Chouhan

(2015RCE9518)



**MALAVIYA NATIONAL INSTITUTE OF TECHNOLOGY
JAIPUR**

CERTIFICATE

This is to certify that the thesis entitled “**Mechanical and Durability Studies on Cement Mortar Containing Kota-Stone (Dimensional Limestone) Waste**” being submitted by Harshwardhan Singh Chouhan (2015RCE9518) is a bonafide research work carried out under my supervision and guidance in fulfillment of the requirement for the award of the degree of Doctor of Philosophy in the Department of Civil Engineering, Malaviya National Institute of Technology, Jaipur, India. The matter embodied in this thesis is original and has not been submitted to any other University or Institute for the award of any other degree.

Place: Jaipur

Dr. Pawan Kalla

Date:

Prof. Ravindra Nagar

Dept. of Civil Engineering
MNIT Jaipur

ACKNOWLEDGEMENT

I humbly grab this opportunity to acknowledge reverentially, may people who deserve special mentions for their varied contributions in assorted ways that helped me during my Ph.D. research and the making of this thesis.

First and foremost, I thank God Almighty for showering with his blessings throughout my life. It is only by his abundant grace that I was able to complete this research work successfully.

I would like to express my deepest sincere and heartfelt gratitude to my supervisors and mentor, **Dr. Pawan Kalla**, Associate Professor, Department of Civil Engineering, Malaviya National Institute of Technology, Jaipur and **Prof. Ravindra Nagar**, Department of Civil Engineering, Malaviya National Institute of Technology, Jaipur for their guidance, advice, criticism, encouragement and insight throughout the Ph.D. From their busy schedule, they always spared time for assessing and critically evaluating the progress of my work. Their wide knowledge helped me in writing this thesis. I am indebted for the kind help and support which made it possible for me to stand up to the challenge offered by the task and come out successfully.

I would like to thank DPGC and DREC committee member, Prof. Sanjay Mathur, Prof. R.C. Gupta, Dr. Rajesh Gupta and Dr. Vinay Agarwal for their insightful comments, criticism and guidance during course of the study.

I am also thankful to Prof. B.L. Swami, Prof. A.K. Vyas, Prof. Gunwant Sharma, Prof. Y.P. Mathur, Prof. A.B. Gupta, Prof. Sudhir Kumar, Prof. Rohit Goyal, Prof. Mahendra Choudhary, Prof. Ajay Singh Jethoo, Prof. Mahesh Jat, Dr. Sandeep Shrivastava, Dr. Arun Gaur, Dr. J.K. Jain and all faculty members of Civil Engineering Department, MNIT Jaipur, for their valuable guidance, help and unflinching encouragement during the research work.

I am grateful to the Director, Head, Civil Engineering Department, Dean Research and Dean Academics for their kind support and cooperation for smooth completion of this research work.

I am extremely grateful to Prof. Amar Nath Arora, Kautilya Institute of Technology and Engineering, Jaipur for their help, support and guidance during the Ph.D. work. Also I thank Dr. Laszlo Csetenyi, University of Dundee, who helped in doing the MIP studies at their institute.

My earnest thanks to all staff and administration at the institute for their help, support and co-operation throughout the course of the study. I would like to thank Mr. Jayesh Agrawal, Office in Charge, Civil Engineering Department, MNIT Jaipur whose generous help in academic related activities has been instrumental. I would like to thank Mr. Sapan Gaur, Mr. Pukhraj, Mr. Rajesh Saxena, Mr. R.S Mandoliya, Mr. Sita Ram Jat, Mr. Ramjilal ji, Mr. Anil Sharma and Mr. Nitesh for their help, guidance and providing research environment and providing me space to carry out my research work. I also would like to acknowledge the Material Research Center, MNIT Jaipur and Center for Development of Stones (CDOS), Rajasthan to provide equipment's for microstudies.

I am particularly in debt to my seniors, friends and batch mates especially Dr. Pradeep Kumar Gautam, Dr. Sayed Ahmed Kabir, Dr. Aditya Rana, Dr. Sarabjit Singh, Dr. Kunal Bisht, Kulvaibhav Sharma, Lalit Kumar Gupta, Sumit Choudhary, Vishal Singhal, Sandeep Singh Shekhawat, Ajay Kumar Mandrawalia, Kusum Rathore, Prarthita Basu, Rohit Kumar Yadav, Abhishek Jain, Rakesh Choudhary, Deepak Mathur, Lilesh Kumar Gautam, Gaurav Singhal, Rakesh Meena, Rajat, Shailesh Meena, Jyotesh Tiwari, Dinesh Verma, and Gaurav Meena for inevitable help, support and motivation to complete this research work successfully.

I also would like to express my whole hearted thanks to my beloved Late Grandfather Sh. Ratan Singh Chouhan and my Grandmother Smt. Lakshmi Kunwar, without whose foresight towards the knowledge our family would not have reached the ocean of education.

It is my proud privilege to acknowledge the blessings, cooperation, and encouragement of my father and mother **Sh. Himmat Singh Chouhan** and **Smt. Sumitra Kunwar** in achieving this life time goal. Their timely guidance, teachings, care and moral support enabled me to sail against the waves. I am obliged to my family members **Sh. Balveer Singh Rathore**, Sh. Lal Singh Chundawat, Sh. Nagendra Singh Chouhan, Sh. Virendrapal Singh Sisodia, Smt. Bhupendra Kunwar and Dharmishtha Kunwar for their care and concern shown throughout the periods of my research work. I also thank to my sister Nisha Chouhan and my brother Ravindra Singh Chouhan who too encouraged me to move forward with positive attitude throughout the duration of research work. I appreciate the love, care and inspiration of cousin brother Bhanu Pratap and Jairaj extended throughout this research.

It would not have been possible to carry out this research work without the active support of my wife Ronika Chundawat, who has boosted my moral during most difficult phases and lit the hope of success throughout the tenure of the research. The words can hardly match her contribution. But still with my utmost sincerity I would like to acknowledge her contribution in the completion of this thesis. I also thank our loving son Krishnaraj Singh whose naughty activities and smile helped me to forget all my tensions.

Last but not the least, I sincerely thank to all who, directly or indirectly, have lent their helping hand in this venture.

Date:

Harshwardhan Singh Chouhan

ABSTRACT

Recent years has recorded a proliferated growth in the construction industry, resulting in massive demand for construction materials such as concrete and mortar. Mortar is the second most used construction material after concrete. Its production consumes a significant quantity of fine aggregate. Excessive exploitation of this natural resource has resulted in its scarcity. This problem demands an alternative material which has the potential to be used as construction material without affecting strength and durability of the structure. Parallel to this, around the globe, another unsustainable practice, i.e. mining of dimensional stone has also increased at an exponential rate. The dimensional stone (DS), i.e. marble, granite, limestone, sandstone etc. industry has grown from an almost manual activity to a highly industrialized business in the last two decades. The quarrying of DS generates a huge amount of waste in both solid and powder form. Sustainable disposal of this waste has emerged as a big challenge around the globe. This waste can be used as a substitute for continually increasing demand for natural fine aggregates.

Kota stone is one of the types of dimensional limestone having fine-grained siliceous calcium carbonate compositions. It is available in eastern Rajasthan of India at Chittor, Ramganj Mandi (Kota) and Jhalawar district. Due to the unplanned disposal of an enormous quantity of solid and slurry waste, produced due to mining and polishing, has posed a severe threat to the regional environment. With various weather conditions like blowing wind and rainwater, the slurry waste gets transported to long distance, thus affecting the ecology of the area. Also, the unplanned disposal of slurry waste has led to degradation of soil properties, converting cultivable area in barren land, migration of species and genesis of various respiratory, vision and skin disorders. The management of this waste has become a significant issue for quarry companies and government organizations. In the past, researchers have used dimensional stone waste like marble, granite, limestone and sandstone as fine aggregate, filler and adhesive in construction materials. Their study claimed that reusing these waste as a construction material can be a gainful practice. Nevertheless, the problem associated with mining of dimensional stones are growing day by day on one hand and on the another hand mining stone waste remains un-utilized due to lack

of comprehensive studies and specifications. In absences of these, persons dealing with construction materials such as engineer, contractor, labour etc. do not rely on stone waste.

Present study aim at utilizing mining and processing waste from Kota stone industry as a fine aggregate material in cement mortar mixes. For this, the generated waste was used in two forms; Kota stone slurry (KSS) and Kota stone crushed sand (KSCS) as fine aggregate in cement mortar mixes (1:3, 1:4 and 1:6). The study was carried out in two stages. Stage first includes a trial study on 1:4 mortar mixes prepared with KSS up to 100% replacement of river sand with an interval of 10%. In stage second, fourteen mortar mixes (1:3 and 1:6) were prepared by replacing river sand between 0 to 60% in steps of 20% with both KSS and KSCS. These mortar mixes were evaluated on the basis of their mechanical and durability properties such as workability, water absorption, porosity, density, ultrasonic pulse velocity, dynamic modulus of elasticity, compressive strength, flexural strength, adhesive strength, tensile bond strengths, drying shrinkage, acid attack, sulphate attack, carbonation, chloride ion penetration, fire resistance and wetting-drying cycle. Results of the study reveal that the use of KSW resulted in a much denser and homogeneous mixture, reducing water-cement ratio, and improving the workability of mortar. Also, inclusion of KSS and KSCS between 20 to 60% had a positive impact on strength properties of mortar mixes. Durability properties of mortars were also enhanced with KSS and KSCS between 30 to 40% replacement of river sand. In addition to this, microstructural analysis of salected mortar mixes was done using scanning electron microscopy (SEM) images, Fourier-transform infrared spectroscopy (FTIR) and X-ray diffraction (XRD) techniques. Above analysis substantiated better performance of KSS and KSCS containing mortars.

CONTENTS

Declaration.....	i
Certificate.....	ii
Acknowledgement	iii
Abstract.....	vi
Contents	viii
List of Tables	xi
List of Figures.....	xii
Abbreviations.....	xviii
CHAPTER 1: INTRODUCTION.....	1
1.1 General.....	1
1.2 Kota stone and its Geographical Availability	3
1.3 Problem Associate with Kota stone Production.....	3
1.4 Research Gaps.....	5
1.5 Objectives of the Study.....	6
1.6 Chapter wise Organization of the Thesis	6
CHAPTER 2: LITERATURE REVIEW	7
2.1 General.....	7
2.2 Use of Limestone Waste in Cement Mortar Mixes	7
2.3 Use of other Dimensional Stone Waste in Mortar Mixes	12
2.4 Influence of Dimensional Limestone Stone Waste on Properties of Mortar Mixes	19
2.4.1 Influence on Strength of Mortar Mixes	19
2.4.2 Influence on Durability Properties of Mortar Mixes	22
2.5 Summary of the Literature Review	31
CHAPTER 3: MATERIALS AND METHODOLOGY.....	33
3.1 General.....	33
3.2 Materials	33
3.3 Material Characterization.....	33
3.4 Methodology	37
3.5 Experimental Program	40
3.5.1 Sample Preparation	40
3.5.2 Workability	42
3.5.2 Compressive Strength	42

3.5.3	Flexural Strength	43
3.5.4	Ultrasonic Pulse Velocity (UPV) and Dynamic Modulus of Elasticity	44
3.5.5	Water Absorption, Density and Percentage Air Voids.....	45
3.5.6	Adhesive Strength Test	45
3.5.7	Tensile Bond Strength	46
3.5.8	Drying Shrinkage	47
3.5.9	Morphology	48
3.5.10	Fourier Transform Infrared Spectroscopy (FTIR) Analysis.....	49
3.5.11	X-ray Diffraction Analysis (XRD).....	49
3.5.12	Mercury Intrusion Porosimetry Test (MIP).....	50
3.5.13	Thermal Gravimetric Analysis (TGA)	51
3.5.14	Acid Attack Test.....	51
3.5.15	Sulphate Attack Test	52
3.5.16	Fire Resistance Test.....	54
3.5.17	Carbonation Test	54
3.5.18	Chloride Ion Penetration Test.....	54
3.5.19	Wetting and Drying Cycle Test.....	56
CHAPTER 4: RESULTS AND DISCUSSIONS.....		57
4.1	General	57
4.2	Stage First.....	57
4.2.1	Workability.....	57
4.2.2	Water Absorption and Density	58
4.2.3	Porosity by Mercury Intrusion Porosimetry (MIP)	59
4.2.4	Compressive and Flexural Strength	60
4.2.5	Ultrasonic Pulse Velocity and Dynamic Modulus of Elasticity.....	61
4.2.6	Morphology	61
4.2.7	Thermogravimetric Analysis (TGA)	63
4.2.8	Summary	64
4.3	Stage Second	65
4.3.1	Workability.....	65
4.3.2	Compressive and Flexural Strength	66
4.3.3	Ultrasonic Pulse Velocity (UPV) and Dynamic Modulus of Elasticity (E_{dy}).....	67
4.3.4	Water Absorption, Porosity and Density.....	69
4.3.5	Adhesive Strength	73
4.3.6	Tensile Bond Strength.....	75
4.3.7	Drying Shrinkage	76

4.3.8 Morphology (SEM).....	78
4.3.9 Fourier-Transformation Infra-Red Spectra (FTIR).....	79
4.3.10 X-ray Diffraction Analysis (XRD)	81
4.3.11 Acid Attack	84
4.3.12 Sulphate Attack.....	91
4.3.13 Fire Resistance	99
4.3.14 Carbonation.....	103
4.3.15 Chloride ion penetration	106
4.3.16 Wetting and drying cycles	108
CHAPTER 5: CONCLUSIONS AND RECOMMENDATIONS.....	110
5.1 Conclusions.....	110
5.2 Recommendations.....	111
REFERENCES.....	112
LIST OF PUBLICATION FROM THESIS.....	121
APPENDIX	122
AUTHOR’S BIO-DATA	1244

LIST OF TABLES

Table No.	Title	Page No.
Table 2.1	Previous Researches on use of Limestone or Limestone Waste and Dimensional Stone in Mortar Production	15
Table 2.2	Chemical Constituents of Stone Waste used in Previous Study for Mortar Production	18
Table 2.3	Physical Properties of Stone Waste used in Previous Study for Mortar Production	19
Table 3.1	Physical Characteristics Materials	34
Table 3.2	Chemical constituents of Cement, River Sand and KSW	34
Table 3.3	Details of Mix Proportion for Stage First	37
Table 3.4	Details of Mix proportion for Stage Second	38
Table 3.5	Mortar Properties	41
Table 4.1	Adhesive Strength of Mortar with KSS and KSCS	74

LIST OF FIGURES

Figure No.	Title	Page No.
Figure 1.1	(a) and (b): Generated Solid and Slurry Waste from Mining and Processing of Dimensional Limestone.	4
Figure 2.1	Compressive Strength of Mortar Containing Limestone Fines at Various Age of Curing	20
Figure 2.2	(a) and (b): Flow Spread and Flow Rate of Mortar Mixes with Various Percentage of Limestone Fines Volume	24
Figure 2.3	Schematic Diagram of Mini Slump Cone with Dimensions and Measurement of Mortar Flow	24
Figure 2.4	Water Absorption and Apparent Porosity of Mortars Containing Various Percentage of Granite Sludge	25
Figure 2.5	Dry Density of Mortar with Varying Percentage of Fine Sanitary Ware	27
Figure 2.6	Specific and Relative Volume Intrusion Curve (A-B) for Limestone Blended Cement Mortars	27
Figure 2.7	Deterioration in Mortar Surface during Sulphate Attack	30
Figure 3.1	River Sand, KSS and KSCS	34
Figure 3.2	Gradation of River Sand, KSS and KSCS	35
Figure 3.3	X-ray Diffraction pattern of Kota Stone Waste	35
Figure 3.4	X-ray Diffraction pattern of River Sand	35
Figure 3.5	SEM images of KSS, KSCS and River Sand	36
Figure 3.6	Methodology	39
Figure 3.7	Mortar Samples	40
Figure 3.8	Flow Table Test	42
Figure 3.9	Compressive Strength Test on Mortar Sample	43
Figure 3.10	Flexural Strength Test on Mortar Samples	44
Figure 3.11	UPV Test on Mortar Samples	44
Figure 3.12	Adhesive Strength of Mortar with Clay Bricks	46
Figure 3.13	Bond Strength Test Setup	47
Figure 3.14	Drying Shrinkage Measurement for Mortar Samples	48

Figure No.	Title	Page No.
Figure 3.15	Image of JSM 7400 F Scanning Electron Microscope	48
Figure 3.16	Image of Fourier Transform Infrared Spectroscopy	49
Figure 3.17	PANalytical X pert PRO Diffractometer	50
Figure 3.18	Mercury Intrusion Porosimetry Machine (Pore Master - 60 GT)	50
Figure 3.19	Simultaneous Thermal Analyzer 6000	51
Figure 3.20	Mortar Samples Exposed to Acid Solution	52
Figure 3.21	Mortar Samples Exposed to Sulphate Solution	53
Figure 3.22	Fire Furnace Apparatus	54
Figure 3.23	Carbonation Chamber	55
Figure 3.24	Depth of Carbonation	55
Figure 3.25	Depth of Chloride Ion Penetration	56
Figure 4.1	Variations in Water to Cement Ratio with KSS	57
Figure 4.2	Water Absorption of Mortar Mixes	58
Figure 4.3	Dry Density and Apparent Density of Mortar Mixes	58
Figure 4.4	Porosity of Mortar Mixes	59
Figure 4.5	Graph for Mercury Intrusion rate versus Pore Size	59
Figure 4.6	Compressive Strength of Mortar Mixes at 7 and 28 Days	60
Figure 4.7	Flexural Strength of Mortar Mixes at 7 and 28 Days	60
Figure 4.8	Ultra Pulse Velocity and Dynamic Modulus of Elasticity of Mortar Mixes	61
Figure 4.9	SEM images of Mortar Mix TS0	62
Figure 4.10	SEM images of Mortar mix TS3	62
Figure 4.11	SEM images of Mortar Mix TS4	62
Figure 4.12	SEM images of Mortar Mix TS5	63
Figure 4.13	SEM images of Mortar Mix TS10	63
Figure 4.14	TGA Curves for Mortar Mixes G0, G3, G4, G5, and G10	64
Figure 4.15	Water-cement ratio v/s % Replacement of KSS/KSCS for series A, B, C and D	65

Figure No.	Title	Page No.
Figure 4.16	Compressive Strength of Mortar with KSS and KSCS at 28 days	66
Figure 4.17	Flexural Strength of Mortar with KSS and KSCS at 28 days	67
Figure 4.18	Ultra Pulse Velocity of Mortar Mixes with KSS and KSCS	68
Figure 4.19	Dynamic Modulus of Elasticity of Mortar Mixes with KSS and KSCS	69
Figure 4.20	Variations in Water Absorption of Mortar Mixes with KSS and KSCS	69
Figure 4.21	Variations in % Air voids of Mortar Mixes with KSS and KSCS	70
Figure 4.22	Porosity of Mortar Mixes with KSS and KSCS	70
Figure 4.23	Mercury Intrusion Porosimetry Graphs for Series A	71
Figure 4.24	Mercury Intrusion Porosimetry Graphs for Series B	71
Figure 4.25	Mercury Intrusion Porosimetry Graphs for Series C	72
Figure 4.26	Mercury Intrusion Porosimetry Graphs for Series D	72
Figure 4.27	Variations in Dry bulk density of Mortar Mixes with KSS and KSCS	73
Figure 4.28	Variations in Apparent Density of Mortar Mixes with KSS and KSCS	73
Figure 4.29	Various type of Cracking between Mortar and Bricks in Adhesive Strength Test	74
Figure 4.30	Variation in Adhesive Strength with KSS and KSCS	75
Figure 4.31	Tensile Bond Strength of Mortar containing KSS and KSCS	75
Figure 4.32	Drying Shrinkage of Mortar Mixes for Series A	76
Figure 4.33	Drying Shrinkage of Mortar Mixes for Series B	77
Figure 4.34	Drying Shrinkage of Mortar Mixes for Series C	77
Figure 4.35	Drying Shrinkage of Mortar Mixes for Series D	77
Figure 4.36	SEM images of Control Mix (1:3)	78
Figure 4.37	SEM images of AS20 Mix	78

Figure No.	Title	Page No.
Figure 4.38	SEM images of AS40 Mix	79
Figure 4.39	SEM images of AS60 Mix	79
Figure 4.40	FTIR Spectra pattern for Control Mix (1:3)	80
Figure 4.41	FTIR Spectra pattern for Mix AS20	80
Figure 4.42	FTIR Spectra pattern for Mix AS40	81
Figure 4.43	FTIR Spectra pattern for Mix AS60	81
Figure 4.44	XRD pattern of Control Mortar (1:3)	82
Figure 4.45	XRD pattern of Mix AS20	83
Figure 4.46	XRD pattern of Mix AS40	83
Figure 4.47	XRD pattern of Mix AS60	83
Figure 4.48	Compressive Strength Loss in Mortar Mixes of Series A	85
Figure 4.49	Compressive Strength Loss in Mortar Mixes of Series B	85
Figure 4.50	Compressive Strength Loss in Mortar Mixes of Series C	85
Figure 4.51	Compressive Strength Loss in Mortar Mixes of Series D	86
Figure 4.52	Weight Loss in Mortar Mixes of Series A	86
Figure 4.53	Weight Loss in Mortar Mixes of Series B	87
Figure 4.54	Weight Loss in Mortar Mixes of Series C	87
Figure 4.55	Weight Loss in Mortar Mixes of Series D	87
Figure 4.56	FTIR Spectra for Control Mix of Series A at 28 Days Acid Immersion Period	88
Figure 4.57	FTIR Spectra for Mix AS20 at 28 Days Acid Immersion Period	89
Figure 4.58	FTIR Spectra for Mix AS30 at 28 Days Acid Immersion Period	89
Figure 4.59	FTIR Spectra for Mix AS40 at 28 Days Acid Immersion Period	89
Figure 4.60	FTIR Spectra for Control Mix of Series A at 90 Days Acid Immersion Period	90

Figure No.	Title	Page No.
Figure 4.61	FTIR Spectra for Mix AS20 at 90 Days Acid Immersion Period	90
Figure 4.62	FTIR Spectra for Mix AS30 at 90 Days Acid Immersion Period	91
Figure 4.63	FTIR Spectra for Mix AS40 at 90 Days Acid Immersion Period	91
Figure 4.64	Changes in Compressive Strength of Mortar Mixes of Series A	92
Figure 4.65	Changes in Compressive Strength of Mortar Mixes of Series B	93
Figure 4.66	Changes in Compressive Strength of Mortar Mixes of Series C	93
Figure 4.67	Changes in Compressive Strength of Mortar Mixes of Series D	93
Figure 4.68	Weight Change in Sulphate Exposed Mortar Mixes of Series A	94
Figure 4.69	Weight Change in Sulphate Exposed Mortar Mixes of Series B	94
Figure 4.70	Weight Change in Sulphate Exposed Mortar Mixes of Series C	95
Figure 4.71	Weight Change in Sulphate Exposed Mortar Mixes of Series D	95
Figure 4.72	FTIR Spectra for Control Mix of Series A at 90 Days Sulphate Immersion Period	96
Figure 4.73	FTIR Spectra for Mix AS20 at 90 Days Sulphate Immersion Period	96
Figure 4.74	FTIR Spectra for Mix AS30 at 90 Days Sulphate Immersion Period	97
Figure 4.75	FTIR Spectra for Mix AS40 at 90 Days Sulphate Immersion Period	97
Figure 4.76	FTIR Spectra for Control Mix of Series A at 180 Days Sulphate Immersion Period	97
Figure 4.77	FTIR Spectra for Mix AS20 at 180 Days Sulphate Immersion Period	98
Figure 4.78	FTIR Spectra for Mix AS30 at 180 Days Sulphate Immersion Period	98

Figure No.	Title	Page No.
Figure 4.79	FTIR Spectra for Mix AS40 at 180 Days Sulphate Immersion Period	98
Figure 4.80	Variation in Compressive Strength of Fire Exposed Mortar Mixes of Series A	100
Figure 4.81	Variation in Compressive Strength of Fire Exposed Mortar Mixes of Series B	100
Figure 4.82	Variation in Compressive Strength of Fire Exposed Mortar Mixes of Series C	101
Figure 4.83	Variation in Compressive Strength of Fire Exposed Mortar Mixes of Series D	101
Figure 4.84	Weight Loss in Fire Exposed Mortar Mixes of Series A	102
Figure 4.85	Weight Loss in Fire Exposed Mortar Mixes of Series B	102
Figure 4.86	Weight Loss in Fire Exposed Mortar Mixes of Series C	103
Figure 4.87	Weight Loss in Fire Exposed Mortar Mixes of Series D	103
Figure 4.88	Carbonation depth in Mortar Mixes of Series A	104
Figure 4.89	Carbonation depth in Mortar Mixes of Series B	104
Figure 4.90	Carbonation depth in Mortar Mixes of Series C	105
Figure 4.91	Carbonation depth in Mortar Mixes of Series D	105
Figure 4.92	Chloride Ion Penetration depth in Mortar Mixes of Series A	106
Figure 4.93	Chloride Ion Penetration depth in Mortar Mixes of Series B	107
Figure 4.94	Chloride Ion Penetration depth in Mortar Mixes of Series C	107
Figure 4.95	Chloride Ion Penetration depth in Mortar Mixes of Series D	107
Figure 4.96	Variations in Weight of the Mortar Mixes after 20 Wetting and Drying Cycles for Series A and B	108
Figure 4.97	Variations in Weight of the Mortar Mixes after 20 Wetting and Drying Cycles for Series C and D	108
Figure 4.98	Physical Appearance of Wetting and Drying Cycle Exposed Mortar Mixes of Series A and B	109
Figure 4.99	Physical Appearance of Wetting and Drying Cycle Exposed Mortar Mixes of Series A and C and D	109

ABBREVIATIONS

ASTM	:	American Society for Testing and Materials
CASH	:	Calcium Alumina Silicate Hydrate
CSH	:	Calcium Silicate Hydrate
CH	:	Calcium Hydroxide
DS	:	Dimensional Stone
DLSW	:	Dimensional Limestone Waste
DSW	:	Dimensional Stone Waste
EDS	:	Energy Dispersive X-Ray Spectroscopy
EN	:	European
ERMCO	:	European Ready-mix Concrete Organization
FA	:	Fly Ash
FTIR	:	Fourier Transform Infrared Spectroscopy
HCL	:	Hydrochloric Acid
IS	:	Indian Standards
ISO	:	International Organization for Standardization
K-Br	:	Potassium Bromide
KSW	:	Kota Stone Waste
KSS	:	Kota Stone Slurry
KSCS	:	Kota Stone Crushed Sand
LP	:	Limestone Powder
LS	:	Limestone
MIP	:	Mercury Intrusion Porosimetry
MPa	:	Mega Pascale's
Mt	:	Million Tones
OPC	:	Ordinary Portland Cement

PU	:	Polyurethane
RH	:	Relative Humidity
RS	:	River Sand
SBR	:	Styrene Butadiene Rubber
SCM	:	Self-Compacting Mortar
SCRM	:	Self-Compacting Repair Mortar
SEM	:	Scanning Electron Microscopy
SF	:	Silica Fume
TGA	:	Thermogravimetric Analysis
UIN	:	Italian National Standards Institute
UPV	:	Ultrasonic Pulse Velocity
XRD	:	X-Ray Diffractometer

CHAPTER 1

INTRODUCTION

1.1 General

Mortar is the most commonly used material in construction industry after concrete. The use of mortar as an adhesive has been reported since ancient times. In the beginning, mortar mix was prepared using mud and gypsum and was employed to joining the mud bricks or curved stone blocks (Moropoulou et al., 2005). Around 3000 BC, use of asphalt to prepare mortar was in trend which later was partially replaced with slaked lime. These mortars were widely used in Roman and Greek buildings. Roman era later introduced pozzolana lime mortar by adding pozzolana material into the lime-based mortar. Cement mortar came into limelight during 1870s when Portland cement was introduced by the United States.

The use of cement based mortar is still widely popular due to its homogenous nature and early strength gaining capacity over lime or pozzolana lime based mortar. (Ballester et al., 2007). A conventional mortar mix is composed of three constituents namely a binder (cement), fine aggregate (river sand or manufactured sand), and water, where binder act as an adhesive unit and water helps in proper mixing; fine aggregate form an integral part in a mortar mix. It provides the required mechanical and durability properties to the overall mortar mix. Hence use of good quality fine aggregate is essential for producing excellent quality mortar (Farinha et al., 2015; Martínez et al., 2013; Turgut and Murat Algin, 2007).

Fine aggregates are procured via mining of sand along river bed. Increase in construction activity has led to a steep increase in demand for this construction and building material. To meet the demand, mining of natural fine aggregates has increased at an exponential rate. To meet the demand, the mining of this natural resources has increased in a very unsustainable way, especially since last few decades (Germano et al., 2018; Shi-cong and Chi-sun, 2009; Thamboo et al., 2019). These unsustainable mining activities have created a natural imbalance by causing changes in channel hydraulics, contaminating water source, polluting the environment and destroying local ecology. Also, the continuous extraction of natural aggregate or natural sand from river beds is one of the reasons for the disparity between sea sand and coastal sand that creates the consequences for coast and flooding in many areas of

the world (Balasubramanian et al., 2016; Rodrigues et al., 2013; Saiz Martínez et al., 2016). To prevent further environmental deterioration, government agencies around the globe have either restricted or prohibited mining of fine aggregates. However, this prohibition is just a temporary solution because fine aggregate is an important constituent of concrete and mortar mixes; two of the most commonly used construction materials and restricting their use will result in severe harm to the infrastructure development of a Nation. Hence, it is the need of the hour to find a sustainable solution to this continuously deteriorating situation.

Parallel to this, around the globe another unsustainable practice, i.e. mining of dimensional stone has also increased at an exponential rate. The dimensional stone (DS), i.e. marble, granite, limestone, sandstone etc. industry has grown from an almost manual activity to a highly industrialized business in the last two decades. Production and consumption of these stones have increased with the help of new technologies. This industry can serve the needs of this significant portion of the construction sector. Globally, 27 countries are producing dimensional stones, among them, China, Turkey, India, Iran and Italy share 72% (125 Mt) of the total production (Chouhan et al., 2018).

India is one of the largest producer of dimensional stones like marble, slate, granite, limestone, quartzite, etc., secure third position with sharing about 30% of total production throughout the world. These stones are mainly quarried from states of Andhra Pradesh, Rajasthan, Madhya Pradesh, Gujrat, Karnataka, Orissa, Tamilnadu, Andman and Nicobar. Also, the Indian stone industries have significantly affect the Indian economy as this generates huge revenue by exporting finished stones. Rajasthan, a state of India is known for its inexhaustible source of various types of dimensional stones which include marble, granite, sandstone, kota stone (flaggy limestone) and slate. Here, It is produced about 90% of the total production of natural stones in India.

Dimensional stones are categorized on the basis of their mineral oxides, geographic availability and are marketed on the basis of their color and locality. After mining, stones are sawed to required dimensions and polished to give it a mirror-like glaze. These operations create a vast quantity of stone waste. Nearly 70% of these valuable mineral reserves get unexploited due to non-upgradation of mining techniques and processing operations. Dumping of these wastes is big issue for mining

industries and cities. Recycling of these wastes in mortar or concrete production could be one of the solutions to this problem.

Researchers have used dimensional stone waste like marble, granite, limestone and sandstone as fine aggregate, filler and adhesive in construction materials like mortar and concrete (Arif et al., 2018; Bilir et al., 2015; Farinha et al., 2015; Jain and Majumder, 2016; Kalla et al., 2015; Khyaliya et al., 2017; Pozo-Antonio, 2015; Rana et al., 2015; Singh et al., 2016). Their results were encouraging for its use as an alternative of natural or conventional resources. Also, some concrete institutions allowed the substitution of natural aggregate up to 20% by recycling aggregates (Saiz Martínez et al., 2016).

1.2 Kota stone and its Geographical Availability

Kota stone is one of the types of dimensional flaggy limestone which is available in eastern Rajasthan of India at Chittor, Ramganj Mandi (Kota) and Jhalawar district, with an annual production of around 17 million tons (Report, Centre for development of stones 2011). Its deposits are located at Vindhya range, under 24° 33' to 24°50' north latitudes and 75°50' to 76°04' east longitudes with an area of approximately 150 square km. This is sedimentary nature rock having fine-grained siliceous calcium carbonate compositions. Physically this is compressed, hard, oil impervious, less water absorbent and non-slippery homogenous natural stone. Because of this, it is used for decorative purpose in commercial and domestic buildings. It is found in different colors blue, green, brown or their combinations (Chouhan et al., 2017).

1.3 Problem Associate with Kota stone Production

The mining of Kota stone has posed a serious threat to the regional environment, due to the disposal of huge quantity of solid and slurry waste from mines and polishing units. Cutting and polishing of Kota stone produce around 10-12Mt of waste each year (Kumar and Lakhani, 2017).

The mining and processing operations generate different types of waste such as solid and semi-liquid (slurry or powder) waste as shown in Figure 1.1 (a) and (b). Solid waste produced during mining and dressing operations. The polishing of stone is carried out by rubbing its exposed face with the polishing machine in the presence of abrasives like sand. The polishing machine requires a large quantity of water to cool,

lubricate and clean the small particles. The fine particles get suspended in the water are then discharged off. The discharged semi-liquid substance termed as stone slurry.

The unsafe disposal of these waste from the mining and processing units is one of the major problems for the environment as well as human health. Forest cover and average rainfall have gradually reduced in the district. Due to poor recovery of fine waste, the land has been degraded and drains in the region have been blocked. The general water table has gone down, creating a severe scarcity of drinking water. A study has revealed that waste dumped over past 50 years is estimated to be over 100 Mt. and stretched over a length of about 35 kilometers all around Ramganj Mandi (Rana et al., 2016).



Figure 1.1 (a) and (b): Generated Solid and Slurry Waste from Mining and Processing of Dimensional Limestone.

In the absence of research on Kota stone waste, dumping of Kota stone slurry is unscientific and continues environmental hazards on land, water, and air. Lack of Kota stone utilization in the industry and construction activities further multiply the complexity. Waterlogging and loss of water table had also compounded the complex situation. Due to the alkalinity of the Kota stone slurry, it reduced the fertility of the soil. Dumped Kota stone slurry gets dry fast and it spread in the air. These wastes are very dangerous to human health. Settling of fine particles of slurry on crops and vegetation threatens the production. Reusing this waste as a construction material can be a gainful practice.

1.4 Research Gaps

From the literature, it is evident that the sustainable disposal of dimensional stone waste is becoming an area of concern for industrial organizations as well as government authorities around the world.

1. The above literature review reveals that limited studies are available on the use of dimensional limestone waste as a construction material.
2. Reported studies on use of limestone in blend with other waste material such as marble dust, silica fume, fly ash, etc., does not provide clear understanding on effect of limestone alone on mortar mix properties. Available studies were focused on mainly workability, density, porosity, strength, drying shrinkage, sulphate attack, and acid attack only. While, other important parameters for mortar mixes containing dimensional limestone like adhesive strength, bond strength, carbonation, and chloride ion penetration have not been evaluated in past. Also, the influence of dimensional limestone waste on mortar mix properties such as wetting-drying cycle, salt crystallization and fire resistance has not been reported in past.
3. The limestone used in past studies was mostly with high calcium oxide (CaO) content, which was either pure or conventional limestone, but comprehensive study on the dimensional limestone used for the present study as mortar material has not been investigated so far.

1.5 Objectives of the Study

In view of above gaps in literature, present study was focused on evaluating the use of Kota stone waste alone as a substitution of conventional river sand in cement mortar mixes.

Following objectives were decided to carry out the study:

1. To determine the physical and chemical characteristics of Kota stone quarry and polishing waste as an engineering material.
2. To find influence of Kota stone waste on physical and mechanical attributes of cement mortar.
3. To determine the long term durability properties of cement mortar containing Kota stone waste.
4. To find optimum dosage of Kota stone waste as substitution of river sand in cement mortar mixes.

1.6 Chapter wise Organization of the Thesis

Chapter one is intended to brief knowledge about study area, problem genus by continuous mining of natural sand, Kota stone production and specific objectives of the study. Chapter two reviews the related literature on the topic. This section includes previous studies on the use of limestone and dimensional stone waste in different mortar mixes and also their impact on various mortar properties are discussed. Chapter three provide characterization of materials, detailing of experimental programme and adequate methodology adopted for the study. In chapter four, the interpretations and discussions based on the results obtained under experimental and investigation programme have been discussed. In chapter five, conclusions of the study based on the results and observations have been included. Also, recommendation with future scope of the study has been included.

CHAPTER 2

LITERATURE REVIEW

2.1 General

Literature review gives a clear picture of the use of dimensional stone waste in cement mortars. It helps to identify, how mortar behaves after introducing dimensional stone industry waste as conventional material such as natural river sand. By this, significant research gaps have been recognized for the present investigation. In past studies, researchers have used dimensional stone waste like marble, granite, and sandstone as fine aggregate, filler and adhesive in cement mortars. Some studies found that these stone wastes have possibility to be used as partial or full substitution of conventional fine aggregate while some claims that same can be used as part of cementitious material. The literature review includes previous study on the use of different limestones (LS), dimensional limestone waste (DLSW) and dimensional stone waste (DSW) such as sandstone, granite, marble and Kota stone etc. in mortar mixes. Also, the influence of stone waste in mortar performance in terms of mechanical and durability properties discussed in detail.

2.2 Use of Limestone Waste in Cement Mortar Mixes

Baldermann et al., (2018) used limestone in his investigation on mortar mixes, where the ordinary cement was replaced with limestone up to 65% level. Total eight proportions were designed including two reference mortar. Durability properties of mortar were determined after 28 days curing in calcium hydroxide solution. To evaluate long term resistance to sulphate attack, specimens were first saturated with calcium hydroxide solution for 14 days then cured in 30g/l sodium sulphate solution at 20°C for 200 days. Solutions were renewed at the end of every two weeks. Observations revealed up to 50% limestone with low water to cement powder ratio reduced porosity of blended mortar resulted in to enhancement in compressive strength and sulphate resistance as compared to conventional mortar mixes.

Similarly, Ballester et al., (2007) prepared a mortar with quarry limestone aggregate and mussel cannery industry obtained limestone waste. Strength properties and microstructure studies like SEM, TGA and MIP were used to examine their effect on internal structure of mortar. Test results indicated that limestone obtained from mussel

cannery industry enhanced the mechanical properties of the mortar when compared with that of quarry limestone. It was observed that mortars with limestone produced from mussel shell exhibited more packed microstructure, resulting in improved mortar strength.

A study by Benabed et al., (2012) investigated the rheological and mechanical properties of self-compacting mortar (SCM) prepared with river sand, dune sand, crushed sand and the mixture of these sands with the limestone fines. Experimental results showed that the mixture of crushed sand and river sand improved the rheological properties and strength of SCM. However a blend of dune sand and crushed sand decreased the mechanical properties of SCM. Crushed sand with limestone fines between 10-15% enhanced the compressive strength of mortar, but above these replacement levels strength was observed reducing gradually.

Bederina et al., (2013) performed an experimental investigation to determine the effect of crushed limestone sand on mortar as replacement of siliceous river sand. In this investigation effect of limestone sand was evaluated upon three different environment exposer: in lime containing solution, in an open air condition and an aggressive solution containing hydrochloride acid. Replacement of river sand was done by limestone crushed sand in the ratio of 0%, 50%, and 100%. Observations revealed that the crushed limestone sand containing mortar reduced the mass loss in all environmental exposures. Mortar containing 100% limestone crushed sand reduced mass change around 21.5%, 7.14% and 84.39% in lime water solution, open air, and hydrochloride acid solution respectively after 180 days. Also, noted improved mechanical strengths of mortar with limestone crushed sand in all environmental exposures. The capillary absorption of the mortars was higher in acid solution as compared to the lime solution due to the formation of voids in acid environment. However capillary action was observed reducing (23.4%) when limestone crushed sand was added to mortar mixes. They concluded the use of limestone sand in mortar better resistance against acid attack.

Bonavetti and Irassar, (1994) used three different waste stone dust i.e. quartz, granite, and limestone as replacement of sand by weight in the proportion of 0 to 20% in Portland cement mortar. The results were evaluated on the basis of change in water requirement, porosity, drying shrinkage, compressive and flexural strength.

Investigation revealed an improvement in mortar strength at initial stage using stone dust, however, higher proportion of stone dust also increased, water absorption and porosity. Enhancement in strength was accredited to accelerated hydration at initial stages due to presence of stone dust.

Corinaldesi et al., (2011), examined mechanical properties and thermal conductivity of cement mortar (1:3) by using various rubber wastes and limestone powder. Several mortar mixes were prepared with polyurethane waste (PU), styrene butadiene rubber waste (SBR) and shoe outsoles rubber waste as replacement of sand up to 30 %. From the experimental study, it was found that mortar with rubber waste reduced the materials thermal conductivity and unit weight. However, the addition of limestone powder increased compressive and flexural strength as well as thermal conductivity.

Felekoğlu et al., (2006) examined the influence of limestone filler and fly ash on compressive strength and viscosity of the self-compacting repair mortar. The study observed that limestone filler containing mortar was more effective than fly ash mortar in attaining early strength. Nevertheless, beyond 28 days fly ash based mortar had better compressive strength than control mortar.

Another study by Haach et al., (2011) used natural lime in order to know their influence on mortar fresh and hardened state properties. For this, total eighteen mortar mixes prepared using two types of sand, natural lime prepared at various water-cement ratio. These samples were analyzed on the basis of their workability and strength parameters such as compressive and flexural strength. From the results, it was stated that the mortar containing lime required more water to achieve same workability to that of mortar without lime content. This is caused by higher specific surface area of lime than cement particle resulting in to reduced properties of mortar.

Similarly, an attempt was made by Kwan and McKinley, (2014), where the performance of mortar by adding limestone fines was investigated. In this study, observations were taken by evaluating different mortar properties such as cohesiveness, flowability and packing density. The limestone fines was used to replace (by volume) fine aggregate without changing mix compositions with a constant water-cement ratio (0.5 by mass) and cement paste volume. From the results, author reported that the inclusion of limestone fines slightly reduced packing density of mortar with considerably decrement in water film thickness and improvement in

powder film thickness. Also, it was observed that the inclusion of limestone fines reduced the flow spread of mortar but cohesiveness and strength were benefited. It was concluded that effect of limestone fines in mortar mixes depends upon water film thickness and powder film thickness.

Another study by Lakhani et al., (2014) used dimensional limestone waste in making of floor tiles. In this study, conventional fine aggregates were replaced between 0% and 100%. Test result showed increase in strength and durability properties till 25% replacement, justifying the use of waste limestone as a building material for floor tiles.

Makhloufi et al., (2014), studied limestone mortars made with blended cement, partially substituting the clinker by blast furnace slag, natural pozzolana, and limestone filler at a combined proportion up to 50%. Test results indicated that the blast furnace slag, natural pozzolana, and limestone filler combined simultaneously with cement enhance the mechanical behavior of this material.

Pliya and Cree, (2015), studied the effect of various limestone like quarried limestone filler (CN), white eggshell derived limestone filler (CW) and brown eggshell limestone filler (CB) on cement mortar. They observed mortar containing CW and CB limestone have inferior properties than that of mortar containing natural limestone filler.

Pozo-Antonio, (2015) studied the behavior of natural lime, pure lime and lime cement-based mortars for repairs mortar. In this study, mortar properties such as mechanical strength, Young's modulus, and the drying shrinkage were monitored. It was observed that for a (1:1.75) mortar, cured for 28 days in a 65 to 75% RH (relative humidity) chamber strength and shrinkage both improved.

Ramezani-pour and Hooton, (2013), in their study, evaluated the effect of limestone on thaumasite sulphate attack. For this, two type mortar bar samples of size 40x40x160 mm were prepared using Portland cement and without limestone. Prepared mortar samples were stored in sodium sulphate solution at 5°C temperature. Observations in terms of length change were recorded after the end of every week. Investigation claimed the mortar with limestone as cementitious material was more susceptible in sulphate environment as compared to Portland cement mortar.

Santos et al., (2018) studied the effect of aggregate grading and mineralogy on porosity of lime-based mortar. For the study, mortar specimens were produced by using five aggregate; siliceous natural sand, siliceous crushed sand, limestone crushed sand, basaltic crushed sand and granite crushed sand with two gradations (standard and optimized). The mechanical behaviour of mortar was observed on the basis of compressive and flexural strength of mortar at the end of 28, 90 and 360 days. Study revealed that the mortar containing limestone and crushed basaltic sand with optimized grading has lowest value of micro pores, which was attributed to the formation of C-A-S-H/C-S-H in the intermediate transition zone. This factor leads to improved mechanical strength of these mortars.

Senhadji et al., (2014) examined the effect of supplementary cementitious materials namely; limestone fines, silica fumes and natural pozzolana at various replacement level on mortar microstructure, strength, and behavior in acidic environment. Porosity of the mortar was assessed by using mercury intrusion porosimetry technique and microstructural phase transformation was observed by scanning electron microscope images and energy dispersive spectrograms. Results suggested that the limestone fines perform well in acidic environment whereas silica fume containing mortar gets damaged in such aggressive conditions. While the compressive strength of mortar was lower with limestone fines as compared to Portland cement mortar.

Another study conducted by Soroka and Setter, (1977), also used limestone fines as filler material in cement mortar mixes. In his study, limestone filler used as fine sand at 10, 20, 30 and 40% replacement level. Obtained results were reported that the limestone filler increased compressive strength about 39% as compared to control mortar. This enhancement was caused by higher density in limestone containing mortar.

Türkel and Altuntaş, (2009), prepared self-compacting repair mortar by using limestone powder, fly ash and silica fume as cement substitution to evaluate their effect on mortar's fresh properties, water absorption, flexural and compressive strength. Observations suggested that the blended of limestone powder, fly ash and silica fume can better perform in workability of mortar as compared to alone limestone powder, fly ash and silica fume. However, strength (early age) of 30% limestone powder containing mortar was more as compared to control mortar. Silica

fume was positively reduced water absorption of mortar as compared to limestone powder and fly ash containing mortar.

Yilmaz and Olgun, (2008) investigated the influence of limestone, fly ash, and dolomitic limestone on cement and cement mortar characteristics. For the investigation mortar mixes were prepared in three different series designed by blending of cement with limestone, fly ash, and dolomitic limestone. Properties of cement and mortar like standard consistency, setting time, soundness and compressive strength were evaluated. This study observed that the compressive strength of mortar was gradually reduced upon increase of fly ash. However, addition of fly ash with limestone and dolomitic limestone improved the strength of mortar as compared to only fly ash contained mortar. Setting time and soundness of mortar were not significantly affected by adding limestone, fly ash, and dolomitic limestone.

2.3 Use of other Dimensional Stone Waste in Mortar Mixes

Apart from limestone other stone waste like granite, marble, sandstones, and solid waste such as ceramic waste, wollastonite, etc. have been used in cement mortars as supplementary cementitious material or substitution of fine aggregate.

An attempt on similar grounds was made by Corinaldesi et al., (2010), where the characterization of marble waste to their possible used in mortar and concrete production was investigated. The study claimed that the marble powder has filler ability, due to this 10% marble powder used as a substitution of sand gives positive effect on compressive strength of mortar than that of control mortar.

Another study by Farinha et al., (2015) examined the mortar properties with addition of fine sanitary ware aggregate. Mortar mixes were prepared using this aggregate as fine aggregate substitution up to 20% with interval of 5%. These mortars were tested through strength, porosity and water absorption parameters. Results from the test suggested that the fine sanitary ware show positive filler effect and contribute in pozzolanic reaction resulting in gain in mechanical strength of the mortar, which was observed highest with 20% replacement level. Also, at the same level, water absorption of mortar was lower as compared to control mortar.

Gupta and Vyas, (2018) reported in their study that the granite has potential to use in cement mortar as substitution of fine natural aggregate. It was found that 30 to 40 percent granite powder as fine aggregate in masonry mortar performed well in bond and adhesive strength parameter whereas mortar with 40% granite powder gave the highest compressive strength among all the mortar mixes. However, the drying shrinkage of mortar was increased by adding granite powder.

Another similar study by Jiménez et al., (2013) used recycled ceramic waste aggregate in mortar production. In this study, five mortar mixes designed using 0, 5, 10, 20 and 40 percent recycled ceramic waste as fine aggregate replacement. Results of the study showed that compressive, flexural and adhesive strength was enhanced with increasing replacement level. However, density and workability was decreased upon the increase of ceramic waste.

Kallel et al., (2016) investigated the influence of sand washing waste on durability of mortar. Mortar mixes containing calcined waste from 0 to 30% replacement of cement were prepared for their acid and sulphate resistivity test. Observations were taken on the basis of weight loss, compressive strength, change in volume and micro study by XRD. The mortar mix containing 10% calcined waste gave superior performance than all mortar mixes.

A study carried out by Khyaliya et al., (2017) investigated the influence of marble waste in lean mortar mixes. Marble waste was utilized as a substitution of fine aggregate with a specific percentage level of 25, 50, 75, and 100. Findings of the study reported that the marble waste up to 50% replacement level was suitable to produce lean mortar mixes. They observed that 50% marble waste used was beneficial for mortar in terms of improved workability, mechanical strength, and durability.

Similarly, Kabeer and Vyas, (2018) used marble powder as fine aggregate in both plaster and masonry mortar. Performance of the mortar was measured on the basis of workability, drying shrinkage and strength parameters. Obtained results revealed that the 20% marble powder as fine aggregate had no derogatory effect on mortar properties.

Mashaly et al., (2018) performed a detailed laboratory investigation on mortar, mortar composites and concrete by using granite sludge as cement substitution. Three series

of mortar or mortar composites and concrete were designed using granite sludge with four replacement level of 10, 20, 30 and 40%. Prepared samples were evaluated on the basis of their physical, mechanical and durability properties like density, water absorption, porosity, compressive and flexural strength, soundness, abrasion resistance and freeze-thaw. Results of the study reported that the inclusion of granite sludge decreased mortar strength as compared to control mortar. However, 20% granite sludge added mortar satisfied the requirement of flexural strength as given in standard EES 269-1. Other parameters like water absorption, porosity, abrasion loss and freeze-thaw negatively affected with incorporation of granite sludge.

Fine ceramic waste in mortar was also utilized by Silva et al., (2009). Performance of mortar mixes was investigated on the basis of physical, strength and durability properties. Study concluded that the 10% fine ceramic waste as filler material improved performance of mortar mixes.

Table 2.1 Previous Researches on use of Limestone or Limestone Waste and Dimensional Stone in Mortar Production

Type of Mortar	Form of Limestone	Replacement	Properties Evaluated	Outcome	Ref.
Mortar (1:3)	Limestone dust	Sand (0 to 20%)	Porosity, shrinkage, flexural and compressive strength, and workability	Improvement in strength at early ages	(Bonavetti and Irassar, 1994)
Cement lime Mortar	Limestone waste	Natural lime (0 to 12%, 4% interval)	Compressive, flexural and adhesive strength, porosity, and microstructure study.	Strength properties were enhanced with limestone waste	(Ballester et al., 2007)
Cement sand mortar	Limestone powder + rubber waste	Filler material	Compressive, flexural, unit weight, thermal conductivity test and SEM	Strength loss due to rubber waste compensated by limestone powder filler	(Corinaldesi et al., 2011)
Self-compacting mortar	Limestone fines	Crushed sand (0 to 30% with 5% interval)	Compressive, flow value test and slump test	Mortar strength was improved with 10 to 15% limestone fines addition in crushed sand	(Benabed et al., 2012)
Cement mortar	Limestone crushed sand	Silica river sand (0%, 25%, 50%, 75% and 100%)	Workability, Compressive and flexural strength, capillarity absorption (in acid and lime solution), and acid attack	Mortar containing limestone crushed sand was more capable to resist against acid attack than that of river sand	(Bederina et al., 2013)
Cement mortar	Limestone	Cement upto 65%	Density, porosity, compressive strength and sulphate resistance	Mortar blended with limestone up to 50% performed better in strength and sulphate resistance	(Baldermann et al., 2018)
Cement mortar	Limestone fines	Fine aggregate	Packing density, flowability, strength and cohesiveness.	Addition of limestone fines reduced the flow spread of mortar whereas cohesiveness and strength were benefited.	(Kwan and McKinley, 2014)

Type of Mortar	Form of Limestone	Replacement	Properties Evaluated	Outcome	Ref.
Cement mortar	Limestone fines	Cementitious material (5, 7.5 and 10%)	Microstructure analysis through MIP, SEM and EDS, XRD and acid attack	Limestone fines containing mortar has high acid resistant capability as compared to silica fume added mortar, while strength of limestone added mortar was less than that of ordinary cement mortar	(Senhadji et al., 2014)
Cement mortar	Limestone filler	10 to 40% of the cement weight	Density and compressive strength	Improvement in compressive strength was about 39% more as compared to control mortar.	(Soroka and Setter, 1977)
Cement mortar	Limestone	Cementitious material	Thaumasite sulphate attack	Mortar containing limestone was more susceptible in sulphate environment as compared to Portland cement mortar	(Ramezaniapour and Hooton, 2013)
Self-compacting repair mortar	Limestone powder	Cementitious material	Fresh properties, water absorption, flexural and compressive strength	Mechanical strength (early age) of 30% limestone powder containing mortar was more as compared to control mortar.	(Türkel and Altuntaş, 2009)
Cement mortar	Limestone and dolomitic limestone	Cementitious material	Standard consistency, setting time, soundness and compressive strength	Addition of fly ash with limestone and dolomitic limestone improved strength of mortar as compared to only fly ash contained mortar. Other properties were satisfactory.	(Yilmaz and Olgun, 2008)
Cement mortar	Granite sludge	Cement up to 40%	Compressive and flexural strength, density, porosity, water	Mortar properties were negatively affected by	(Mashaly et al., 2018)

Type of Mortar	Form of Limestone	Replacement	Properties Evaluated	Outcome	Ref.
			absorption, soundness, abrasion resistance and freeze-thaw	incorporating granite sludge	
Cement mortar	Granite powder	Natural sand up to 40%	Workability, water absorption, compressive strength, tensile bond strength, drying shrinkage and adhesive strength,	Mortar prepared with 30 to 40% granite powder can be used as masonry purpose	(Gupta and Vyas, 2018)
Lean mix mortar	Marble powder	Natural sand up to 100% with steps of 25%	Workability, water absorption, drying shrinkage, compressive strength, acid attack and sulphate attack	50% marble waste as natural sand substitution was feasible to enhanced mortars mechanical and durability property	(Khyaliya et al., 2017)
Cement mortar	Marble powder	Natural sand up to 100% with steps of 20%	Workability, compressive strength, water absorption, drying shrinkage, adhesive strength, and microstructure analysis	20% marble powder was suitable to use as fine aggregate.	(Kabeer and Vyas, 2018)
Cement mortar	Marble powder	River sand up to 10%	Workability, compressive strength and pulse velocity	Mortar containing 10% marble powder better performed than that of control mortar.	(Corinaldesi et al., 2010)
Cement mortar	Fine sanitary ware waste	Fine aggregate up to 20% with 5% interval	Water absorption compressive strength, flexural strength, porosity and microstructure	Highest strength of the mortar was found with 20% fine sanitary ware aggregate.	(Farinha et al., 2015)
Cement mortar	Ceramic waste	Fine aggregate up to 40% replacement	Compressive, flexural and adhesive strength, water absorption and density	Study claimed 40% ceramic waste containing mortar improved strength parameters. However, density and water absorption was decreased	(Jiménez et al., 2013)

Table 2.2 Chemical Constituents of Stone Waste used in Previous Study for Mortar Production

Type of solid waste	SiO ₂	CaO	Al ₂ O ₃	Fe ₂ O ₃	MgO	Na ₂ O	K ₂ O	LOI	Ref.
Limestone powder	6.50	86.94	0.11	0.06				7.30	(Corinaldesi et al., 2011)
Limestone fines	1.0	52.6	0.2	0.2	2.1			43.6	(Benabed et al., 2012)
Lime stone	0.76	54.9	0.41	0.23	0.61			36.3	(Makhloufi et al., 2014)
Limestone crushed sand	20.14	63.47	3.71	4.74	2.12			1.72	(Bederina et al., 2013)
Limestone fines	7.89	45.45	2.58	1.13	1.72			42.4	(Senhadji et al., 2014)
Limestone powder	0.45	52.35	0.33	0.14	1.05			42.5	(Türkel and Altuntaş, 2009)
Limestone	2.58	52.39	0.68	0.33	0.64			41.8	(Yilmaz and Olgun, 2008)
Granite sludge	58.17	3.27	11.96	13.35	0.36	4.69	3.84	2.58	(Mashaly et al., 2018)
Granite powder	74.39	0.41	13.5	0.86	0.38	4.16	4.79	-	(Gupta and Vyas, 2018)
Marble waste	3.75	33.12	-	0.13	17.91	-	-	45.0	(Khyaliya et al., 2017)
Marble powder	1.57	32.19	0.18	1.18	-	-	-	-	(Kabeer and Vyas, 2018)

LOI- Loss on ignition

Table 2.3 Physical Properties of Stone Waste used in Previous Study for Mortar Production

Type of solid waste	Specific gravity	Water absorption (%)	Loos bulk density	Fineness modulus	Ref.
Limestone dust	2.72				(Bonavetti and Irassar, 1994)
Limestone fines	2.7				(Benabed et al., 2012)
Limestone	2.7			2.30	(Makhloufi et al., 2014)
Limestone crushed sand	2.7	4.3		2.30	(Bederina et al., 2013)
Limestone fines	2.7				(Senhadji et al., 2014)
Limestone powder	2.65				(Türkel and Altuntaş, 2009)
Granite	2.46	15.29	1368	0.9	(Gupta and Vyas, 2018)
Marble powder	2.7	9.89	1380	2.13	(Kabeer and Vyas, 2018)

2.4 Influence of Dimensional Limestone Stone Waste on Properties of Mortar Mixes

2.4.1 Influence on Strength of Mortar Mixes

2.4.1.1 Compressive and Flexural Strength

Strength of mortar is the desired mechanical parameter which provides overall picture of mortar quality. Strength is dependent on type of binding material, curing conditions and adequate gradation of fine aggregate. However, long term durability or performance of mortar depends on several other parameters. In recent years, researchers have tried to improve strength parameters by inclusion of dimensional stone waste or solid stone waste in different ways such as cementitious material, as filler material and as fine aggregate replacement. Bonavetti and Irassar, (1994) observed an increase in compressive and flexural strength with increase of limestone dust up to 20% replacement level. Strength was found 44% to 72 % more as compare to control mortar at early age of testing however in the later age results were comparable. Another study by Ballester et al., (2007), used limestone waste which was obtained by cannery industry having 96% CaCO₃ to replace natural lime from cement-lime-sand mortar. They found mortar with 12% waste limestone in addition of

silica enhances both compressive and flexural strength at longer curing ages. In fact limestone powder also compensates the flexural strength loss due to rubber waste which was used as silica sand replacement. These were rectified with scanning microscope images that shows mortar containing mussle cannery industry obtained limestone waste have dense and major calcium silicate hydrated product which stands for high compressive strength of mortar. Corinaldesi et al., (2011) used limestone as filler material in cement sand mortar mixes. From the study they concluded that the limestone powder addition improved compressive and flexural strength of mortar. Similar to that Türkel and Altuntaş, (2009) observed limestone powder can improve mechanical performance of self-compacting repair mortar at early ages.

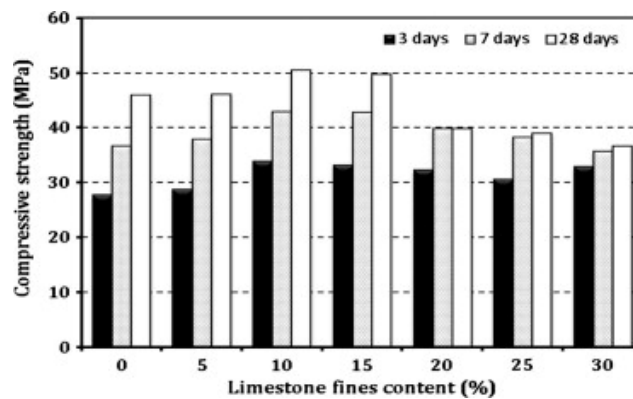


Figure 2.1 Compressive Strength of Mortar Containing Limestone Fines at Various Age of Curing (Benabed et al., 2012).

Benabed et al., (2012) used limestone fines to prepare self-compacting mortar. The results of compressive strength obtained in this study are shown in Figure 2.1. It was observed that the compressive strength of mortar was enhanced with increase of limestone fines up to 15% replacement of fine aggregate. Improvement in strength was attributed to small particles size of limestone fines resulting in to denser microstructure. Kwan and McKinley, (2014) used cement paste volume replacement method to explain effect of limestone fines on the compressive strength of mortar. They observed it was dependent on cement paste volume and found compressive strength was increased with increasing limestone fines but strength was decreased when cement paste volume was below 50%. Similarly, Soroka and Setter, (1977) found improvement in compressive strength of mortar with limestone fillers. They noticed compressive strength of mortar was superior with higher content (40%) of limestone filler. Improvement in strength was claimed due to high fineness nature or filler effect and may be formation of calcium-carbo-aluminates. Above filler effect

was also reported by Kabeer and Vyas, (2018) in their study, where mortar mixes were prepared using 20, 40, 60, 80 and 100% marble powder as opposed to river sand. The results from the study indicated that the compressive strength of mortar containing 20% marble powder was superior to that of control mortar. This improvement was due to fineness of marble powder which enhanced the packing density of mortar resulting in to more strength in mortar. The densify nature of mortar was justified with Scanning electrons microscopy images (SEM), reported by Chouhan et al., (2018). In this study, SEM micro images showed, mortar containing 40 to 50% dimensional limestone slurry waste has denser CSH formation in microstructure as compared to reference mortar resulted in to maximum compressive and flexural strength found at these replacement level. However, Senhadji et al., (2014) observed low compressive and flexural strength with limestone fines in OPC mortar. It was found that strength reduced from 45.5MPa to 38.5MPa with inclusion of 15% limestone fines when used as cementitious material.

2.4.1.2 Tensile Bond strength

Martínez et al., (2013), evaluate the bond strength of mortar produced with recycled aggregate as 100% replacement of natural aggregate, also used three types of filler material namely: hydrated lime, limestone and white slag (by product of steel industry). Bond strength test was performed over concrete blocks in accordance to standard NC 172:200. Study observed that the recycled aggregate (composed of ceramic material) containing mortar achieved highest bond strength about 0.51 MPa than other recycled aggregate containing mortar. Moriconi et al., (2003) reported that the bond strength with red bricks and recycled aggregate mortar was high as compared to yellow brick attributed to large number of pores in red bricks, which allows mortar paste to penetrate in to top brick layers, this also ensures suitable water-cement ratio required for interfacial transition zone. Similarly, a study by Corinaldesi and Moriconi, (2009), evaluate the mortar-brick bond test derived according to UNI EN 1052-3. For this, the behaviour of masonry during the absence of normal stress was evaluated. Author observed recycled aggregate mortar gave superior mortar brick bond strength as compared to control mortar and was related to adhesion between fresh mortar and brick surface. A recent study by Kabeer and Vyas, (2018) observed that the tensile bond strength between mortar paste and bricks was maximum with

20% marble powder for 1:3 and 1:4 mortars whereas for 1:5 and 1:6 mortar superior with 40% marble powder.

2.4.1.3 Adhesive Strength

Adhesive strength of mortar was found improved with cannery industry obtained limestone waste due to spike of workability with high consistency as compared to mortar containing natural limestone (Ballester et al., 2007). Similar observations were found by Kabeer and Vyas, (2018), where they evaluated adhesive strength for 1:3, 1:4, 1:5 and 1:6 proportion mortars with addition of marble powder between 20 to 100% replacement of river sand. The adhesive strength was found maximum with 20% marble powder for all mortar proportions however, improvement in adhesive strength was observed with 40% and 60% marble powder in rich (1:3 and 1:4) and lean mixes (1:5 and 1:6) respectively. Farinha et al., (2015) noticed that the adhesive strength of mortar containing 20% fine sanitary ware was more as compared to control mortar. This improvement exhibited by the formation of strong interface between substrates due to penetration of fine sanitary ware into capillary pores. However, one more study by Jiménez et al., (2013) on use of sanitary ware waste in cement mortar as the 10, 20, and 40% replacement of fine aggregate reported that the adhesive strength was not affected by sanitary ware incorporation. Similar results observed in a study by Gupta and Vyas, (2018), where they used granite powder in cement mortar for fine aggregate replacement between 30 to 40%. Improvement in adhesive strength was about 9 to 23% more than that of reference mortar.

2.4.2 Influence on Durability Properties of Mortar Mixes

2.4.2.1 Workability

Workability of any mortar depends on the fineness of the aggregate used. More fine particles get increased specific surface area of the paste resulted into more water required to achieve desired workability. Bonavetti and Irassar, (1994) used quartz dust, limestone dust and granite dust as replacement (by weight) of sand from 0 to 20% with interval of 5%. They observed that mortar with limestone and granite dust increased water requirement to achieve constant flow (between 105 to 115 mm) due to increase in specific surface area of the mortar. Water demand of mortar containing 20% granite and limestone dust has 17% more as compared to control mortar. This phenomena also reported by Benabed et al., (2012) in their study, where,

mortar flow decreased with addition of limestone fines. This was due to increase in fines content in aggregate resulted in to large specific surface area of fine aggregates that demand extra water to flow mortar paste. Bederina et al., (2013) observed that the mixing of mortar containing limestone sand quite difficult than quartz sand mortar, while water-cement ratio was same. This could be described as the fact that limestone has more water absorbent capacity than quartz sand, and on the other hand friction developed by angular shaped limestone aggregate, therefore more water needed to get desired flow.

Kwan and McKinley, (2014) investigated the influence of limestone fines on flowability of mortar. Mortar mixes were designed by adding limestone fines as equal volume fine aggregate replacement with constant cement paste volume. Flowability of the mortar was evaluated in terms of mortar flow spread and mortar flow rate conducted with mini slump cone and mini V- funnel as established by Okamura and Ouchi, (2003). Observations as seen in Figure 2.2, noted that the flow spread and flow rate of mortar were zero at 46% cement paste volume. When cement paste volume increased, flow started and improved with addition of limestone fines at certain percentage level of about 4, 8 and 12% for 50, 54 and $\geq 58\%$ cement paste volume respectively. However, flow rate of the mortar was decreased with increase in limestone fines due to its cohesive nature. This behaviour was attributed to increased cohesiveness and plasticity of mortar with limestone fines (Kwan and McKinley, 2014).

A similar study conducted by Türkel and Altuntaş, (2009) determined the workability of the self-compacting repair mortar (SCRM) using silica fume, limestone powder and fly ash. For this mini slump flow test performed on fresh mortar according to (ERMCO, 2005) standard shown in Figure 2.3. Workability of the self-compacting repair mortar (SCRM) was reported in terms of variation in spread value and required dosage of super plasticizers. Minimum and maximum spread value of the mix was decided as 200 and 280 mm. It was noticed that the silica fume utilization increased dosage of super plasticizers due to their large specific surface area. Dosage of super plasticizers for 30% fly ash and limestone powder was 0.8% while 30% silica fume containing mortar has required 5% super plasticizers to spread the mix as same value of control mortar. Previous study by (Corinaldesi et al., 2010; Kabeer and Vyas, 2018) on marble containing mortar reported that the workability of mortar was

dependent on amount of fine content added. Initially, within a certain percentage level, it was benefited to workability due to its thixotropic behaviour.

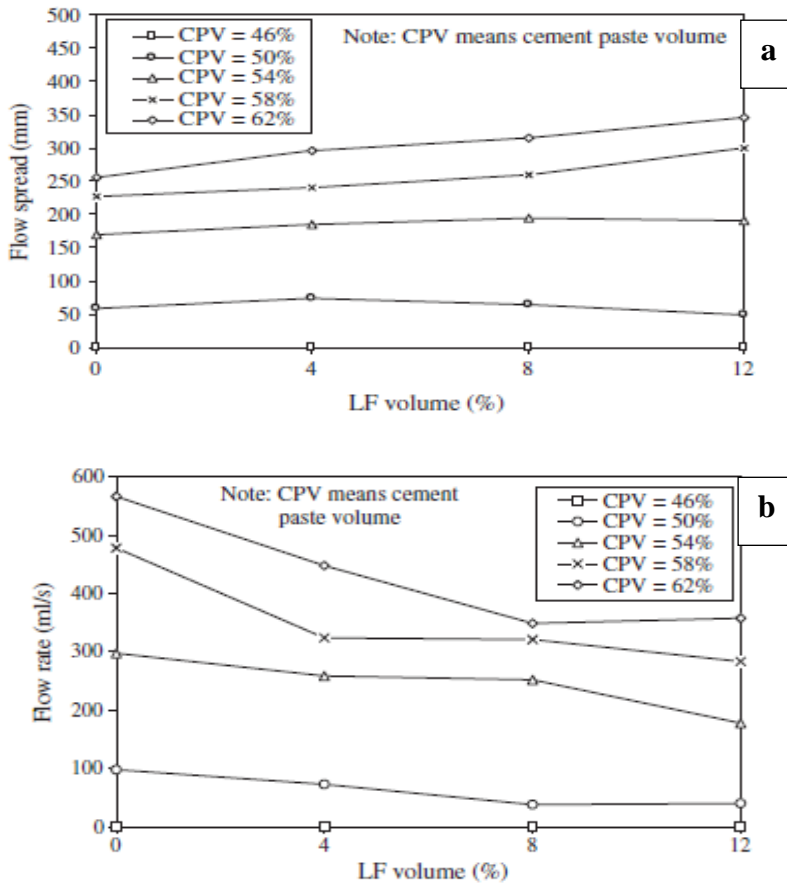


Figure 2.2 (a) and (b) Flow Spread and Flow Rate of Mortar Mixes with Various Percentage of Limestone Fines Volume (Kwan and McKinley, 2014)

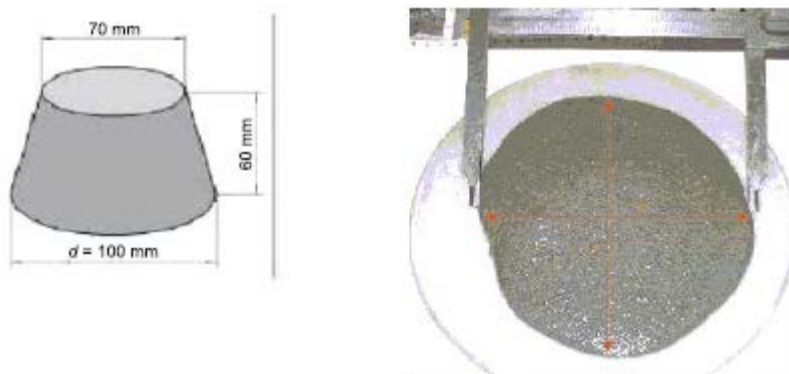


Figure 2.3 Schematic Diagram of Mini Slump Cone with Dimensions and Measurement of Mortar Flow (Türkel and Altuntaş, 2009)

2.4.2.2 Water Absorption, Density and Porosity.

Türkel and Altuntaş, (2009) determined total and capillary water absorption of mortar prepared using limestone powder (LP), silica fume (SF), and fly ash (FA). Capillary water absorption was evaluated according to specifications given in TS4045 (1984). For total water absorption test, samples were immersed in water completely, while in capillary absorption test samples base of size 40X40 mm were dipped into water upon a depth of 1mm from the bottom. Results from the tests revealed that the mortar containing 30% LP and 30% FA alone has greater water absorption value than the control mortar while 30% SF containing mortar has lower water absorption value as compared to control mortar. However, the minimum water absorption value was found in mortar with combination of 20% FA, 5% LP and 5% SF.

Mashaly et al., (2018) evaluated the effect of granite sludge on mortar properties, water absorption, porosity and bulk density in accordance to (ASTM C20 2000). Results of the study (summarized in Figure 2.4) indicated that the water absorption and porosity of the mortar were increased with the amount of incorporated granite sludge. Reason behind this improvement was reported as high specific surface area of granite containing mortar, needed more water to lubricate the mortar paste. However, mortar up to 20% granite sludge improvement in water absorption and apparent porosity was minor compared to control mortar.

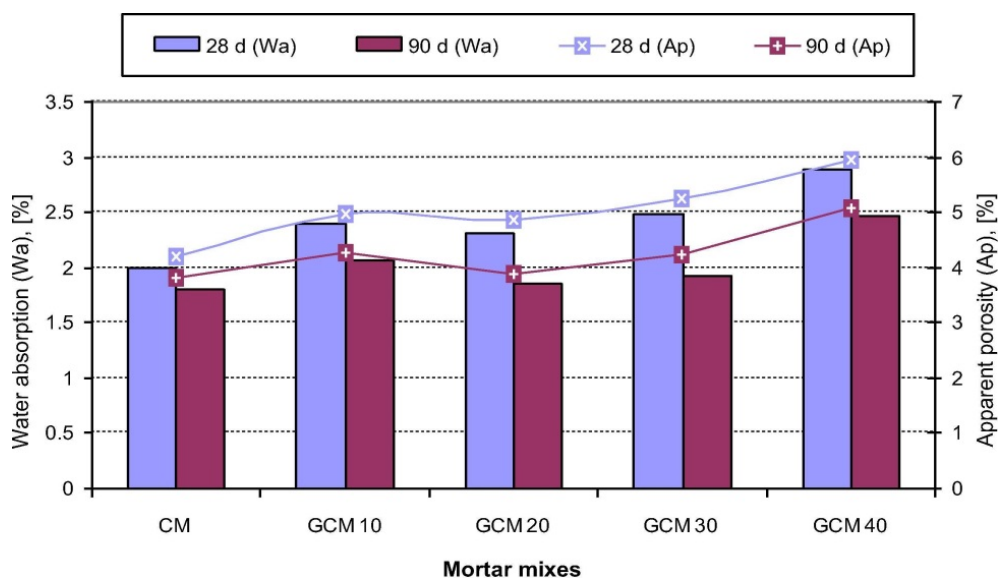


Figure 2.4 Water Absorption and Apparent Porosity of Mortars Containing Various Percentage of Granite Sludge (Mashaly et al., 2018)

Bonavetti and Irassar, (1994) found minimum air content in mortar with 10% limestone dust that reduced porosity of the mortar by pore filling effect. This effect was better understood in a study by Ballester et al., (2007), where they used mercury intrusion porosimetry (MIP) method to determine the porosity of mortar mixes. This study reveals that the fine particle content in cannery industry obtained limestone waste were more efficient in filling of pores resulting in to high strength of mortar mixes.

Baldermann et al., (2018) noticed that, the blended mortar with $\leq 50\%$ limestone as cement substitution produces higher size of pores as compared to conventional mortar. This was attributed to coarser particles of limestone than cement particles; however average pore structure was reduced, which resulted into better performance against compressive strength and sulphate attack. Mostly mortar pore diameters were observed around 0.03 to 0.3 μm which represent total porosity in MIP curves (shown in Figure 2.5). This result was also correlated with the density of mortar, which was observed increasing up to 50% limestone addition. Bulk density and apparent density of mortar having 50% limestone were about 2.26 and 2.57 respectively, which is 7.11% and 2.39% more as compared to conventional mortar. Similarly, Soroka and Setter, (1977) found improvement in mortar mix density (in terms of lower air content) by addition of dolomite, limestone and basalt fillers.

Another attempt by Farinha et al., (2015), determined the density of mortar using 5, 10, 15 and 20% fine sanitary ware as fine aggregate replacement. The effect on dry bulk density upon the inclusion of waste is shown in Figure 2.6. From the figure, it is noted that the mortar incorporation up to 20% fine sanitary ware had highest density relative to other mortar mixes. On the contrary to this, Kwan and McKinley, (2014) found that the packing density of the mortar reduced with increase in cement paste volume and limestone fines. They observed that it was reduced from 0.723 to 0.704 with increase in limestone fines from 0 to 12%.

Reduction in packing density was understood by packing theory. According to this, a certain amount of powder content is required for filling voids between aggregate and to provide maximum packing density. Above a certain limit of powder content, the existing aggregates are trying to adjusting extra particles this resulted in to lower the packing density (Larrard, 1999).

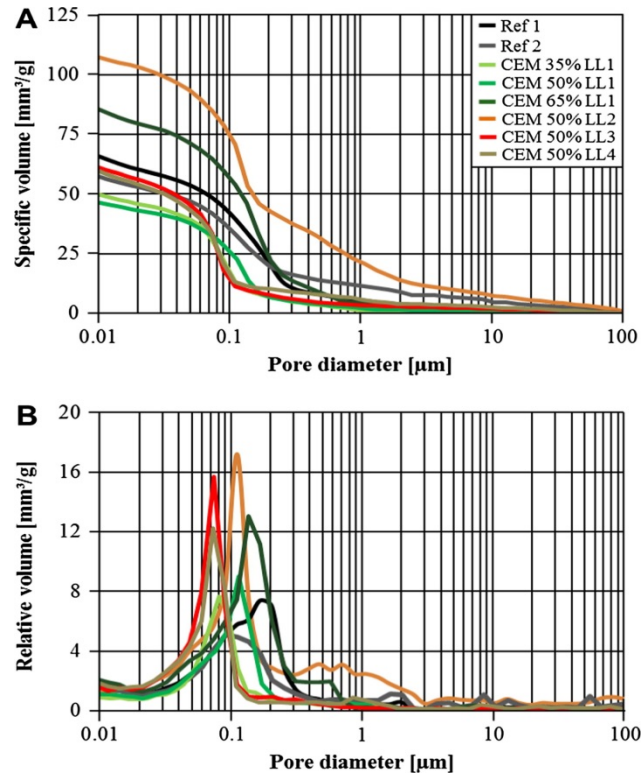


Figure 2.5 Specific and Relative Volume Intrusion Curve (A-B) for Limestone Blended Cement Mortars (Baldermann et al., 2018).

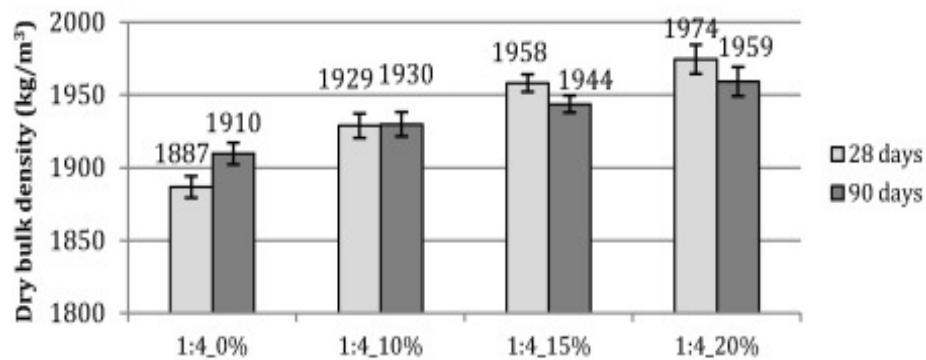


Figure 2.6 Dry Density of Mortar with Varying Percentage of Fine Sanitary Ware (Farinha et al., 2015)

2.4.2.3 Acid Attack

Acid attack is one of the important durability properties which directly affect the performance of mortar or concrete. During the acid attack degradation takes place due to the production of highly soluble salts (gypsum) as a byproduct of the reaction between cement hydrated products (CH) and acid. These salts are highly water soluble, resulting in the weakening of the cement paste and deteriorating the mortar in terms of spalling, strength loss, and weight loss. Sulfuric acid attack in mortar or concrete can

be caused by its availability in groundwater, chemical waste, etc. (Skariah et al., 2017).

Makhloufi et al., (2014) observed a synergistic effect of quaternary binder containing limestone in mortar mixes, causing this perform better as compared to reference mortar in aggressive medium. They followed two protocols to know the effect of limestone mortar in acid solution; one was slow attack and another was rapid attack. In slow attack, mortar samples were continuously immersed in lime water solution and 3% sulfuric acid solution with normal temperature of 22 to 24°C whereas in fast acid attack, mortar samples were subjected to seven drying and heating-cooling cycles. In slow method, solution was changed every month. In fast acid attack method, one cycle required 7 days, in which samples were drying in oven for three days at constant 60°C temperature and remaining three days it was immersed in lime water and 5% sulphuric acid solutions. Authors concluded that the fast acid attack gets more decalcification of hydrated products such as calcium hydroxide than that of slow acid attack method. Also, they found mortar having 30% limestone, 10% blast furnace slag and 10% natural pozzolana as cement replacement improves the mortar behaviour in aggressive medium.

Bederina et al., (2013) studied the performance of mortar containing limestone sand in 3% HCL (hydrochloric acid) solution till the age of 180 days. After 180 days, reduction in mass and strength of mortars was observed. However, this reduction was minimum in limestone containing mortar. Maximum and minimum mass loss was about 16.4% and 2.53%, in control mortar and 100% limestone sand mortar respectively. Whereas compressive strength loss in mortar with 0% 50% and 100% limestone sand was 13.45, 11.12 and 9.73% respectively. Thus limestone in mortar was resistant against the acid attack. Similar observations were found by Ghrici and Kenai, (2007), when they used limestone fines as Portland cement replacement up to 20% in mortar production. They concluded limestone fines containing mortar was better performed against sulfuric acid attack than ordinary OPC containing mortar.

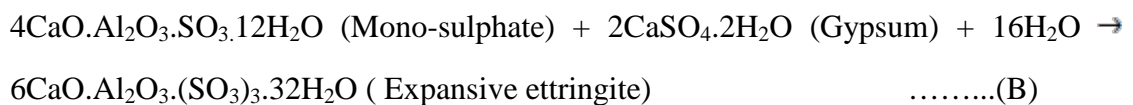
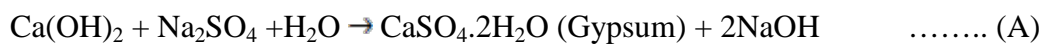
Senhadji et al., (2014) reported that the cement with addition of 15% limestone fines had lowest weight loss in sulfuric acid solution as compared to other mortar. This behaviour of limestone fines was attributed to high calcium carbonate content (CaCO_3), which improved acid consuming capacity of mortar. Also, low cement

reduced production of portlandite (C-H), which in turn result in to better performance against acid attack.

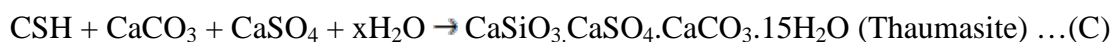
2.4.2.4 Sulphate Attack

Sulphate attack in mortar or concrete occurs due to reaction between sulphates presents in groundwater, drainage solutions and hydrated products. This reaction leads to generate gypsum, expansive ettringite and thaumasite as byproduct and causes deterioration of mortar in terms of cracking, expansion, strength loss and spalling, etc. as shown in Figure 2.7. In sulphate attack test, initially mass of the mortar are increases because of formation of expansive ettringite or gypsum, which reduce the pore volume of the mortar. However in later age's weight loss happens due to formation of thaumasite (Kallel et al., 2016).

Formation of gypsum, expansive ettringite and thaumasite can be understood by following reactions A, B and C:



Thaumasite is formed by the reaction between calcium silicate hydrates (CSH) and sulphate with presence of carbonates, resulting in to loss in binding material occurs and hence the depletion of the mortar or concrete surfaces.



The formation thaumasite is extremely high in wet environment with low temperature (Hooton and Thomas, 2002). It was reported that the below 15 °C temperature, particularly from 0 to 5 °C are the most favorable to thaumasite formation (Bensted, 1999). However (Colleparidi, 1999; Sims and Huntley, 2004) mentioned in their study, the thaumasite sulphate attack can be arisen at 20 °C or more.

Irassar, (2009) reported that the thaumasite sulphate attack in mortar with limestone takes place by exposed the sulphate solution that disintegrates the CSH in cement matrix with the presence of Ca^{2+} .

Ramezaniapour and Hooton, (2013) reported that, at low temperature below 5°C, Portland-limestone cement was highly susceptible in thaumasite sulphate attack as compared to ordinary Portland cement. Baldermann et al., (2018) observed that the cement blended with 35 to 50% limestone, outstandingly performed in sulphate resistant test in both 8° C and 20° C temperatures.



Figure 2.7 Deterioration in Mortar Surface during Sulphate Attack
(Ramezaniapour and Hooton, 2013).

2.4.2.5 Drying Shrinkage

Bonavetti and Irassar, (1994) reported that the drying shrinkage of the mortar containing granite (10-15%) and limestone (10%) dust was high due to more water absorbed and formation of carbo-aluminates in internal mortar structure. However, mortars incorporating quartz dust has lower drying shrinkage than the control mortar while increasing water demand.

Pozo-Antonio, (2015) evaluated drying shrinkage of limestone based mortar in accordance to standard ASTM C490. For drying shrinkage measurement, samples were casted in standard size mould of 285mm x 25mm x 25mm and noted in terms of length change. This study reported that the mortar with pure lime has higher value of shrinkage as compared to mortar with natural hydraulic lime based mortar.

Khyaliya et al., (2017) investigated the effect of marble powder on drying shrinkage of mortar. They observed that the marble powder used up to 50% as river sand substitution, performed satisfactorily in drying shrinkage. This phenomenon was

attributed to lower water-cement ratio for given cement content. However mortar with more than 50% marble powder increased the drying shrinkage, reason behind this would be the higher specific surface area of the aggregates which increase the drying shrinkage of mortar.

2.5 Summary of the Literature Review

Previous studies were exploring the use of various limestones or dimensional stone waste as mortar constituents either filler or cementitious material. These studies suggest that addition of limestone leads to loss in workability of mortar due to its high fineness and cohesive nature. However, some author noticed reduction in workability at higher percentage of limestone, while at below 20% replacement improved due to its thixotropic nature. Water absorption and porosity of mortar were increased with increase of fine, due to high specific surface area, this resulted in to high pores formation in mortar mixes.

Compressive and flexural strength of mortar was increased with the inclusion of limestone fines, marble powder, granite sludge and fine ceramic waste, as fine aggregate replacement (between 20 and 40%). In addition to this, limestone combining with other material like silica fume, fly ash and rubber waste gives better performance in strength of mortar. Tensile bond strength, adhesive strength and drying shrinkage of the mortar mixes were benefited as incorporation of granite powder, ceramic waste and marble powder.

Inclusion of dimensional stone waste improves the durability of mortar mixes. Contrary to their respective control mixes, mortar with limestone and marble powder exhibited superior resistance against acid attack. This behaviour was attributed to high calcium carbonate content (CaCO_3), which improves resistance to acid attack and acid consuming capacity of mortar.

Nevertheless, available investigations on said properties were limited, even these properties with dimensional limestone waste are still missing. Additionally, the reported studies on use of limestone in combination with other waste material such as fly ash, silica fume, marble dust etc., does not provide clear understanding on effect of limestone alone on mortar mix properties. Also, the limestone used in these studies was mostly highly calcium oxide (CaO) contained, which was either pure or

conventional limestone. Some other important parameters of mortar such as carbonation, chloride ion penetration, wetting and drying cycle and fire resistance, have not been evaluated in past with addition of dimensional limestone waste.

CHAPTER 3

MATERIALS AND METHODOLOGY

3.1 General

For the present study mortar mixes were produced by using cement, fine aggregate (river sand) and Kota stone waste. These materials were characterized on the basis of their physical, chemical, morphological and microstructural analysis. Initial part of this chapter gives details about material used for mortar production, including procurement of raw materials, their physical and chemical characterization according to relevant standards, and microstructure analysis to identified major components and morphology with the help of SEM and XRD analysis.

3.2 Materials

a) Cement

Portland pozzolana cement conforming standard (IS 1489, 1991) was used as binding material, procured from local market.

b) Fine Aggregate (River Sand)

Fine aggregate (river sand) conforming standard (IS 2116, 1980), was procured from local suppliers.

c) Kota Stone Waste (KSW)

Kota stone waste was procured from processing units located at Ramganj Mandi, Rajasthan, India. At processing units, this waste accumulates in two forms slurry and cutting waste. In the present study, slurry and cutting waste as shown in Figure 3.1, has been used for partial replacement of conventional river sand. Dry Kota stone slurry (KSS) waste was used as it is, cutting waste crushed into desired gradation and reformed into manufactured crushed sand, designated as Kota stone crushed sand (KSCS). Particle size of both KSS and KSCS was kept below 1.18 mm to achieve required gradation for plaster and masonry mortar.

3.3 Material Characterization

Gradation of river sand, KSS and KSCS, as shown in Figure 3.2 was observed in accordance with the specifications of (IS 1542: 1992, 1999; IS 2116, 1980). It was found that 36.4% and 13% particles in KSS and KSCS were < 0.15 mm, whereas in river sand 6.3% particles were < 0.15 mm. This indicates presence of more fines in KSS and KSCS as compared to river sand.

Physical characterization and chemical constituents of cement, river sand, KSS and KSCS are given in Table 3.1 and Table 3.2 respectively. Table 3.2 shows Kota stone waste has significant quantity of calcium oxide (CaO) and silicon oxide (SiO₂), which identifies its calcareous nature. It was also noticed by X-ray diffraction patterns shown in Figure 3.3-3.4. Difference in texture of these materials was identified by Scanning Electron Microscopy images as shown in Figure 3.5. It was observed that KSS has smooth surface as compared to river sand, and KSCS has an irregular shape with flaggy appearance.

Table 3.1 Physical Characteristics Materials

Property	Materials			
	Cement	River sand	KSS	KSCS
Specific gravity	2.9	2.65	2.7	2.7
Water absorption (%)	-	2.49	8.8	3.5
Bulk density (Loose) (kg/m ³)	1100	1552	956	1291
Fineness modulus	-	1.9	1.29	1.99
Compressive strength after 28 days (MPa)	36.5	-	-	-
Initial setting time (minutes)	136	-	-	-
Final setting time (minutes)	225	-	-	-
Consistency (%)	32	-	-	-

Table 3.2 Chemical constituents of Cement, River Sand and KSW

Material	Chemical Constituents					Loss of ignition
	SiO ₂	CaO	MgO	Al ₂ O ₃	Fe ₂ O ₃	
Cement	32.01	44.75	1.11	8.47	3.83	9.4
River Sand	97.4	0.56	-	-	1.2	0.4
Kota stone waste	23.5	37.85	-	3.1	1.94	31.4



Figure 3.1 River Sand, KSS and KSCS

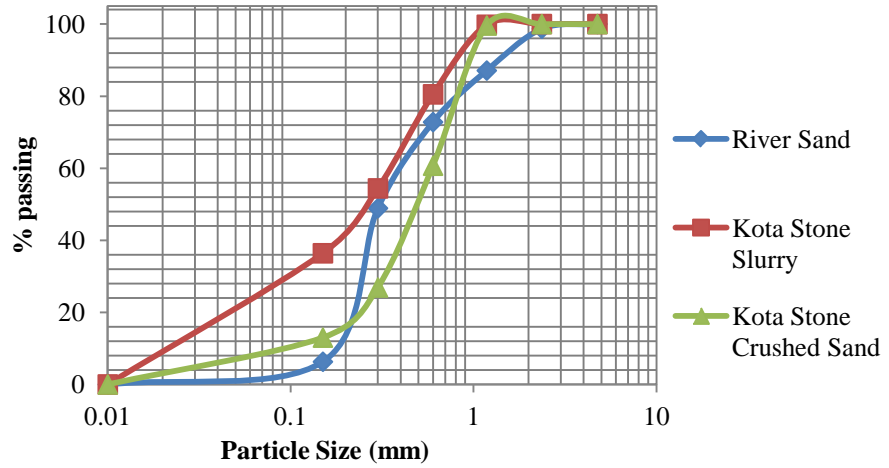


Figure 3.2 Gradation of River Sand, KSS and KSCS

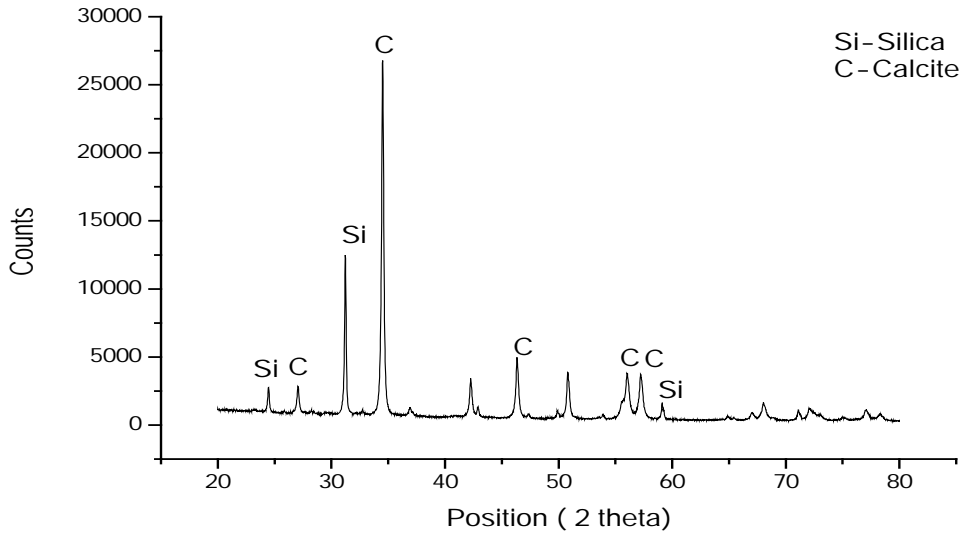


Figure 3.3 X-ray Diffraction pattern of Kota Stone Waste

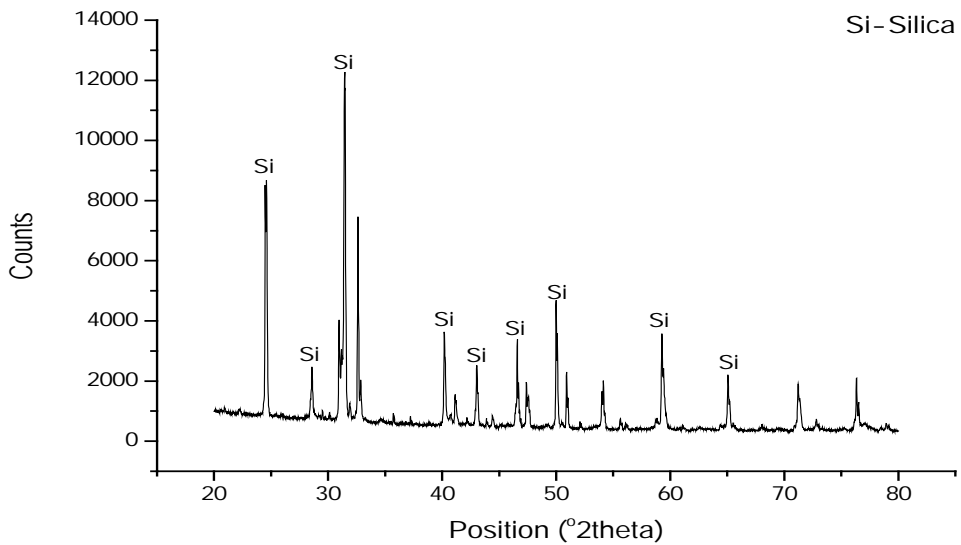
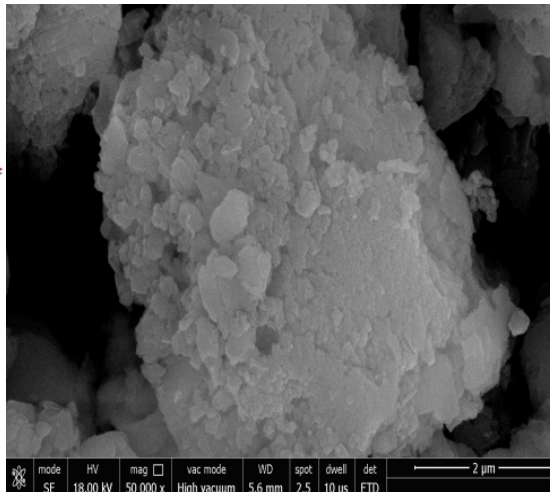
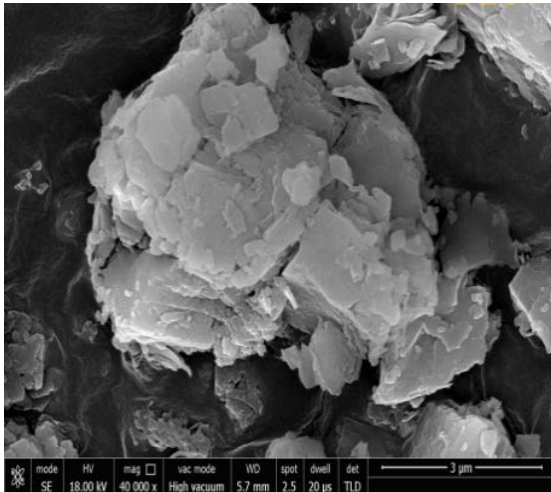


Figure 3.4 X-ray Diffraction pattern of River Sand

Kota Stone Slurry (KSS)



Kota Stone Crushed Sand (KSCS)



River Sand (RS)

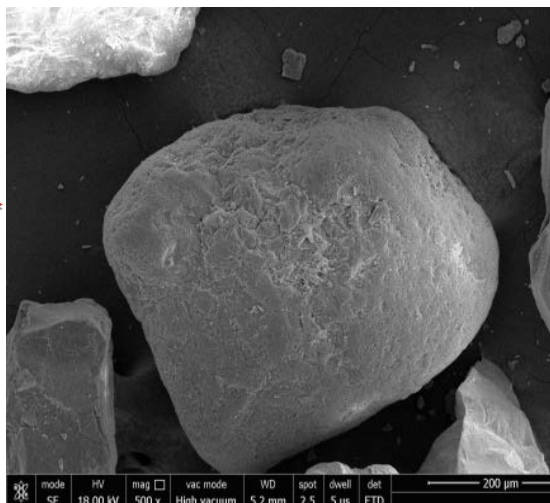


Figure 3.5 SEM images of KSS, KSCS and River Sand

3.4 Methodology

Present study was conducted in two stages. First stage included trial study whereas second stage comprised detailed investigations on mortar mechanical and durability properties with microstructure analysis.

a) Stage First:

In this stage, eleven mortar mixes were prepared with 1:4 (cement: sand) volumetric ratio. In these mixes, Kota stone slurry was used as a substitution (by volume) of river sand between 0 to 100% in steps of 10%. Details of mix proportions as shown in Table 3.3, mixes were designated as TS0, TS1, TS2,..... TS10. Here mix TS0 indicate mortar without replacement whereas TS1, TS2, TS3, TS4, TS5, TS6, TS7, TS8, TS9 and TS10 are mixes containing KSS as replacement of river sand in proportion of 10%, 20%, 30%, 40%, 50%, 60%, 70%, 80%, 90% and 100% respectively. These mortar mixes were designed at different water-cement ratio obtained by flow of the mortar paste described in workability section. Properties of these mortar mixes such as workability, compressive and flexural strength, water absorption, density, porosity and dynamic modulus of elasticity were evaluated. Also, microstructure of mortar mixes was analyzed using mercury intrusion porosimetry (MIP), thermogravimetric analysis (TGA) and scanning electron microscopic (SEM) images.

Table 3.3 Details of Mix Proportion for Stage First

Mix designation	Replacement (%)	Cement (kg)	River sand (kg)	KSS (kg)	Water (kg)	w/c ratio
TS0	0	300.0	1693.6	0.0	330.0	1.10
TS1	10	300.0	1524.3	104.3	315.0	1.05
TS2	20	300.0	1354.9	208.6	300.0	1.00
TS3	30	300.0	1185.5	312.9	300.0	1.00
TS4	40	300.0	1016.2	417.2	330.0	1.10
TS5	50	300.0	846.8	521.5	336.0	1.12
TS6	60	300.0	677.5	625.7	360.0	1.20
TS7	70	300.0	508.1	730.0	405.0	1.35
TS8	80	300.0	338.7	834.3	420.0	1.40
TS9	90	300.0	169.4	938.6	426.0	1.42
TS10	100	300.0	0.0	1042.9	435.0	1.45

(b) Stage Second:

In this stage, study was conducted with fourteen mortar mixes having two volumetric ratios of 1:3 and 1:6. For this KSS and KSCS were used as a volumetric replacement of river sand between 0 to 60% in steps of 20%. As observed for trial mixes that above 60% replacement level mixing becomes difficult this requires extra water to achieve desired workability. Mixes above 60% replacement levels were not included in this stage. For the investigation, prepared mixes were separated into four different series of A, B, C and D. Series A and B include mortar mix prepared at 1:3 volumetric ratio with KSS and KSCS respectively, similarly C and D series were designated for 1:6 volumetric ratio. Details of mix proportions for this stage mortar mixes are given in Table 3.4. Fresh and mechanical properties of mortar were evaluated for all mortar mixes, whereas in long term durability test 60% replacement level was eliminated from all the series because of its high shrinkage and poor adhesive nature. In place of 60% replacement, 30% replacement level added in all series for durability studies only. Details of fresh, mechanical and durability properties listed in Figure 3.6.

Table 3.4 Details of Mix proportion for Stage Second

Mix designation	Replacement (%)	Cement (kg)	River sand (kg)	KSS (kg)	KSCS (kg)	Water (kg)
Control (1:3)	0	350	1481.9	0	-	315.0
AS20	20	350	1185.5	182.5	-	290.5
AS30	30	350	1037.4	273.8		297.5
AS40	40	350	889.2	365.0	-	315.0
AS60	60	350	592.8	547.5	-	357.0
BC20	20	350	1185.5	-	246.5	304.5
BC30	30	350	1037.4		369.7	304.5
BC40	40	350	889.2	-	492.9	304.5
BC60	60	350	592.8	-	739.4	304.5
Control (1:6)	0	200	1693.6	0		350.0
CS20	20	200	1354.9	208.6		282.0
CS30	30	200	1185.6	312.9		276.0
CS40	40	200	1016.2	417.2		290.0
CS60	60	200	677.5	625.7		340.0
DC20	20	200	1354.9	-	281.7	346.0
DC30	30	200	1185.0		422.5	346.0
DC40	40	200	1016.2	-	563.3	340.0
DC60	60	200	677.5	-	845.0	340.0

In mix designation, numeric value denotes % of replacement of river sand and alphabetic letters represent series name and types of waste (*S: slurry waste and C: crushed sand*).

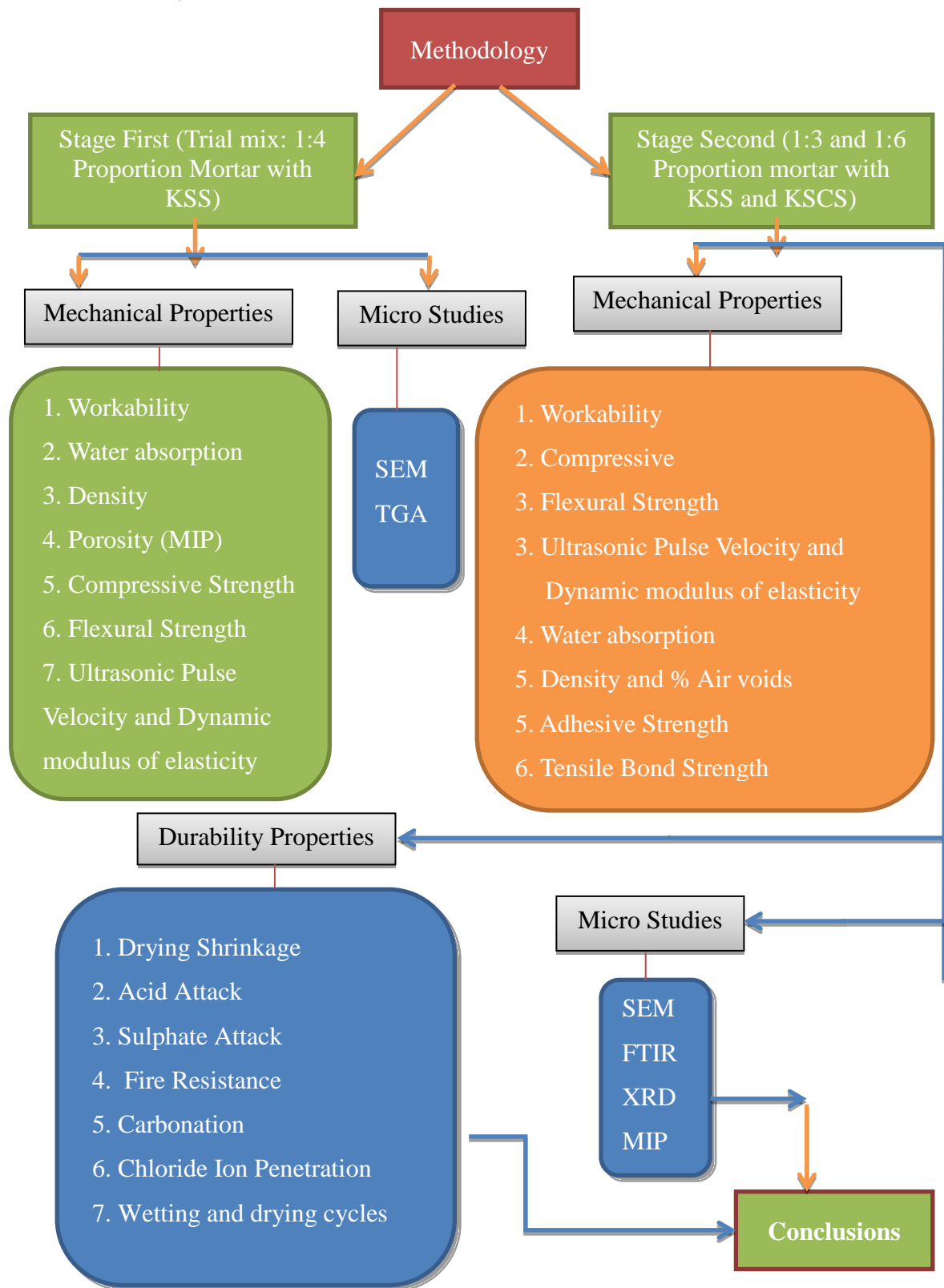


Figure 3.6 Methodology

3.5 Experimental Program

3.5.1 Sample Preparation

Before casting of samples, materials were brought to normal temperature of about $27 \pm 2^\circ\text{C}$. Quality of cement maintained uniform throughout the casting. Quantity of materials required for each batch was calculated according to Table 3.3 and Table 3.4, and then placed into tilting drum type mixer as shown in Figure 3.7. The mixer was rotated for 2 to 3 minutes to keep the mix homogenous. After this, water added in to the dry mixture and was mixed properly for 2 to 3 minutes. Prepared mortar was filled in to the moulds of specified size as prescribed in Table 3.5 (Mortar Properties). Before filling, the inner surface of each mold was oiled thoroughly. Filled specimens were compacted using plate vibrator of constant rate to avoid air voids in mortar mix. Then top surface of each specimen was leveled using trowel. Specimens were demoulded after 24 hours and were placed in to curing tank until the day of testing. Temperature of curing tank was maintained at about $27 \pm 2^\circ\text{C}$, and water renewed after seven days. Samples preparation for adhesive strength, tensile bond strength and drying shrinkage of these mortar mixes described in section 3.5.6, 3.5.7 and 3.5.8.



Figure 3.7 Mortar Samples

Table 3.5 Mortar Properties

Property	Sample used	Standards
Compressive strength	50 mm cube	(IS 2116: 1980, 1999)
Flexural strength	40x40x160 mm beam	(ASTM C348, 1998)
Ultrasonic pulse velocity and Dynamic Modulus of elasticity	40x40x160 mm beam	(ASTM C348, 1998); (Pozo-Antonio, 2015)
Water absorption	70 mm cube	(ASTM C642, 2008)
Density	70 mm cube	(ASTM C642, 2008)
Percentage air voids	70 mm cube	(ASTM C642, 2008)
Adhesive strength	-	(EN 1015-12, 2000)
Tensile bond strength	-	(ASTM C952, 2003)
Drying shrinkage	25x25x285 beam	(ASTM C1148-92, 2014)
Acid Attack	50 mm and 70 mm cube	(ASTM C 267, 2001)
Sulphate Attack	50 mm and 70 mm cube	(ASTM C 267, 2001)
Fire test	50 mm and 70 mm cube	(Kumar et al., 2018)
Carbonation	50 mm and 70 mm cube	(RILEM CPC 18, 1988)
Chloride ion penetration	40x40x160 mm beam	(Singh, 2016)
Wetting and drying cycle	70 mm cube and 40x40x160 mm beam	(BS EN 14066, 2013)

3.5.2 Workability

Workability of mortar mixes was assessed using flow of the mortar as shown in Figure 3.8, obtained via flow table test as per (ASTM C230, 2010). Flow value in the range of $110 \pm 5\%$, as recommended by (IS: 2250-1981, 1981) was adopted for this study. Water quantity adjusted till desired flow value in the range of 205-215 mm was achieved.



Figure 3.8 Flow Table Test

3.5.2 Compressive Strength

The compressive strength of mortar mixes was assessed using compressive testing machine (Figure 3.9) with constant loading rate of 2 kN/s recommended by (IS: 2250-1981, 1981). To carry out this test four cube specimens of 50 mm size were cast for each mix. Specimens were stored in water until the day of testing. Strength was evaluated immediately after removal from the curing tank. Compressive strength of mortar mixes was determined as the maximum applied load per unit specific surface area. Expression of compressive strength is:

$$\text{Compressive Strength (MPa)} = \frac{F(N)}{A (mm^2)} \dots\dots\dots (1)$$

Here:

“F” is the maximum applied load on the sample

“A” is the surface area



Figure 3.9 Compressive Strength Test on Mortar Sample

3.5.3 Flexural Strength

Flexural strength of mortar mixes was determined as per (ASTM C348, 1998). Compression testing machine with flexural testing assembly (shown in Figure 3.10) was used in this experiment. Beam moulds of size 40mmx40mmx160mm were cast in two layers with tamping, followed by putting in a vibrating table for 15 sec to achieve uniform compaction. The center point loading method was used to conduct flexural test on mortar samples. For this, the flexural assembly designed such that forces applied to the sample in vertical direction only without any eccentricity. The distance between end supports and point of loading remains constant and the direction of reactions is parallel to the direction of applied load at all times during the test. The maximum load applied on the sample was noted, and flexural strength was calculated in MPa as follows:

$$\text{Flexural Strength (MPa)} = 0.0028 P \dots\dots\dots (2)$$

Here:

“P” is the maximum point load in newton.



Figure 3.10 Flexural Strength Test on Mortar Samples

3.5.4 Ultrasonic Pulse Velocity (UPV) and Dynamic Modulus of Elasticity

For this test, Ultrasonic Pulse Velocity machine as shown in Figure 3.11 used to evaluate the uniformity, homogeneity, crack detection, and hardening characteristics of mortar specimens. The procedure was followed in accordance to (ASTM C597, 2016). Dynamic modulus of elasticity was measured by using following equation (Pozo-Antonio, 2015).

$$E = 0.001 \times v^2 \times \rho \dots\dots\dots (3)$$

Here:

"E" is the dynamic modulus of elasticity (MPa), "v" (m/s) is the speed of the wave in beam and "ρ" (gm/cc) is the dry density of mortar.



Figure 3.11 UPV Test on Mortar Samples

3.5.5 Water Absorption, Density and Percentage Air Voids

Water absorption, density and percentage air voids of mortar mixes were evaluated according to (ASTM C 642-06, 2008). For each mix, three specimens of 70 mm cubes were prepared, and after 28 days water curing, cubes were placed in an oven at 100°C for 24 hours. Repeat this procedure until it comes to the 100 percent dry condition. After that samples were placed into the water for 24 hours to find weight in saturated surface dry (SSD) condition. Then, submerge weight of mortar samples was calculated. By using these weights, water absorption, density and percentage air voids of mortar mixes were calculated with following equations:

$$W = \frac{(B-A)}{A} * 100 \dots\dots\dots (4)$$

$$\rho_{dry} = \frac{A}{B-C} \dots\dots\dots (5)$$

$$\rho_a = \frac{A}{A-C} \dots\dots\dots (6)$$

$$\% \text{ Air voids} = \frac{\rho_a - \rho_{dry}}{\rho_a} \dots\dots\dots (7)$$

Here:

“W”: water absorption (%)

“A”: Dry weight of samples (in gm)

“B”: Weight in SSD condition (in gm)

“C”: Weight of samples in water (gm)

“ ρ_{dry} ”: Dry density (gm/cc); and

“ ρ_a ”: Apparent density (gm/cc);

3.5.6 Adhesive Strength Test

Adhesion of each mix with brick was evaluated using Pull off test. The test was conducted as per (EN 1015-12, 2000). Each mix sample was replicated with three specimens. The mortar was plastered on the brick surface with a depth of 10 mm. Samples were left to air dry for 24 hours after which samples were sealed in an airtight plastic bag for seven days at room temperature. After this, the specimens were removed and placed in controlled temperature (20±2°C) with constant relative

humidity (55±5) for 21 days. At the time of testing a circular groove having diameter of 50 mm diameter prepared on plastered surface shown in Figure 3.12, and then glued a metal bit on circular groove using adhesive. Then samples were left for 48 hours to set adhesive between groove and metal bit. After 48 hours samples were tested for their adhesive strength using following expression:

$$\text{Adhesive Strength (MPa)} = \frac{F(N)}{A(\text{mm}^2)} \dots\dots\dots (8)$$

Here:

“F” is the maximum load at failure

“A” is the cross-section area of groove



Figure 3.12 Adhesive Strength of Mortar with Clay Bricks

3.5.7 Tensile Bond Strength

Tensile bond strength test was preceded as per (ASTM C952-02, 2003). It was determined using crossed-brick couplets method. In this method, two bricks were joint perpendicular to each other by mortar mix of size 92×92 mm with a depth of 13 mm. These specimens were compacted by using a standard wooden hammer having weight

of 900 gm. Similar to adhesive strength, specimens were initially kept in an airtight polybag for 7 days and then transferred into the control environment chamber for the remaining 21 days. The whole set-up of the test assembly as shown in Figure 3.13, and tensile bond strength was calculated by using following equation:

$$\text{Tensile Bond Strength (MPa)} = \frac{F(N)}{A (mm^2)} \dots\dots\dots (9)$$

Here:

“F” is the maximum load at failure

“A” is the cross-section area



Figure 3.13 Bond Strength Test Setup

3.5.8 Drying Shrinkage

This test was performed on mortar shrinkage bar, prepared by using shrinkage mould of inner dimensions 25mm×25mm×285mm as prescribed in (ASTM C1148-92, 2014). For each mix, five samples were prepared and allowed to moist curing by covering wet jute bags for two days. After demoulding, samples were again moist cured for one day, and then placed in control environment chamber with first measurement. From the first measurement, shrinkage of mortars was calculated after every 7 days up to 28 days and then after every 15 days, until the variations in the length were observed constant.



Figure 3.14 Drying Shrinkage Measurement for Mortar Samples

3.5.9 Morphology

Surface morphology was used to get the in-depth perspective of interface characteristics of Kota stone waste with conventional materials. JSM 7400 F scanning electron microscope as shown in Figure 3.15 was used to carry this study, operated in secondary electron mode.



Figure 3.15 Image of JSM 7400 F Scanning Electron Microscope

For this, thin 5 mm square (10 mm x 10 mm) polished mortar specimens were placed inside the SEM. A beam of primary electrons was focused on the specimen, resulting in the transfer of energy to the specimen and formation of secondary electrons. These secondary electrons were attracted and collected by the detector or biased grid, translated into a signal which was then amplified, analyzed, and converted into the topographical image for examination.

3.5.10 Fourier Transform Infrared Spectroscopy (FTIR) Analysis

FTIR analysis was used, to assess potential change in molecule bonds and properties upon addition of Kota stone waste in mortar mixes. For this study, a thin film prepared with mortar powder and potassium bromide (K-Br) was used for spectrum analysis. Different bond groups with corresponding wavenumbers in samples were identified by the peaks corresponding to the Si (Silica) Al (Alumina), S (Quartz), C (Calcium) and OH (Water molecules) bond.



Figure 3.16 Image of Fourier Transform Infrared Spectroscopy

3.5.11 X-ray Diffraction Analysis (XRD)

Presence of crystalline substances in mortar matrix was identified by X-ray diffraction (XRD) analysis. XRD test was performed using PANalytical X pert PRO diffractometer as shown in Figure 3.17 with scanning range between 5° to 90°; obtained XRD pattern was analyzed by using X'Pert high score plus and Origin Pro-8 software.



Figure 3.17 PANalytical X pert PRO Diffractometer

3.5.12 Mercury Intrusion Porosimetry Test (MIP)

The porosity of the mortar mixes was evaluated by Mercury Intrusion Porosimetry test (MIP) using Pore Master - 60 GT machine. This test work on the principle that percolation of mercury into the void of mortar mixes can only be possible upon action of an external force. Hence, higher the pore size, lesser is the pressure requirement and vice versa (Kalla et al., 2015). Washburn equation and pressure versus intrusion data were used to evaluate size and volume of pores.



Figure 3.18 Mercury Intrusion Porosimetry Machine (Pore Master - 60 GT)

3.5.13 Thermal Gravimetric Analysis (TGA)

This technique was used to analyze the rate of mass change (a function of time and temperature) in controlled atmosphere conditions. For present study prepared samples were placed into a Simultaneous Thermal Analyzer 6000 in a nitrogen environment with the continuously increasing temperature at the rate of 10°C/min. The temperature range was taken between 30°C to 900°C.



Figure 3.19 Simultaneous Thermal Analyzer 6000

3.5.14 Acid Attack Test

Acid resistance test on mortar mixes was performed according to (ASTM C 267, 2001). To perform this test, 5% sulfuric acid (H₂SO₄; 1N) solution prepared using distilled water. Then 28 days cured 70 mm and 50 mm mortar cubes (three of each mix) were dipped in to the sulfuric acid solution. Before this, oven dry weight of 70 mm cube samples was noted. The effect of sulfuric acid on mortar samples was determined in terms of change in weight and change in compressive strength at the end of 1, 7, 14, 28, and 90 days. After every observation solution was renewed. Calculation of compressive strength was according to expression 1, and variation in weight was calculated by following expressions:

$$\text{Change in compressive strength (\%)} = \left(\frac{F_c - F_{ab}}{F_c} \right) * 100 \dots \dots \dots (10)$$

$$\text{Change in weight (\%)} = \left(\frac{W_a - W_{ab}}{W_a} \right) * 100 \dots \dots \dots (11)$$

Here:

“Fc” is the compressive strength of mortar sample after 28 days curing

“Fab” is the compressive strength of acid exposed mortar sample at particular day of testing

“Wa” is the oven dry weight of mortar sample after 28 days curing

“Wab” is the weight of acid exposed mortar sample at particular day of testing

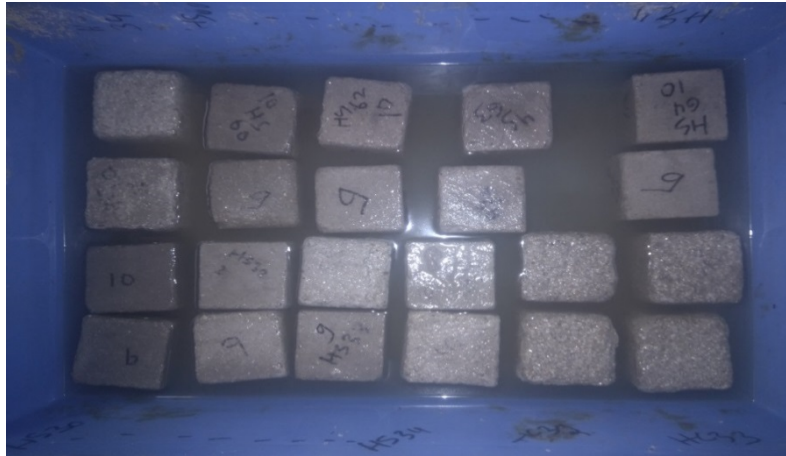


Figure 3.20 Mortar Samples Exposed to Acid Solution

3.5.15 Sulphate Attack Test

This test was followed as in accordance to (ASTM C267, 2001). For this, sulphate solution was prepared using 5 % (by weight of water) sodium sulphate (Na_2SO_4) stirred in to distilled water. As similar to acid resistance test, 50 mm and 70 mm cube three of each mix were immersed in to prepared solution. Effect of sulphate was determined by observing the variation in compressive strength and weight of the mortar mixes after the end of 1, 7, 14, 28, 90 and 180 days. At the day of observation solution was renewed. Variation in mortar samples due to exposed in to sulphate solution was calculated by using an expression as follows:

$$\text{Change in compressive strength (\%)} = \left(\frac{F_c - F_{sb}}{F_c} \right) * 100 \dots \dots \dots (12)$$

$$\text{Change in weight (\%)} = \left(\frac{W_a - W_{sb}}{W_a} \right) * 100 \dots \dots \dots (13)$$

Here:

“Fc” is the compressive strength of mortar sample after 28 days curing

“Fsb” is the compressive strength of sulphate exposed mortar sample at particular day of testing

“Wa” is the oven dry weight of mortar sample after 28 days curing

“Wsb” is the weight of sulphate exposed mortar sample at particular day of testing



Figure 3.21 Mortar Samples Exposed to Sulphate Solution

3.5.16 Fire Resistance Test

Damage of mortar during fire action was evaluated by exposing fire on mortar samples. For this, 50 and 70mm mortar samples three of each mix, used to fire exposed into the fire furnace as shown in Figure 3.22 at 200, 400, 600, and 800 °C. The rate of fire exposed on mortar samples was followed according to standard fire curve stipulated by ISO 834. After the fire exposure at a particular temperature, compressive strength and weight of the samples were determined. Then variation in compressive strength and weight in particular fire temperature was calculated using expression:

$$\text{Change in compressive strength (\%)} = \left(\frac{Ca - Ct}{Fa} \right) * 100 \dots \dots \dots (14)$$

$$\text{Change in weight (\%)} = \left(\frac{Wa - Wt}{Wa} \right) * 100 \dots \dots \dots (15)$$

Here:

“Ca” is the compressive strength of mortar sample after 28 days curing

“Ct” is the compressive strength of fire exposed sample at a particular temperature

“Wa” is the oven dry weight of mortar sample after 28 days curing

“Wsb” is the weight of fire exposed mortar sample at a particular temperature

“t” is the temperature (200, 400, 600 and 800 °C) on which fire exposed



Figure 3.22 Fire Furnace Apparatus

3.5.17 Carbonation Test

Carbonation test was performed on mortar samples of size of 40x40x160 mm as per specifications given by (RILEM CPC 18, 1988). Sample preparation method for the test was similar as adopted for chloride ion penetration test. Prepared samples were placed in to carbonation chamber shown in Figure 3.23 with constant relative humidity about 50% and carbon dioxide concentration of about 5%. Penetration of carbon dioxide in to mortar samples was evaluated in terms of carbonation depth (mm), which was calculated by spraying phenolphthalein solution on split mortar samples. In split samples, colour less portion from the edge (Figure 3.24) indicates carbonation of cement hydrated product due to the concentration of carbon dioxide. Remaining colourful area represented as free from carbonation.

3.5.18 Chloride Ion Penetration Test

This test was performed on 28 days water cured beam samples of size 40x40x160 mm. Before testing, they were placed in to oven at $60\pm 5^{\circ}$ C for 24 hours. Then samples were coated with epoxy paint on five sides. One surface of size 40x40mm was uncoated to allow for penetration of chloride ion into the mortar samples. After that samples were immersed in to 1% sodium chloride solution and then rate of chloride ion penetration was observed in terms of depth of chloride ion penetration in mm. On the day of testing, samples were longitudinally split up from the middle and then 0.1 M silver nitrate (AgNO_3) solution sprayed on split mortar samples. The depth of chloride ion penetration was measured by measuring white colour depth (Figure 3.25) which was appeared by penetration of chloride ions.

Remaining from white colour area in the split sample was noted as free from chloride ions. This process was followed for every observation at 1, 7, 14, 28, 56 and 90 days.



Figure 3.23 Carbonation Chamber

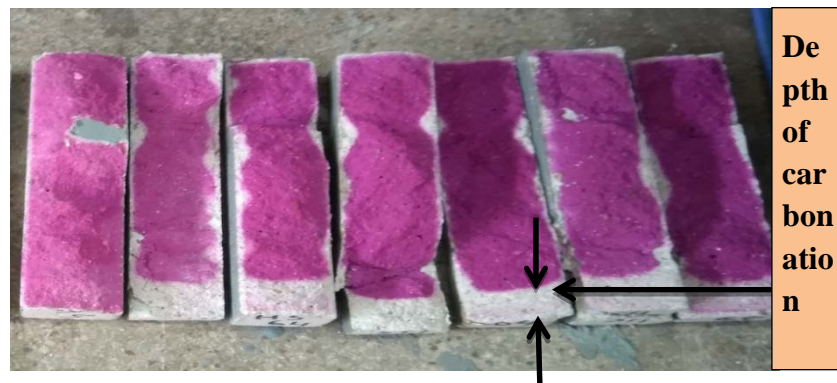


Figure 3.24 Depth of Carbonation

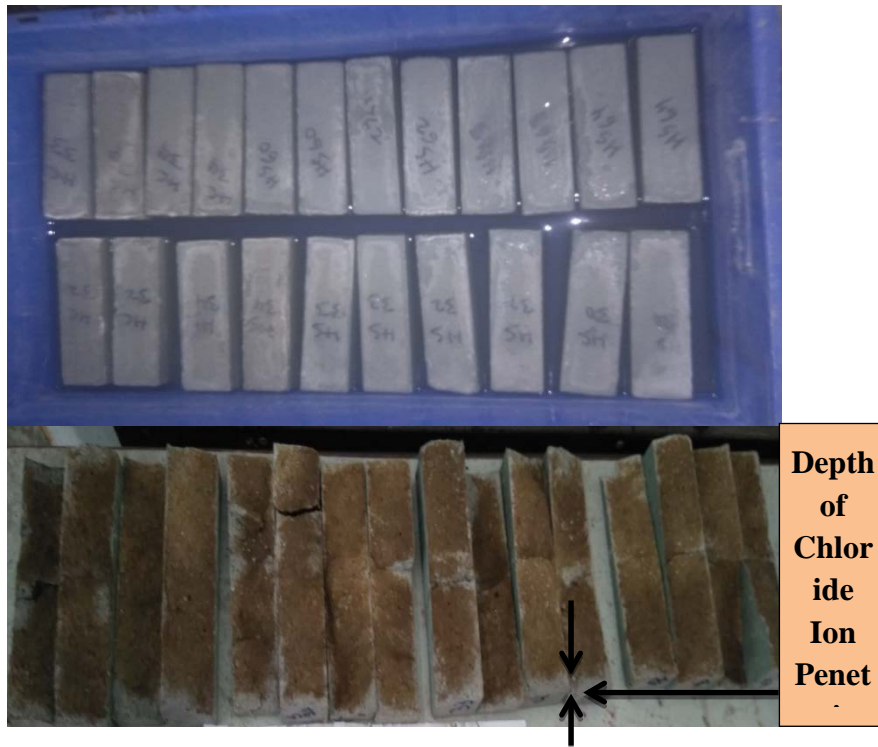


Figure 3.25 Depth of Chloride Ion Penetration

3.5.19 Wetting and Drying Cycle Test

Wetting and drying cycle test was performed in accordance with (BS EN 14066, 2013). For this, cube and beam samples were first oven dry for 24 hours at $110 \pm 5^\circ\text{C}$ temperature, then initial weight of samples noted. After that samples were immersed into the distilled water at 20°C temperature for 6 hours then shifted to the oven at 70°C for 18 hours. At that time one wetting and drying cycle completed. For preceding next cycle, samples from oven were immediately immersed in to distilled water then continued above process till the end of 20 cycles. Effect of wetting and drying cycle was observed in terms of physical appearance and change in weight.

$$\text{Change in weight (\%)} = \left(\frac{W_a - W_{wb}}{W_a} \right) * 100 \dots\dots\dots (16)$$

Here:

“ W_a ” is the oven dry weight of mortar sample after 28 days curing

“ W_{wb} ” is the weight of mortar sample after completion of 20 wetting and dry cycles

CHAPTER 4

RESULTS AND DISCUSSIONS

4.1 General

Various properties of mortar mix (listed in Table 3.5) containing Kotastone slurry (KSS) and Kotastone crushed sand (KSCS) were evaluated according to their standards. Results obtained from the experimental investigations have been elaborated in two stages. Stage first include results of trial mortar mixes (1:4 proportion) containing KSS whereas stage two describe mechanical and durability properties of mortar mixes containing 1:3 and 1:6 proportion) KSS and KSCS.

4.2 Stage First

4.2.1 Workability

Workability of the mortar was understood by water demand of mortar to achieve specified flow (205-215 mm) for common site exercise. Figure 4.1 presents the change in the water-cement ratio on the inclusion of KSS. The test result shows that 30% replacement of conventional river sand with KSS reduced water-cement ratio of mixes which means that incorporation of KSS (up to 30 %) gives same workability as control mix with less amount of water. This fall in water demand was attributed to the filler effect since the gaps between sand particles, now filled by KSS which is previously filled by water. Therefore, available water was used more efficiently to lubricate the mortar paste and hydrate the cement. Further at 40% replacement level water-cement ratio of mortar was same as control mortar. Replacement beyond 40% leads to an overall increase in surface area of the paste that may be result in to increased water demand to achieve desired flow (205-215 mm).

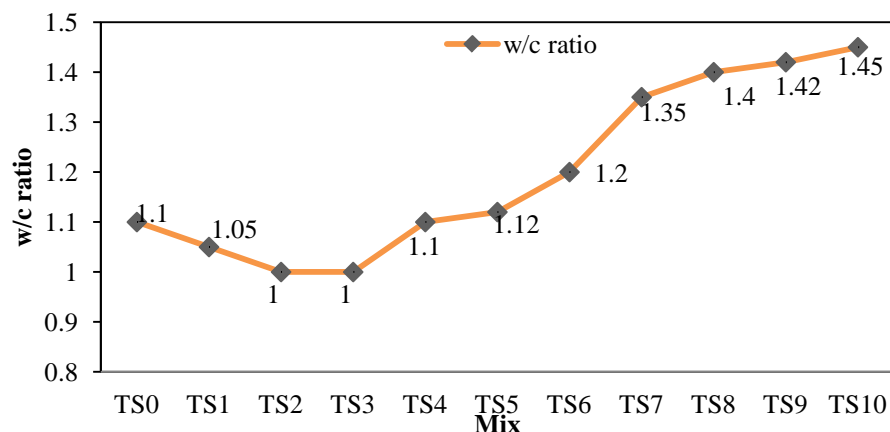


Figure 4.1 Variations in Water to Cement Ratio with KSS

4.2.2 Water Absorption and Density

Results of water absorption, bulk density, and apparent density tests were presented in Figure 4.2-4.3. An increase in water absorption with an increase in KSS replacement was observed. For TS10 mix, water absorption was found 23.11% which is 13.4% more than that of control mix.

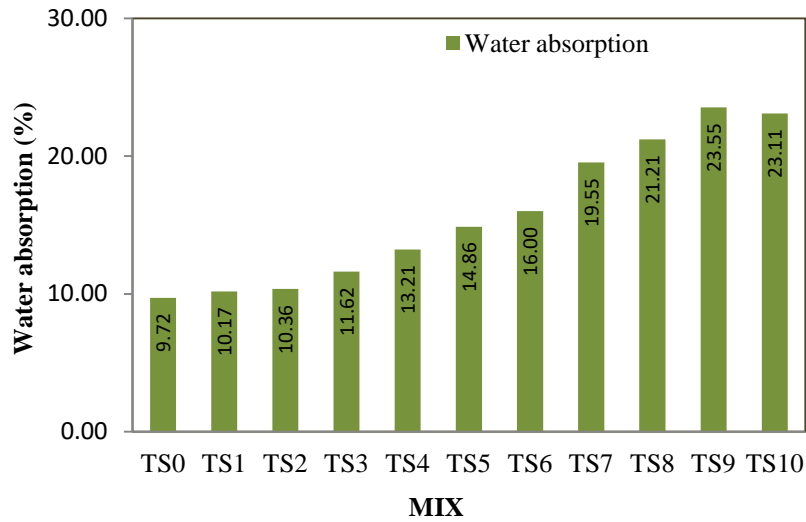


Figure 4.2 Water Absorption of Mortar Mixes

Inclusion of slurry improved dry bulk density of mortar mixes up to 30% replacement level, this improvement could be due to the low water-cement ratio of the mixes. At higher replacement, a declining pattern was observed. Increase in proportion of KSS as river sand resulted in to increase in apparent density, with maximum value at TS4 mix.

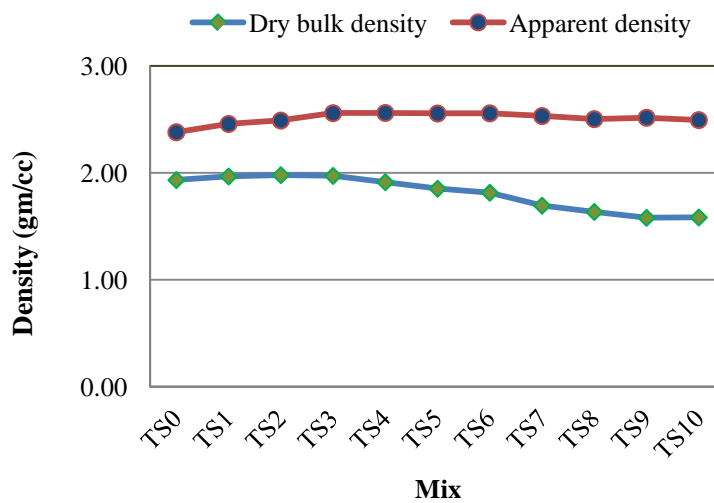


Figure 4.3 Dry Density and Apparent Density of Mortar Mixes

4.2.3 Porosity by Mercury Intrusion Porosimetry (MIP)

Figure 4.4 presents the MIP results. The porosity of mortar mixes increased with increase in KSS replacement. Up to 40 % replacement, results were comparable to control sample. However further substitution of KSS resulted in to high porosity in mortar mixes, indicating reduction in packing efficiency due to more fine particles.

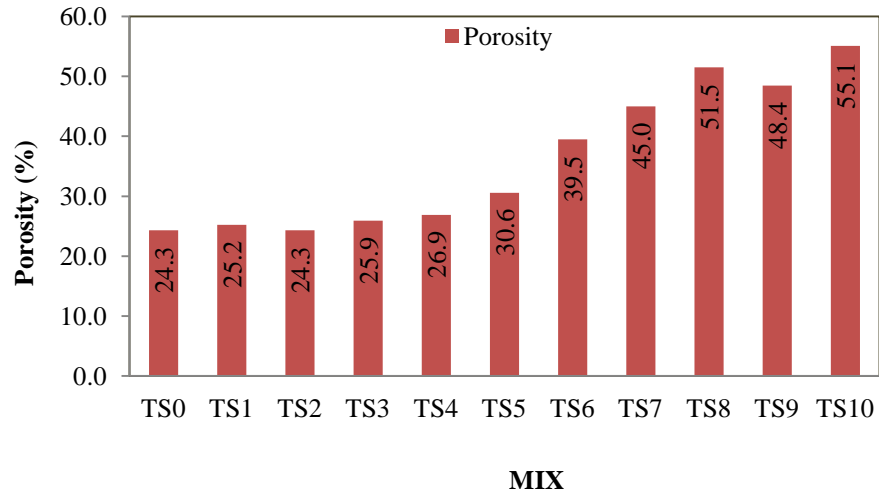


Figure 4.4 Porosity of Mortar Mixes

The differential intrusion peak of selected samples TS0, TS3, TS4, TS5, and TS10 are shown in Figure 4.5. For Mix TS0, this peak was slightly sharp indicating the discontinuous pore structure of the mix. However, low peaks were observed for mixes with KSS as a set of crooked peaks which indicate interconnected pores and weak micro-structure of the samples.

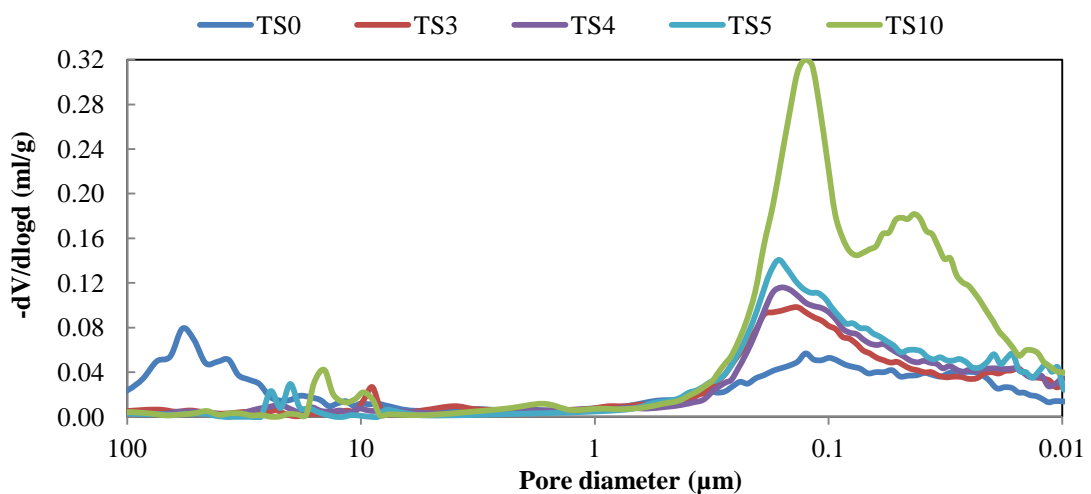


Figure 4.5 Graph for Mercury Intrusion rate versus Pore Size

4.2.4 Compressive and Flexural Strength

The effect of KSS on the compressive and flexural strength of mortar mixes at 7 and 28 days are shown in Figure 4.6 and Figure 4.7, respectively. Overall, an incremental trend was observed with increase in the proportion of KSS in mixes. The maximum compressive strength at 7 and 28 days was observed for TS4 mix that is 6.88 and 9.21 MPa respectively. Similarly, for flexural strength, it was observed maximum for TS5 mix (2.50 and 4.10 MPa at 7 and 28 days respectively). However, flexure strength was reduced after 50% replacement whereas compressive strength of mix TS10 mix was comparable to that of control mix (TS0). This increase in strength was attributed to filling of voids by fine slurry particles and reduced water-cement ratio of mixes resulting in to an overall dense and compact structure (Farinha et al., 2015).

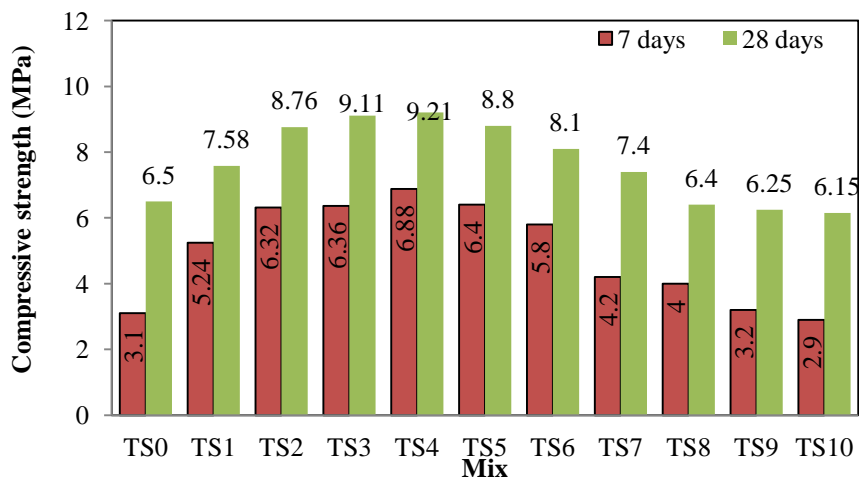


Figure 4.6 Compressive Strength of Mortar Mixes at 7 and 28 Days

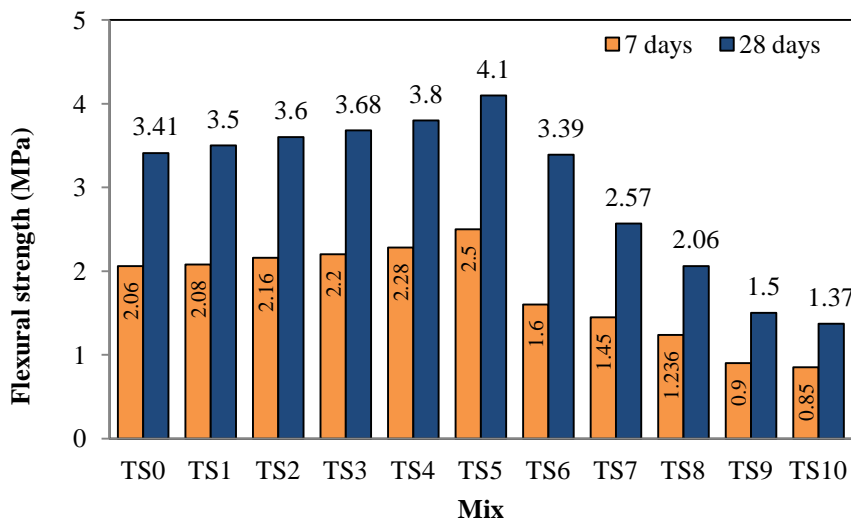


Figure 4.7 Flexural Strength of Mortar Mixes at 7 and 28 Days

4.2.5 Ultrasonic Pulse Velocity and Dynamic Modulus of Elasticity

UPV test is used to observe denseness of the mix. The plotted graph in Figure 4.8 shows that the ultrasonic pulse velocity is maximum for 40% substitution indicating well compacted and dense structure. This is because as the quantity of KSS increases up to 40%, the overall gradation of the mixture improved. Beyond 40% replacement, slurry particles improved the non-uniformity of mix, making it porous. These voids lead to reduction in the pulse velocity.

In Figure 4.8, dynamic modulus of elasticity was also observed to be higher than control mix up to 40% replacement; with a maximum value observed for TS3 mix. At this replacement, the increment in dynamic modulus of elasticity was observed around 7.9%. Replacement beyond 40%, gave detrimental trend which could be attributed to increase in water-cement ratio resulting in to poor compaction and cracks in the structure.

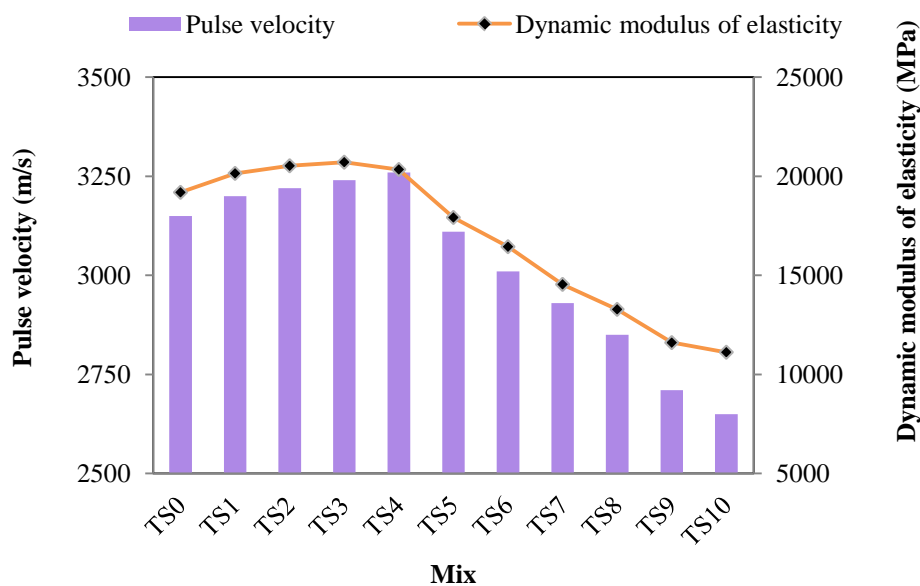


Figure 4.8 Ultra Pulse Velocity and Dynamic Modulus of Elasticity of Mortar Mixes

4.2.6 Morphology

The ettringite, calcium silicate hydrates (C-S-H), and the pores present in the microstructure were mainly studied in SEM analysis. SEM analysis was carried out on TS0 (control), TS3, TS4, TS5, and TS10 mortar mixes, presented in Figures 4.9-4.13 respectively. In the images dark portions are voids; Ca(OH)_2 or (CH) appears in large crystals as hexagonal prisms; small rubbery crystals indicate C-S-H gel/paste, and

large whisker-like particles denote ettringite (Singh et al., 2015; Yilmaz and Olgun, 2008). A significant amount of CH, C-S-H and voids were observed in KSS containing mortars. As the replacement level increases, more packed structure with dense C-S-H formation results in to strength enhancement. However, at a higher replacement level, internal cracks were also seen in Figure. 4.13, which indicates deterioration in performance of mortar mixes containing 100% KSS.

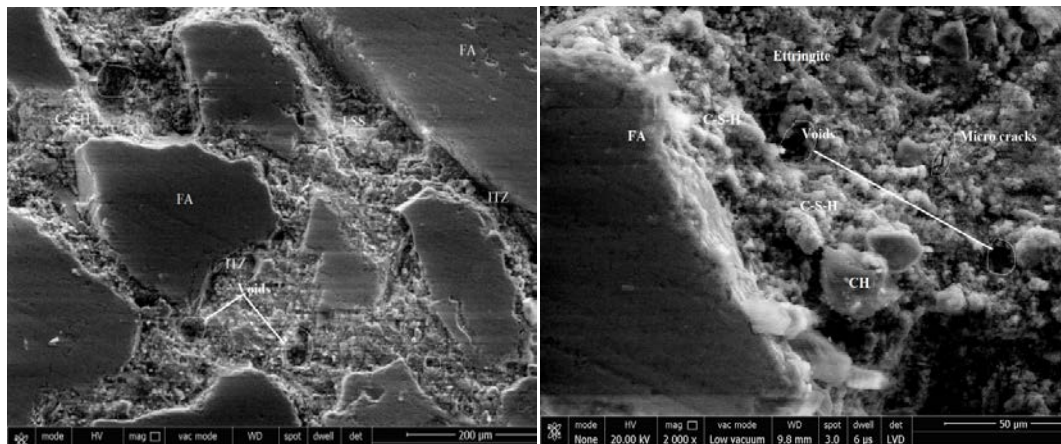


Figure 4.9 SEM images of Mortar Mix TS0

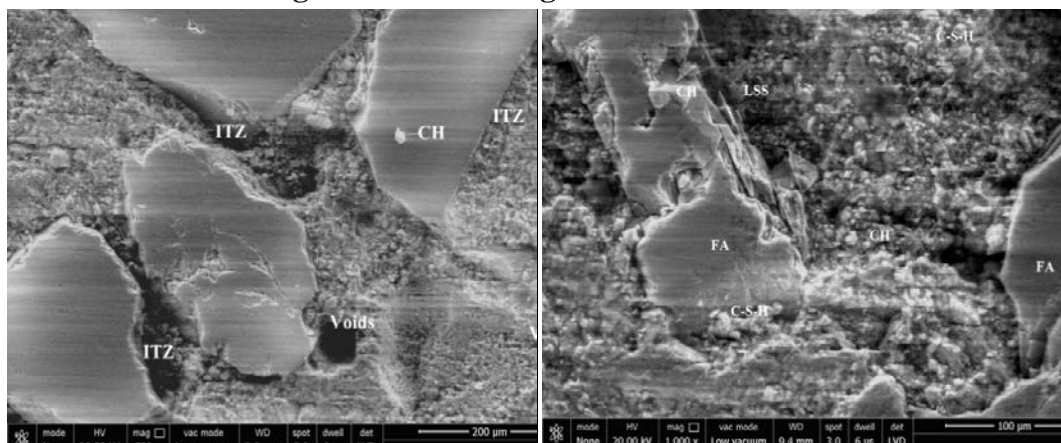


Figure 4.10 SEM images of Mortar mix TS3

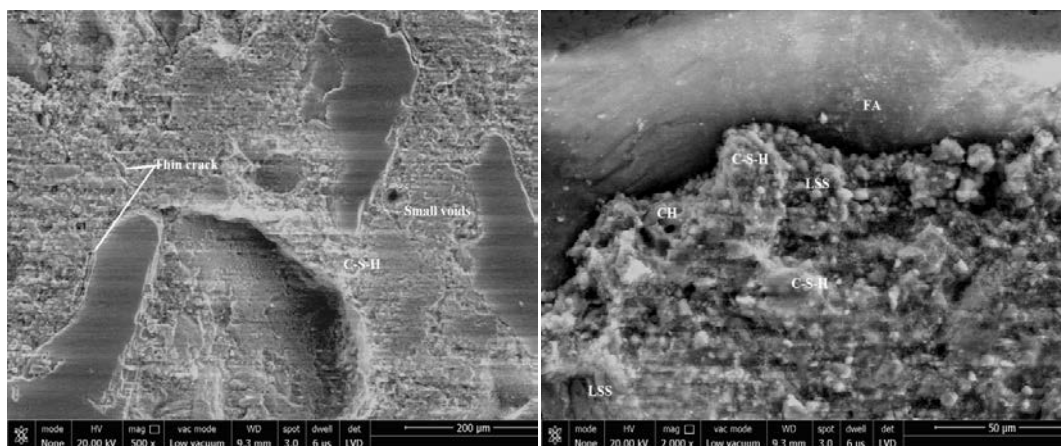


Figure 4.11 SEM images of Mortar Mix TS4

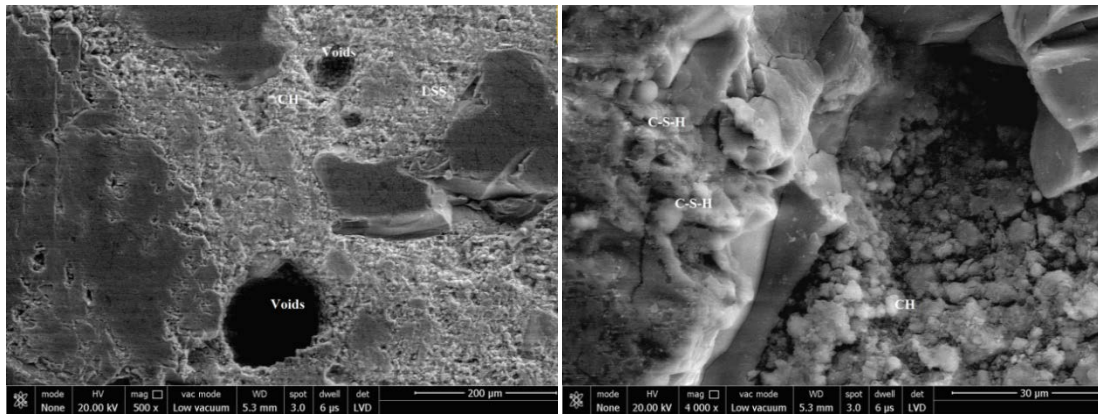


Figure 4.12 SEM images of Mortar Mix TS5

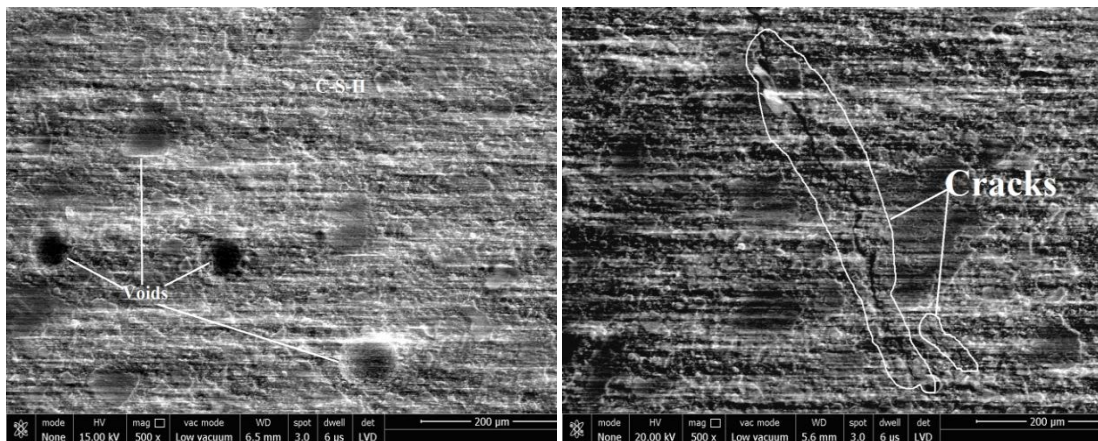


Figure 4.13 SEM images of Mortar Mix TS10

4.2.7 Thermogravimetric Analysis (TGA)

Mortar samples TS0, TS3, TS4, TS5, and TS10 were investigated through their TGA curve to analyze change in weight during thermal exposure, shown in Figure 4.14. Weight loss of the mixes has been worked out by dividing the curve into four temperature regions. In the first region of the range between 30°C to 300°C, the trend of the curve was the same for all the mixes, which show a gradual decrement in weight indicating moisture evaporation. Curves TS3, TS4, TS5, and TS10 were slightly down compared to the control mix (TS0), due to the greater water absorption capacity of KSS than river sand. Additionally, this loss in water was due to hydration of cement, mainly C-S-H gel, which tends to increase with KSS content in mortar mixes. A similar trend was seen in the second region (300°C to 450°C), where a gradual loss in weight was observed, it was 4% for the control mix and 5 to 6 % for TS3, TS4, TS5 and TS10 mixes. This fall in weight was attributed to dihydroxylation of $\text{Ca}(\text{OH})_2$. Similarly, in the third region between 450°C to 600°C, a constant drop in the curve was observed, which indicate weight loss to about 5% for the control mix

and 6 to 7.5% for TS3, TS4, TS5 and TS10 mixes. This loss in weight indicates beginning of phase transition or decomposition of calcite into CaO. Finally, in the last region between 600°C, to 800°C a sudden drop in the curve was observed. Here the weight loss was 6.5%, 14.5%, 16.5%, 19% and 31% for control, TS3, TS4, TS5 and TS10 respectively, due to the decomposition of CaCO_3 into calcium oxide and release of CO_2 . Beyond 800°C, the weight remained constant.

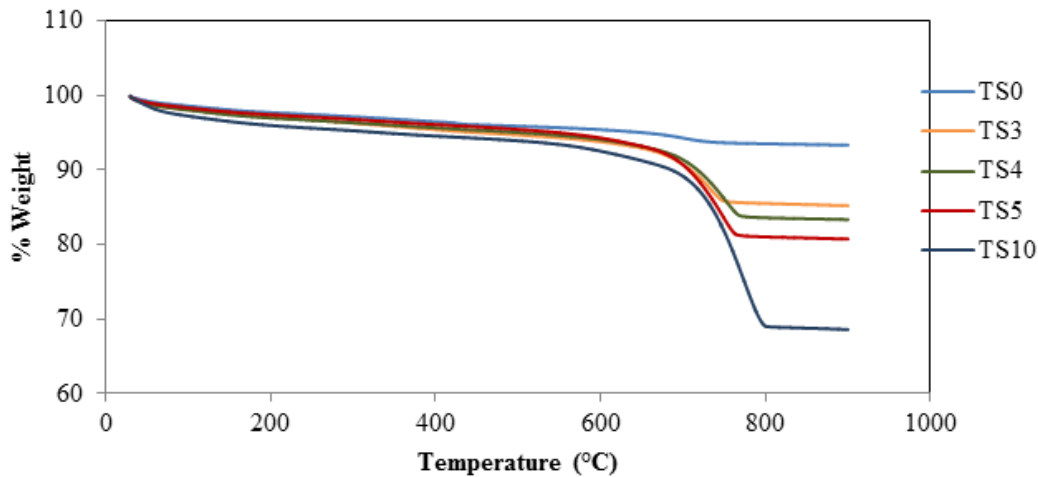


Figure 4.14 TGA Curves for Mortar Mixes G0, G3, G4, G5, and G10

4.2.8 Summary

First stage test results reveal that the mortar mixes containing up to 40% KSS were observed with reduced water-cement ratio and improved workability. Also, compressive and flexural strength of mortar mixes were found improved with increasing of KSS. Compressive strength was observed maximum at 40% replacement level, whereas flexural strength was found maximum at 50% replacement of river sand. Water absorption and porosity of mortar mixes found increasing with the increase in KSS this was attributed to higher water holding capacity of KSS compared to river sand. However at 20% and 40% substitution, water absorption and porosity were comparable to that of the control mix. The microstructure of mortar mixes containing 40% KSS showed a homogeneous and well compact internal structure resulting in to superior strength of the mix. These results indicated that the addition of Kota stone slurry as river sand replacement has positive impact on mortar strength properties. Also, it encouraging for detailed investigation on most commonly used mortar proportions 1:3 and 1:6 on the basis of mechanical and durability.

4.3 Stage Second

4.3.1 Workability

Figure 4.15 presents the variation in the water-cement ratio on the addition of KSS and KSCS. It was seen that water-cement ratio of mixes reduced with the increase in replacement level. Decrease in water-cement ratio was observed up to 40% sand replacement in series A, whereas for series B, C and D it was reduced at each replacement level as compared to their respective control mortar. The minimum water-cement ratio was found at 20% substitution of river sand with KSS for series A and C, this was 7.8% and 19.4% less compared to their control mix. However, for series B and D, the minimum water-cement ratio was observed at highest replacement of river sand with KSCS, this was 3.3% and 2.9% less than their respective control mix. This indicates that mixes containing KSS and KSCS give similar workability as control mortar with lower water demand. The fall in water demand may be attributed to filler effect created by KSS and KSCS. The voids between sand particles which were earlier occupied by water, now replaced by KSS and KSCS in their respective mixes. This resulted in higher water availability for lubrication of particles and hydration of cement. Additionally, thixotropic nature of slurry particles may be responsible for this behavior resulting less energy required to achieve desired flow of the mortar compared to control mix (Bederina et al., 2013; Khyaliya et al., 2017).

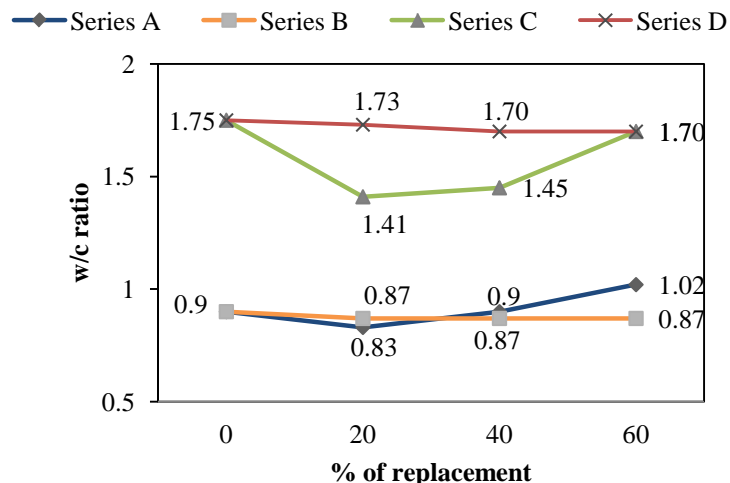


Figure 4.15 Water-cement ratio v/s % Replacement of KSS/KSCS for series A, B, C and D

Gradation of material in Figure 3.2 shows that KSS has more fine particles compared to the KSCS, due to this, above effect is more significant in series A and C

than series B and D. In series A, beyond 40% substitution of river sand with KSS, water cement ratio observed 11.8% (AS60) more than control mortar. This behaviour can be attributed to increase in surface area of the paste resulting in an overall increased water demand to achieve desired flow (205-215 mm). Previous studies also report increased water demand due to a higher specific surface area of limestone slurry as compared to river sand (Haach et al., 2011).

4.3.2 Compressive and Flexural Strength

The results obtained from compressive and flexural strength tests are graphically presented in Figures 4.16 and 4.17, respectively. Figure 4.16 shows that, compared to conventional mix, an incremental trend was observed in all mortar series with the addition of KSS and KSCS till maximum replacement. For series A and C, maximum compressive strength was observed at 20 % substitution of river sand with KSS, which was 13.13 MPa (AS20) and 6.84 MPa (CS20) respectively. This improvement in compressive strength for series A and C was observed 34.1% and 145.1% more than that of their respective control mix, whereas for series B and D highest compressive strength was observed at 40% (BS40 and DC40) substitution of sand with KSCS and it was 16.5% and 89.6% (11.4 MPa and 5.29 MPa) more as compared to their counter control (9.79 MPa and 2.79 MPa).

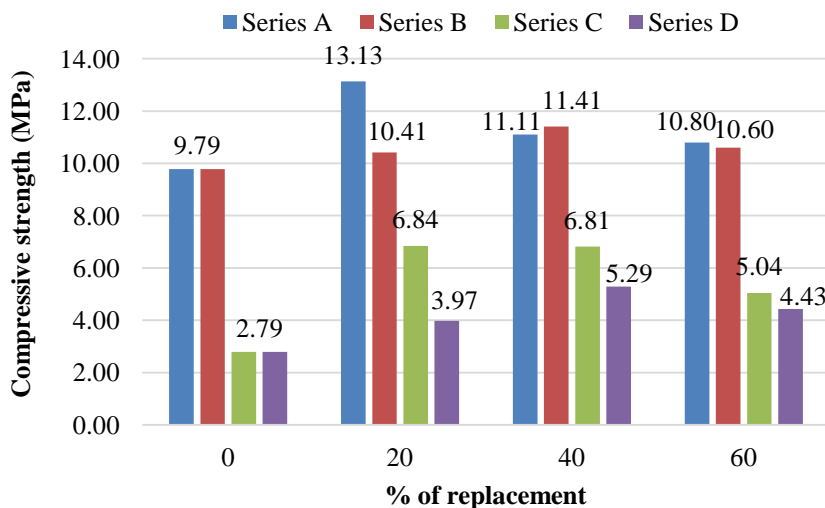


Figure 4.16 Compressive Strength of Mortar with KSS and KSCS at 28 days

Flexural strength results for series A through D are presented in Figure 4.17. It is evident from Figure 4.17 that series A, B, C and D provided increase in strength with respect to corresponding control specimens up to a replacement level of 40%,

20%, 60% and 60%, respectively. For series C and D maximum flexural strength was found at 40% substitution of river sand with KSS and KSCS, which was 1.85 MPa and 1.80 MPa respectively, whereas in series A and B, it was maximum at 20% replacement of sand that is about 3.90 MPa and 3.61 MPa, respectively.

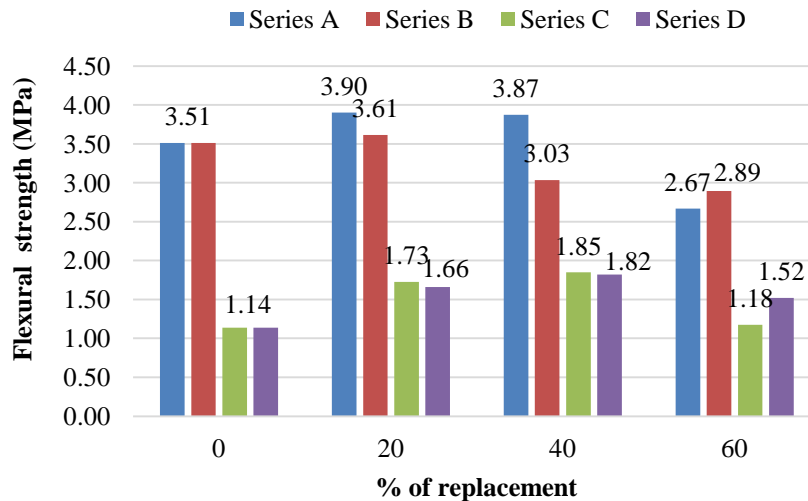


Figure 4.17 Flexural Strength of Mortar with KSS and KSCS at 28 days

Improvement in compressive strength and flexural strength was mainly due to the filling of voids by fine particles presents in KSS and KSCS, resulting in an overall dense and compact structure. Scanning electron microscope images (Figures 4.36-4.39) also justified this filler effect in mortar mix. Reduction in water-cement ratio also improves strength of the mortar mixes. However, beyond 20% replacement, flexural strength observed reducing in series B which was attributed to smooth surface with sharp edges of KSCS, resulting in weak bonding between sand particles. Also, pozzolanic reactions between lime content and cement matrix play a dominant role in strength enhancement. Similar behaviour was also reported by (Benabed et al., 2012), and (Corinaldesi et al., 2011) where loss in strength was compensated by using limestone fines.

4.3.3 Ultrasonic Pulse Velocity (UPV) and Dynamic Modulus of Elasticity (E_{dy})

UPV test was performed to evaluate the effect on denseness and compactness of mortar mixes with inclusion of KSS and KSCS. Variation in UPV of different mortar mixes has been presented in Figure 4.18.

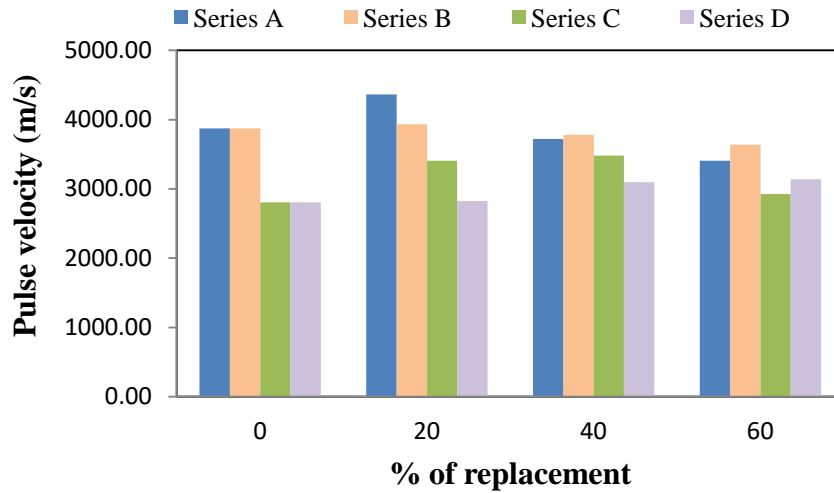


Figure 4.18 Ultra Pulse Velocity of Mortar Mixes with KSS and KSCS

It was observed that for series A and B, the value of UPV increased till 20% substitution of river sand by KSS and KSCS. Whereas for the lean mixes (C and D), it improved up to highest replacement level with a maximum of 40% substitution of sand. Maximum improvement in UPV value was observed 12.73%, 1.65%, 23.5% and 10.29% for series A, B, C and D respectively. Hence mortar with KSS and KSCS, create a denser medium for transport of ultrasonic waves than the river sand. Improvement in denseness was observed due to optimum doses of KSS and KSCS, which improves the overall gradation of the mixture. Further increase in KSS and KSCS replacement resulted in to non-uniformity of the mix, making it more porous leading towards poor compaction reduced pulse velocity.

A similar trend was observed for dynamic modulus of elasticity as shown in Figure 4.19. For series A, B, C, and D, maximum dynamic modulus of elasticity was about 27.23% (AS20), 3.38% (BC20), 55.76% (CS40) and 22.65% (DC60) more as compared to their respective control mix. The result clearly establish that mortar with KSS has more dynamic modulus of elasticity compared to mortar with KSCS, this behaviour was attributed to lower water-cement ratio (Figure 4.15) of mortar mixes containing KSS. In addition to this, modulus of elasticity may have influenced by formation of calcium carbo-aluminates results in to strong interfacial transition zones (Khyaliya et al., 2017). Fall in dynamic modulus was noticed for rich mixes (series A, B) containing KSS and KSCS beyond 20%, this could be due to the lower density of mixes, resulting in to more deformation at same stress application.

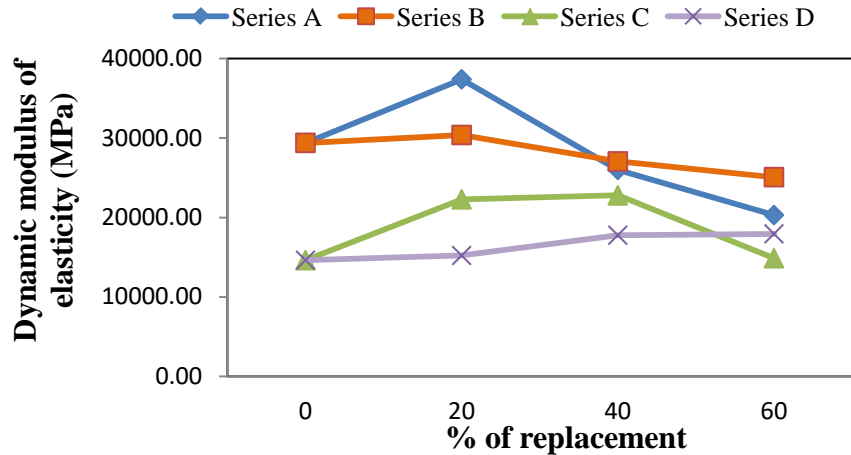


Figure 4.19 Dynamic Modulus of Elasticity of Mortar Mixes with KSS and KSCS

4.3.4 Water Absorption, Porosity and Density

Results obtained from water absorption, porosity and density were graphically presented in Figures 4.20-4.28. In Figure 4.20, improvement in water absorption for all series was observed with increase in KSS and KSCS. Maximum water absorption was found at highest replacement level (60%), which was about 107.16%, 47.63%, 75.18% and 37.5% more than that of control mixes. Reason behind improvement in water absorption was high water holding capacity and specific surface area of KSS, KSCS as compare to the river sand. Due to this phenomenon, more voids were generated in mortar mix with KSS and KSCS as seen in Figure 4.21.

Similar to water absorption maximum voids were generated at 60% replacement level. At 20% substitution of river sand voids were about 4 to 15 percent that is comparatively very less than the maximum substitution of river sand with both KSS and KSCS.

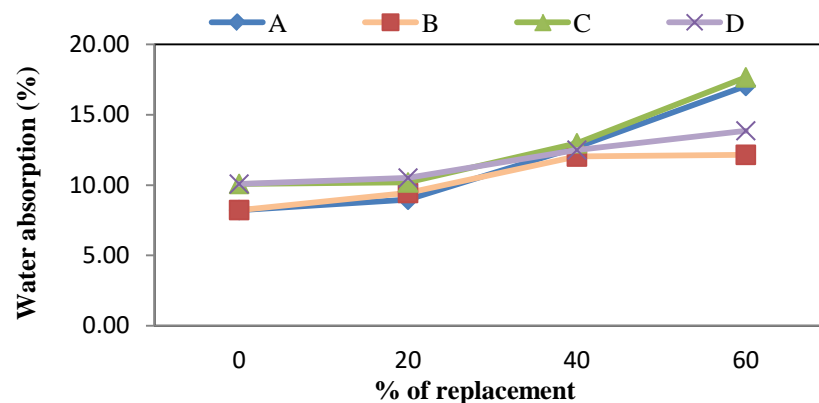


Figure 4.20 Variations in Water Absorption of Mortar Mixes with KSS and KSCS

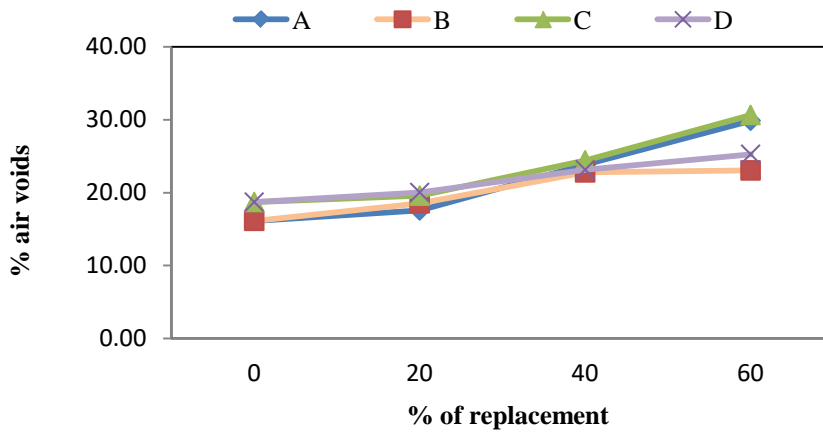


Figure 4.21 Variations in % Air voids of Mortar Mixes with KSS and KSCS

Porosity of the mortar mixes was determined through mercury intrusion porosimetry technique. This is most appropriate method to determine total pore volume of mortar matrix. For the test, samples were cured for 28 days and variation in porosity of mortar with incorporation of KSS and KSCS were presented in Figure 4.22. Similar to percentage air voids and water absorption, total porosity of rich mortar mixes of series A and B increased with inclusion of KSS and KSCS, however up to at 40% replacement level, variation in porosity was comparable to that of control mixes. In lean mixes of series C and D at 20% replacement level, porosity was observed less or equal to their control mixes. At Further replacement level, improvement in porosity observed with increase in KSS and KSCS. This could be more understood by mercury intrusion graphs presented in Figure 4.23-4.26.

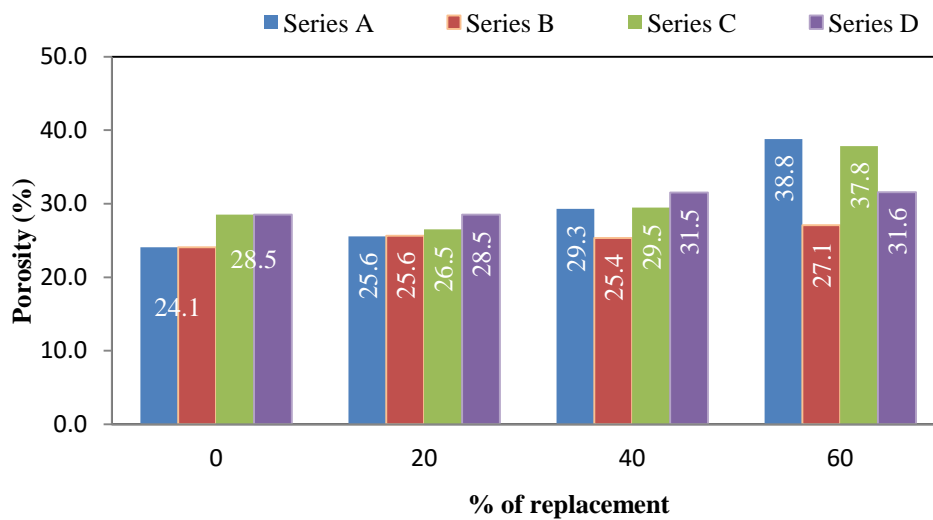


Figure 4.22 Porosity of Mortar Mixes with KSS and KSCS

In series A and B, mercury intrusion peaks in the pore size range between 0.5 to 0.02 μm were observed high in KSS and KSCS containing mortars, which indicates large number of small size pores formed by the presence of KSS and KSCS. Similar trend observed in series C and D in the pore size range between 1 to 0.035 μm . Pores of less than 1 μm were exhibited to formation of capillary pores in CSH (Ballaster et al. 2007). It was less significant as compared to large size pores present in mortar mixes. Large size pores in the range between 1 to 10 μm were observed maximum in control mixes because of poor cohesion between cement and aggregate, whereas in KSS and KSCS containing mortar has lesser pore volume due to their high cohesive nature and pore filling effect resulted into better performance against mechanical properties mortar mixes.

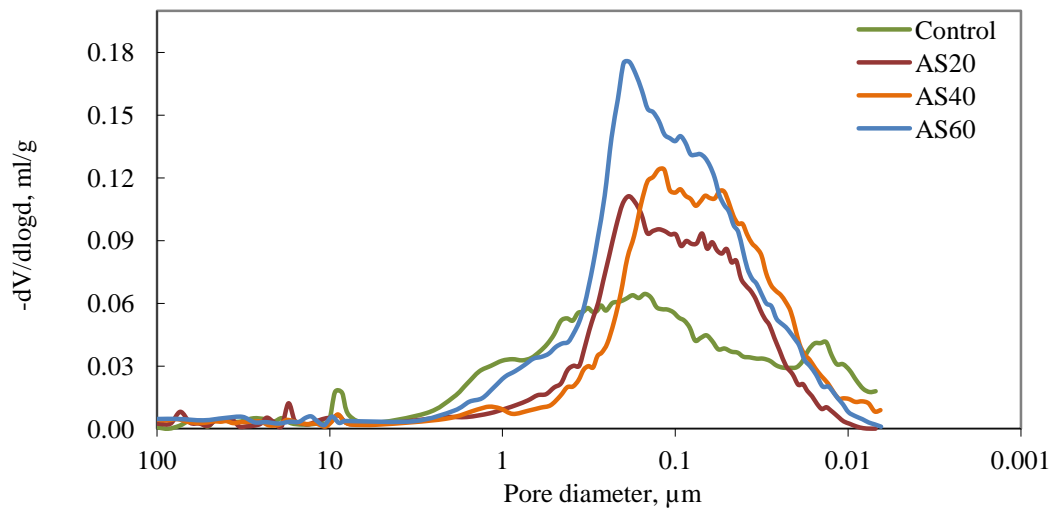


Figure 4.23 Mercury Intrusion Porosimetry Graphs for Series A

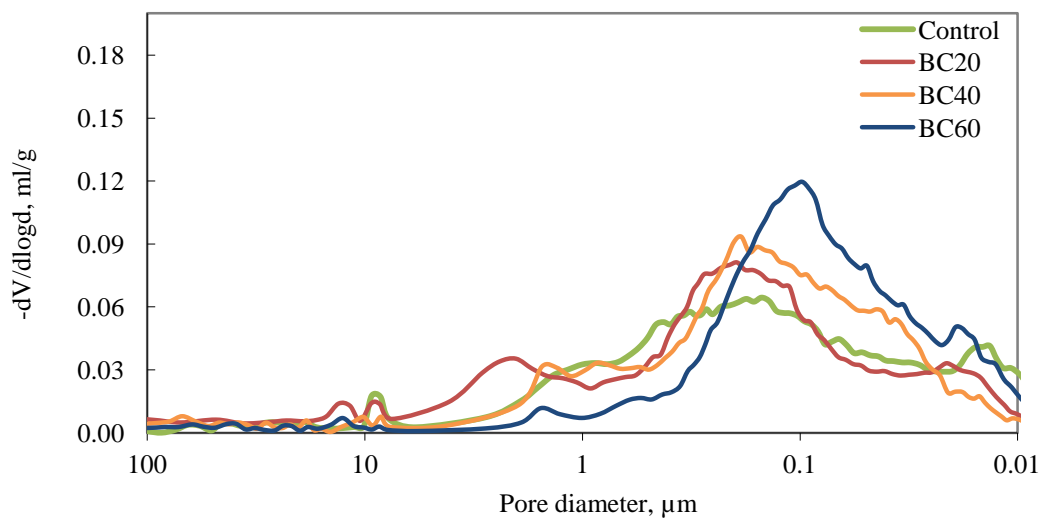


Figure 4.24 Mercury Intrusion Porosimetry Graphs for Series B

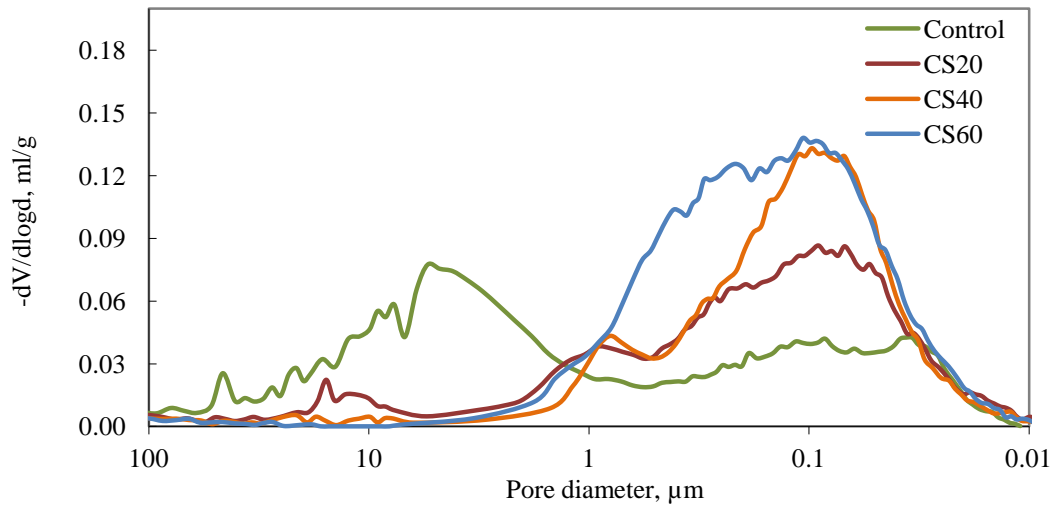


Figure 4.25 Mercury Intrusion Porosimetry Graphs for Series C

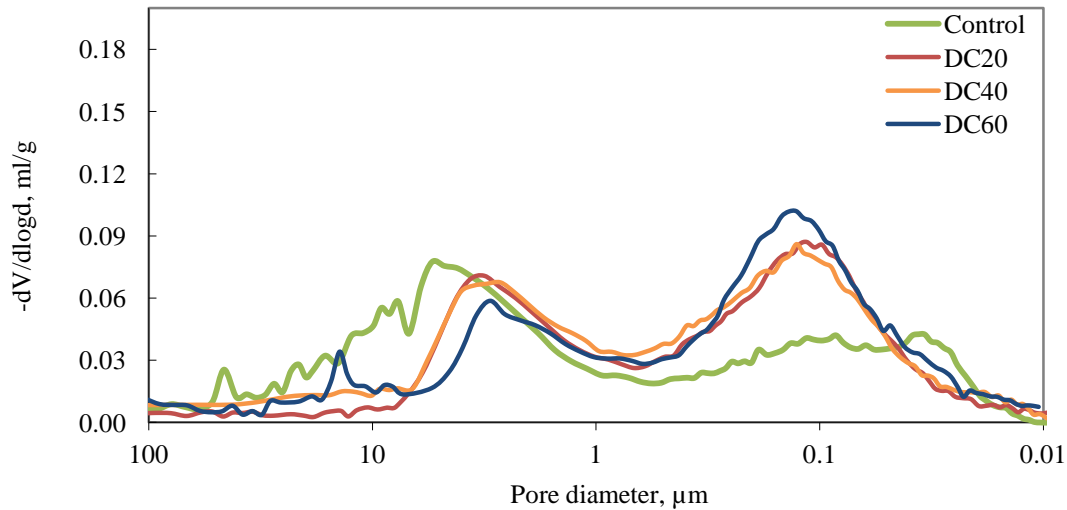


Figure 4.26 Mercury Intrusion Porosimetry Graphs for Series D

Figure 4.27 shows the addition of KSS and KSCS improved the dry bulk density of mortar mixes up to 20% replacement for all series (Except series C). This improvement can be due to the minimum water-cement ratio at this replacement level. At higher replacement, a declining pattern was observed due to high water absorption and porosity of the mixes.

Figure 4.28 shows the inclusion of KSS and KSCS as fine aggregate leads to improvement in apparent density, with maximum at highest substitution of river sand for all series. This improvement can be accredited to improvement in hydration process with KSS and KSCS resulting in higher compressive strength compared to

control mix. Earlier study by (POWERS, 1958) reported that for a given volume of cement, hydration product increases with reduction in water to cement ratio. Also results found were analogs to a study carried out by (Kabeer and Vyas, 2018) where dolomite dimensional slurry waste was used as fine aggregate to improve mortar properties.

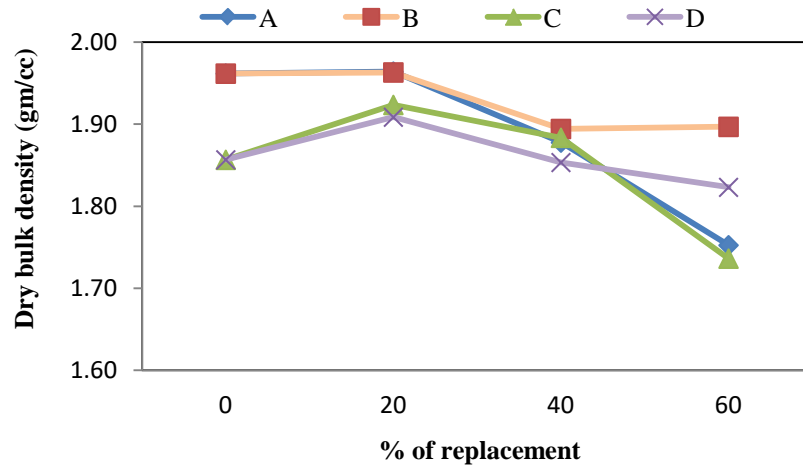


Figure 4.27 Variations in Dry bulk density of Mortar Mixes with KSS and KSCS

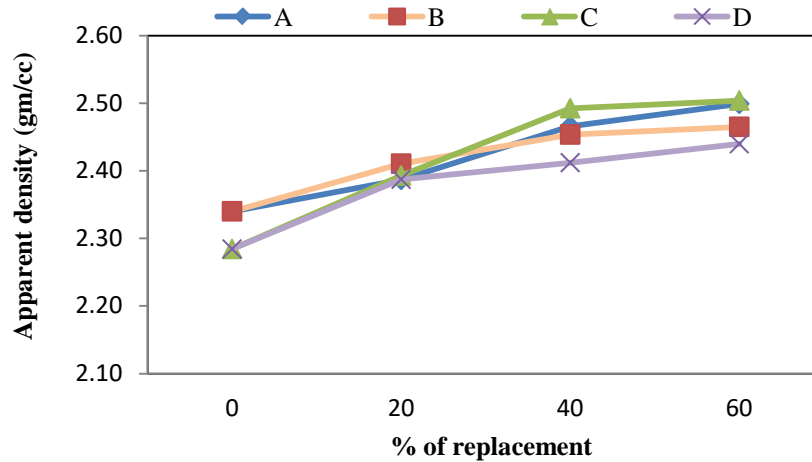


Figure 4.28 Variations in Apparent Density of Mortar Mixes with KSS and KSCS

4.3.5 Adhesive Strength

Results of adhesive strength of mortar mixes are presented in Table 4.1 and Figure 4.30. There is two types of failure pattern observed during the testing. Type 1 (T1) cracking seen in Figure 4.29, is an adhesive rupture in the interface of mortar and brick whereas type 2 (T2) cracking is a cohesive rupture of mortar itself.

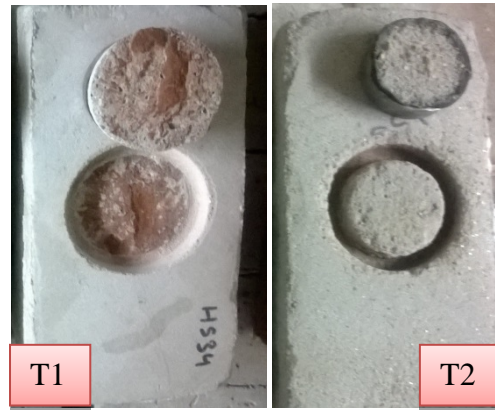


Figure 4.29 Various type of Cracking between Mortar and Bricks in Adhesive Strength Test

Table 4.1 shows the improvement in adhesive strength of mortar with incorporation of KSS and KSCS. Inclusion of KSS in both rich and lean mixes (series A&C), gives maximum adhesive strength at 40% substitution, while in mortar mixes with KSCS observed maximum strength at 20% replacement level. This improvement was around 10 to 100% as compared to control mortar. High water absorption property of KSS and KSCS compared to river sand could be one of the reason for such behavior played a significant role in the hydration reaction. For series C and D, mode of failure was T2 for control mortar which was attributed to less amount of binding material compared to series A and B. With incorporation of KSS, mode of bond rupture was changed to T1 type indicating improved hydration process of mortar matrix. Whereas in rich mixes mostly mortar mixes have adhesive rupture between the interfaces of mortar and brick layer due to the higher tensile strength of mortar (Braga et al., 2012). For series D at 60% replacement, the adhesive strength was not calculated due to the poor bonding between mortar and brick surface. Lower adhesive strength at 60% and 40% replacement for series A, B and D was attributed to more fine content introduced in mortar matrix. Similar results were also observed by (Lenart, 2013) in their studies about cement-lime mortar.

Table 4.1 Adhesive Strength of Mortar with KSS and KSCS

Substitution (%)	Adhesive strength (MPa)/(Mode of cracking)			
	Series A	Series B	Series C	Series D
0	0.29 (T1)	0.29 (T1)	0.07 (T2)	0.07 (T2)
20	0.35 (T1)	0.32 (T1)	0.13 (T1)	0.14 (T1)
40	0.37 (T1)	0.27 (T1)	0.14 (T1)	0.05 (T2)
60	0.13 (T1)	0.25 (T1)	0.11 (T2)	-

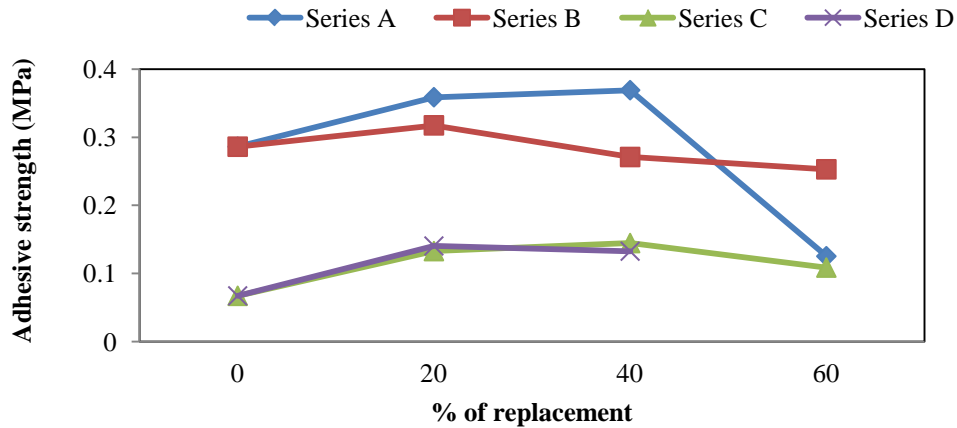


Figure 4.30 Variations in Adhesive Strength with KSS and KSCS

4.3.6 Tensile Bond Strength

The calculated tensile bond strength is graphically presented in Figure 4.31. An incremental pattern was observed for all series except series B where inclusion of KSCS resulted in declining strength. At 20% replacement, this decrement was not very significant as compared to control mix, but further replacement resulted in to considerable loss in adhesion property with respect to control mix. This behavior was attributed to irregular shape and smooth surface texture (formed due to cutting process) of KSCS particles. But for lean mixes (series D) tensile strength was not observed affected by the particle shape and surface texture as finer content in KSCS improved overall gradation resulting in well graded mixture.

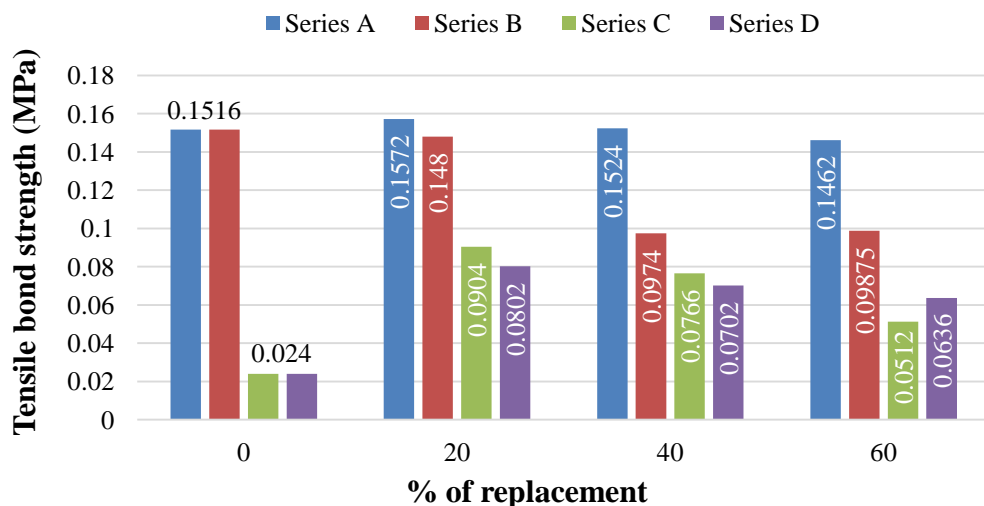


Figure 4.31 Tensile Bond Strength of Mortar containing KSS and KSCS

For series A, the tensile bond strength increased up to 40% replacement level and in series C and D, strength was more than that of control mix till maximum

replacement level. For all mixes, maximum strength was obtained at 20% replacement that is about 0.15 MPa, 0.09 MPa, and 0.08 MPa. This could be due to the low water-cement ratio of mortar mixes leading to strong bond between brick and mortar.

4.3.7 Drying Shrinkage

Drying shrinkage test is one of the important parameter to observe the ability of mortar for their practical application. This property of the mortar is mainly related to the available cement content, water content and relative humidity. Figure 4.32-4.35 presents the percentage variation in drying shrinkage of mortar with KSS and KSCS. It was noticed that drying shrinkage of mortar increases with increase in KSS and KSCS proportion. The reason behind this negative effect was improvement in fineness of the mix upon inclusion of KSS and KSCS; however, at 20% substitution level, this effect was very insignificant. At 20% substitution level water-cement ratio was lowest and almost similar to control mixes, justifies the obtained comparable drying shrinkage value. Beyond 20%, fineness becomes a dominating factor resulting in to increase in drying shrinkage. Similar to that (Bilir et al., 2015) found incremental trend for drying shrinkage of mortar with inclusion of fly ash as fine aggregate.

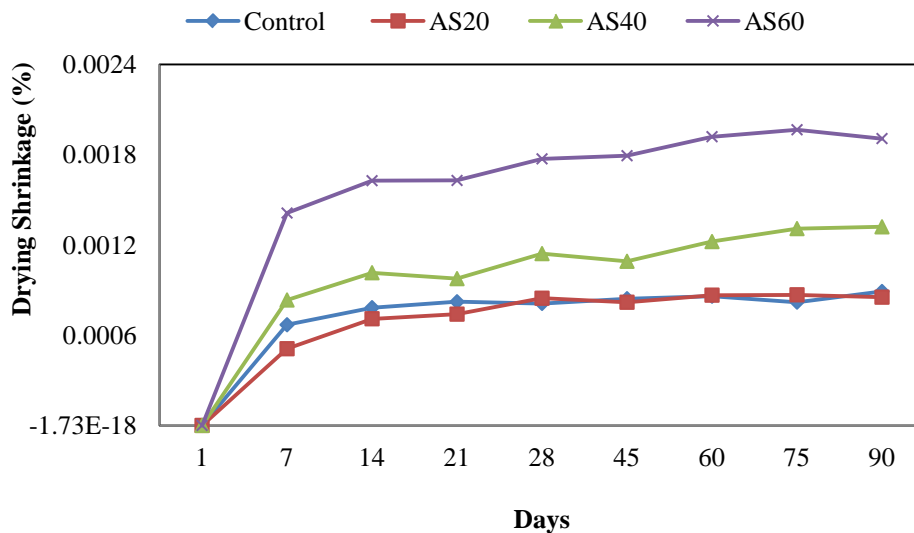


Figure 4.32 Drying Shrinkage of Mortar Mixes for Series A

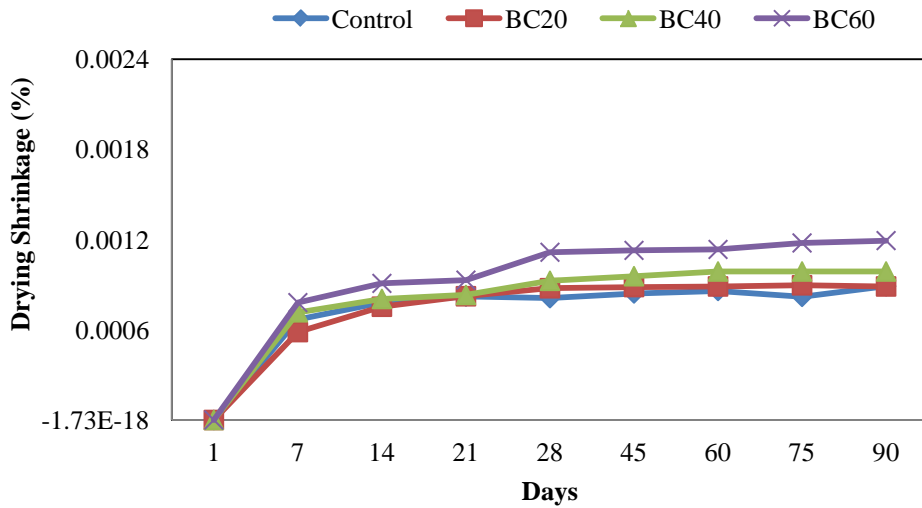


Figure 4.33 Drying Shrinkage of Mortar Mixes for Series B

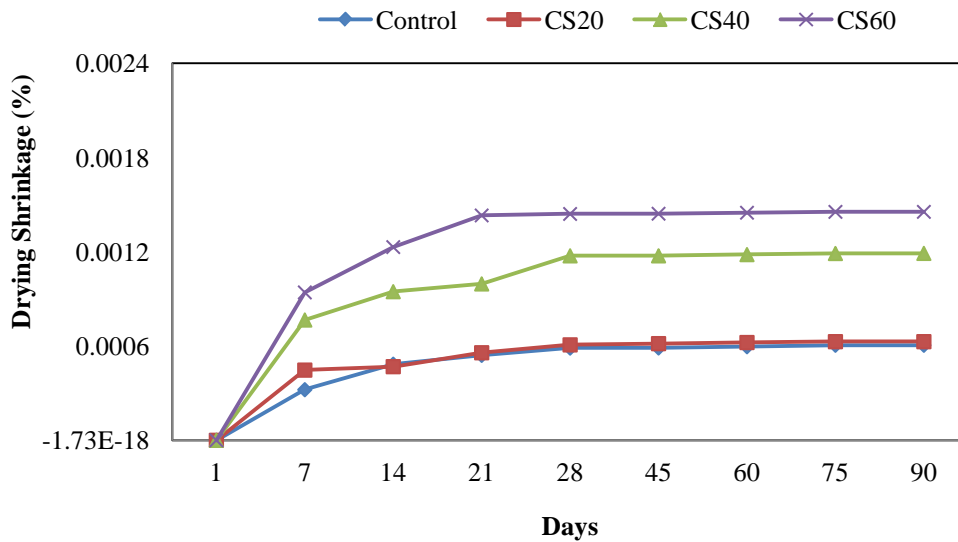


Figure 4.34 Drying Shrinkage of Mortar Mixes for Series C

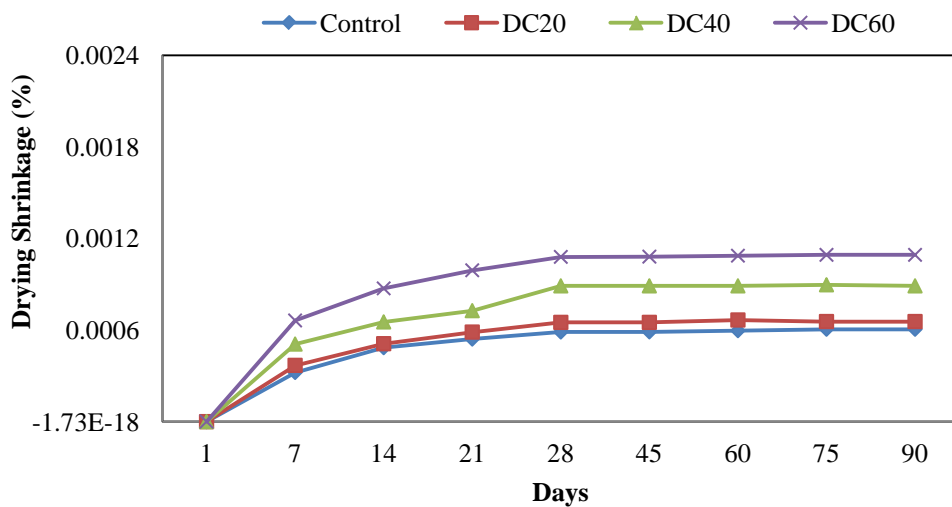


Figure 4.35 Drying Shrinkage of Mortar Mixes for Series D

4.3.8 Morphology (SEM)

Images obtained by SEM were presented in Figure 4.36-4.39. In Figure 4.36(a), voids were observed in large size, indicates weak compacted area whereas mortar inclusion with KSS gives very few amount of voids. The portion of ITZ was observed weak for the control mix as compared to mortar with KSS. This indicates that mortar with KSS formed more dense and compact structure compared to control mix. This was attributed to dense C-S-H formation observed in Figure 4.37(b)-4.38(b) resulting in to improved strength properties of mortar mixes. However at 60% replacement level, number of voids are maximum with large crystal of calcium hydroxide (CH/Ca(OH)₂) (Singh et al., 2015) indicates porous structure resulted into more water absorption shown in Figure 4.39.

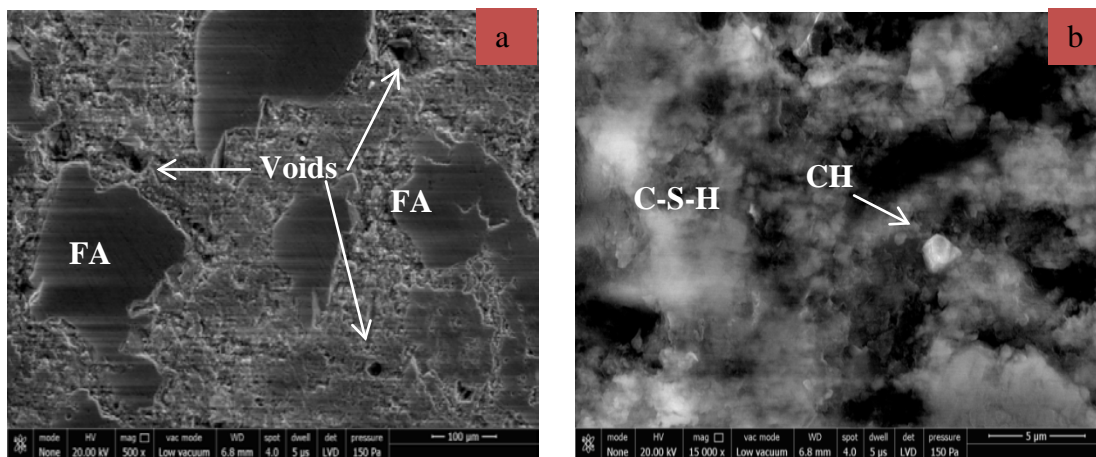


Figure 4.36 SEM images of Control Mix (1:3)

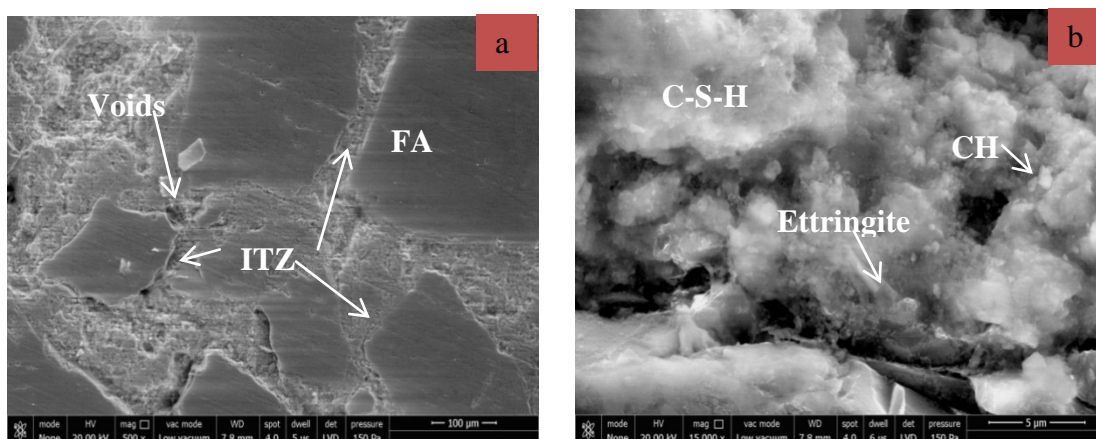


Figure 4.37 SEM images of AS20 Mix

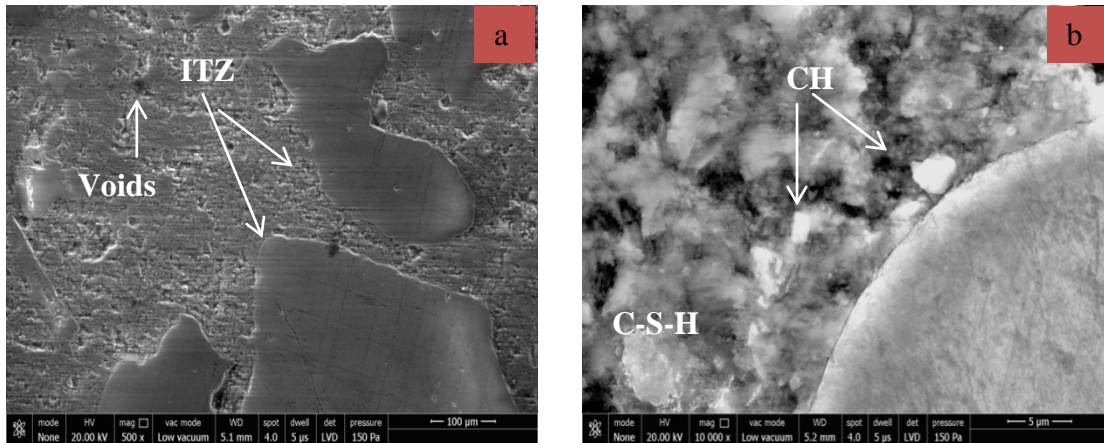


Figure 4.38 SEM images of AS40 Mix

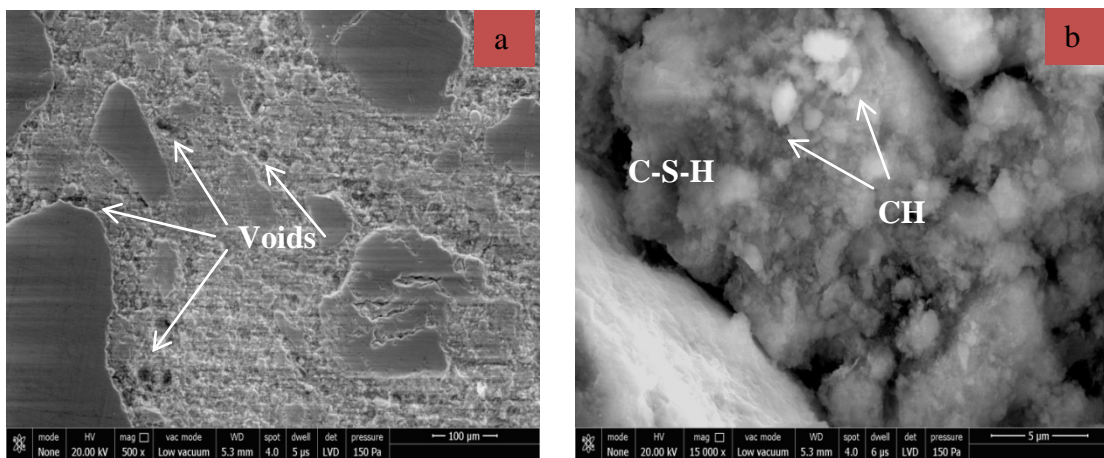


Figure 4.39 SEM images of AS60 Mix

4.3.9 Fourier-Transformation Infra-Red Spectra (FTIR)

Fourier-transformation infrared spectra (FTIR) analysis was done on rich mortar mixes of series A. The equipment used was ‘Spectrum Two’ with K-Br beam splitter having resolution of 4 cm^{-1} with eight scans. A powder sample of mortar was used for the test and spectra of the samples were presented in Figure 4.40-4.43.

Strong narrow absorptions at band 1477 cm^{-1} , 1429 cm^{-1} , 1489 cm^{-1} , 1484 cm^{-1} and sharp deep band at $872\text{-}876\text{ cm}^{-1}$ were attributed to CaCO_3 or limestone (Pozo-Antonio and Dionísio, 2017). Also with lesser extent calcite peaks were detected at $1794\text{-}1800\text{ cm}^{-1}$, $2515\text{-}2517\text{ cm}^{-1}$, and $2925\text{-}2929\text{ cm}^{-1}$ (C-H), (Lu et al., 2018) and it was observed that these peaks were well defined in the mortar incorporation of KSS, whereas in control mortar these appeared with very low intensity. Peaks appear around 475 cm^{-1} (Al-O), 1000 cm^{-1} (Si-O-Si) and $711\text{-}792\text{ cm}^{-1}$ were responsible for silicates and presence of quartz in mortar mixes (Kabeer and Vyas, 2018; Yilmaz and

Olgun, 2008) The peaks observed around 1000 cm^{-1} were shifted from 983 cm^{-1} to 969 cm^{-1} due to presence of KSS in mortar mixes. This change in band indicates the change in microstructure with better interlinking between Si-O and Al-O bond resulting increase of calcium alumina silicate hydrate (C-A-S-H) in mortar with KSS. This result was justifying the improvement in compressive strength and flexural strength of mortar. However the intensity of this band appeared in 60% KSS was low as compared to other mixes, which justified minimum adhesive, flexural and bond strength at this replacement level in their series. A well-defined broad band at 3460 cm^{-1} was appeared due to the presence of water molecules in mortar samples.

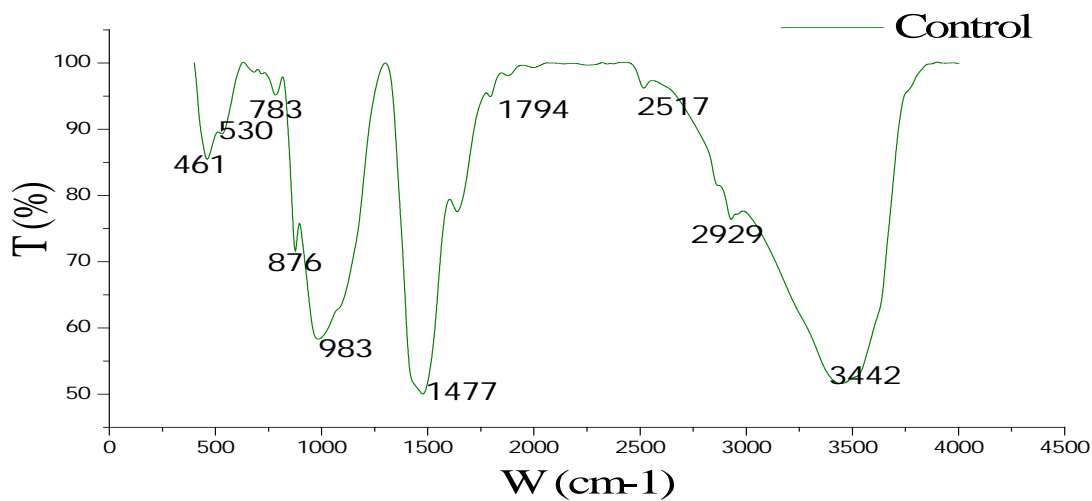


Figure 4.40 FTIR Spectra pattern for Control Mix (1:3)

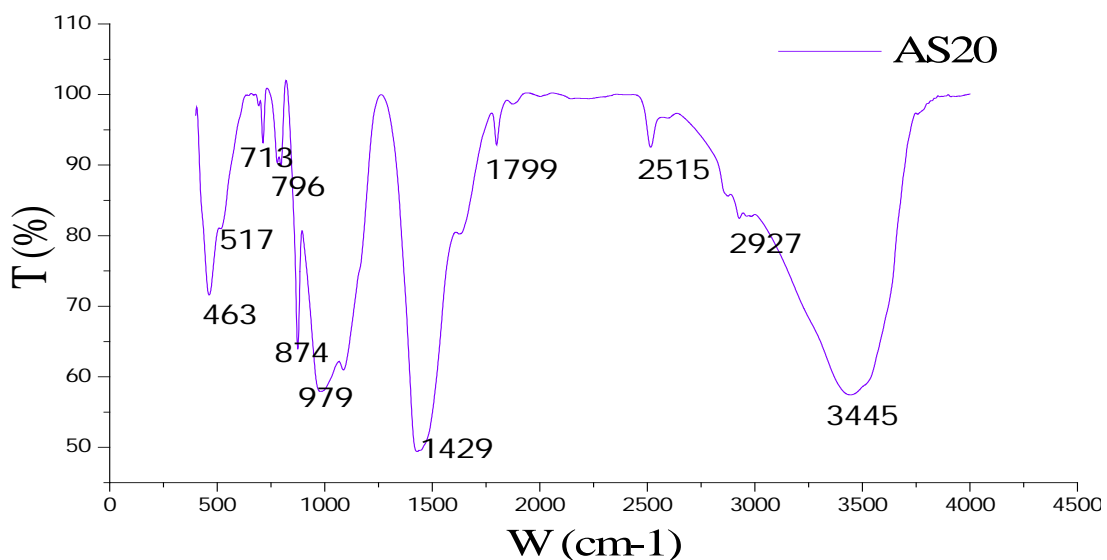


Figure 4.41 FTIR Spectra pattern for Mix AS20

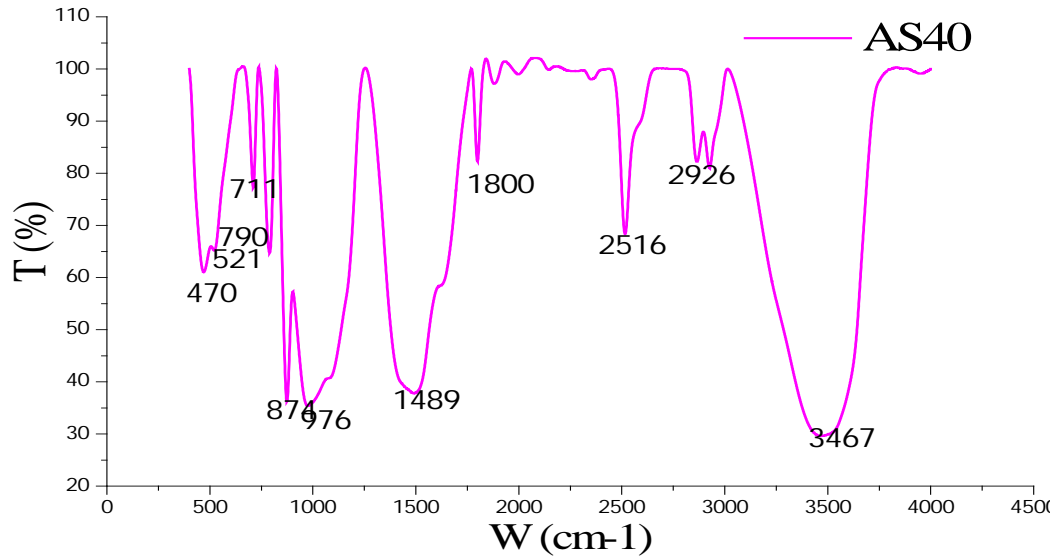


Figure 4.42 FTIR Spectra pattern for Mix AS40

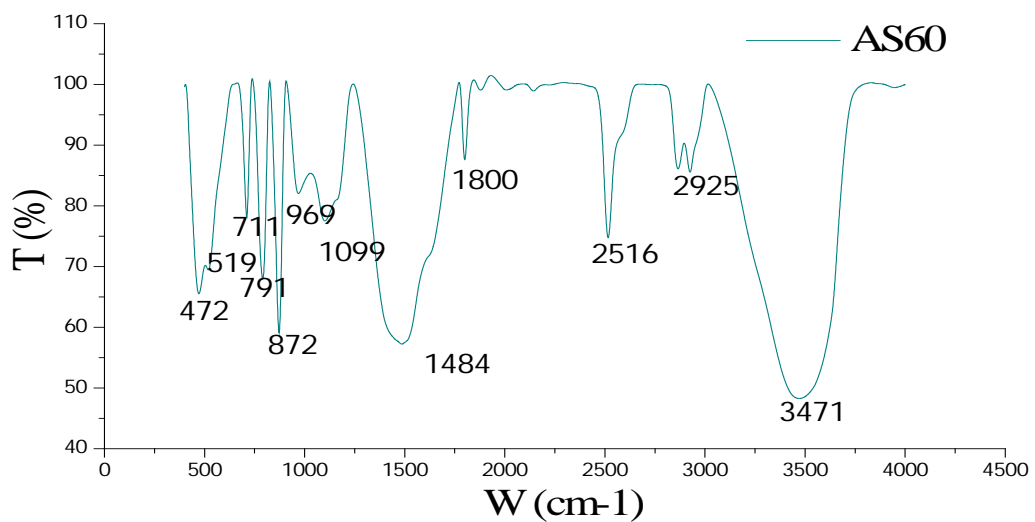


Figure 4.43 FTIR Spectra pattern for Mix AS60

4.3.10 X-ray Diffraction Analysis (XRD)

The X-ray diffraction analysis was done on powder sample of mortar mix which was obtained by grinding small piece from inner part of the mortar specimen formed by extracting 10 mm upper surface from all sides. Different mortar spectrograms are shown in Figure 4.44-4.47.

For comparison between control mortar and mortar containing KSS, peaks of Quartz (form of free silica), hydrated product calcium hydroxide (CaOH₂) and calcium aluminum silicate hydrate (C-A-S-H), calcium carbonate (CaCO₃) and

ettringite have been analyzed. Major peaks of quartz present in control mix and AS20 mix with higher intensity as compared to mix AS40 and AS60. It indicates free quartz available on the surface of the material shows less consumption in making of hydrated product C-S-H (Makhloufi et al., 2016). C-H (Portlandite) peaks were traced at angle 18.09, 34.11, 36.62, 47.14, 62.68 and 77.55 in control and AS20 mix. Intensity of C-H peaks in control mix was higher as compared to mix AS20, whereas in mortar AS40 and AS60, C-H peaks were absent. It means that mortar mix containing KSS enhance the reaction between silica and calcium hydroxide (C-H) resulting into more hydrated products like C-S-H (calcium silicate hydrate). In addition to that, presence of KSS in mortar leads to formation of carbo-aluminates resulting into reduction of calcium hydroxide product (Weerdt et al., 2011). C-A-S-H peaks were observed due to presence of mullite of pozzolana cement that reacts with hydrated product tri-calcium silicate resulted in to product C-A-S-H. In all mortar mixes C-A-S-H peaks were well visualized but the intensity of these peaks were quite high in mortar containing KSS resulting in to enhanced compressive strength. The major calcite (CaCO_3) peaks were observed at angle 29.41, 39.39, 43.21, 47.59, 48.47 and 57.41. Calcite peaks appeared in AS20, AS40, and AS60 with high intensity than that of control mortar. This was due to the presence of more calcite in mortar mixes with KSS that played a dominant role in strength enhancement of mortar mixes.

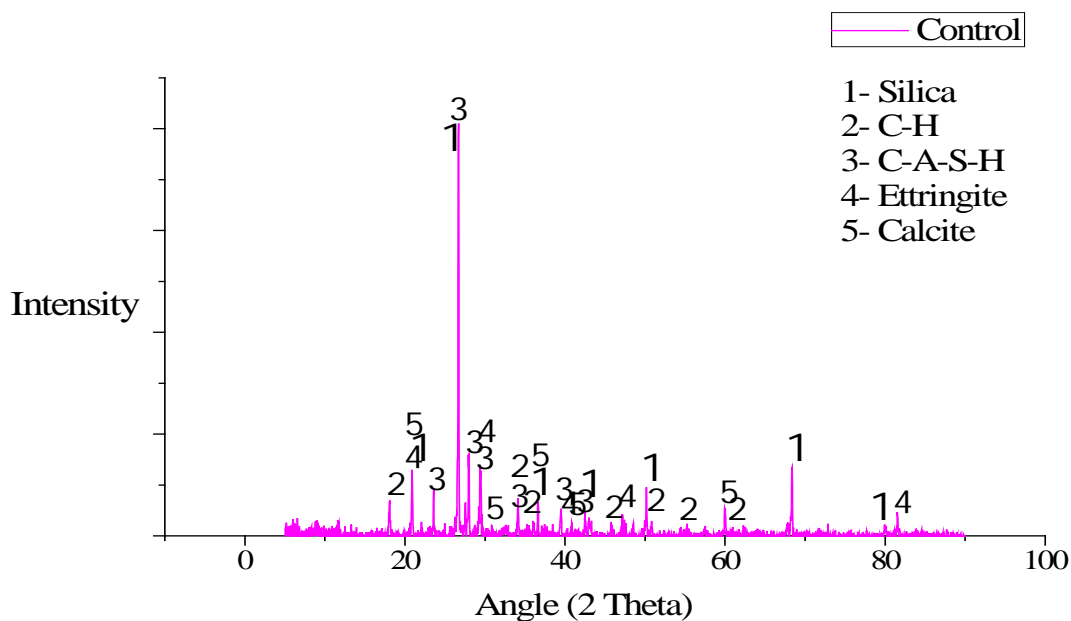


Figure 4.44 XRD pattern of Control Mortar (1:3)

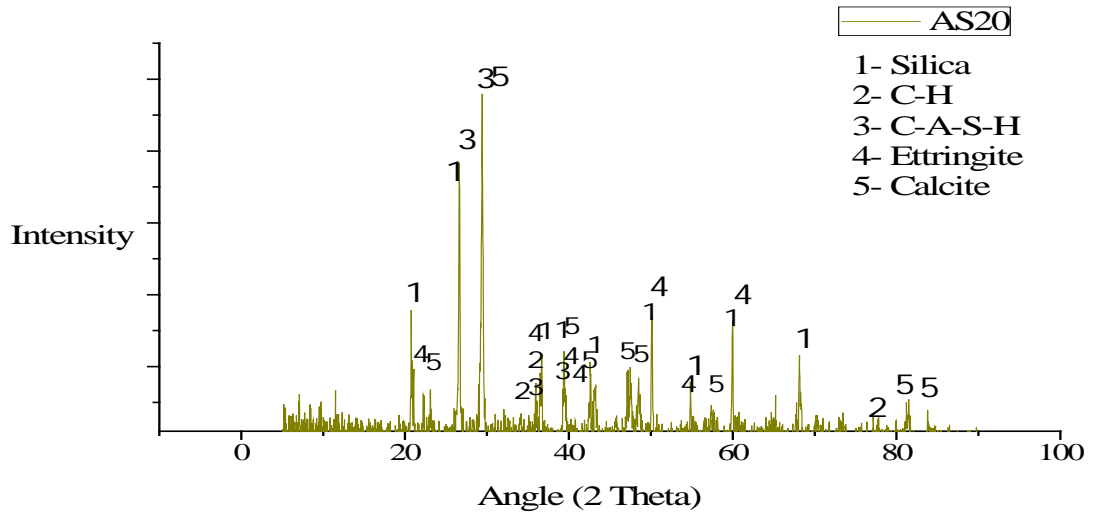


Figure 4.45 XRD pattern of Mix AS20

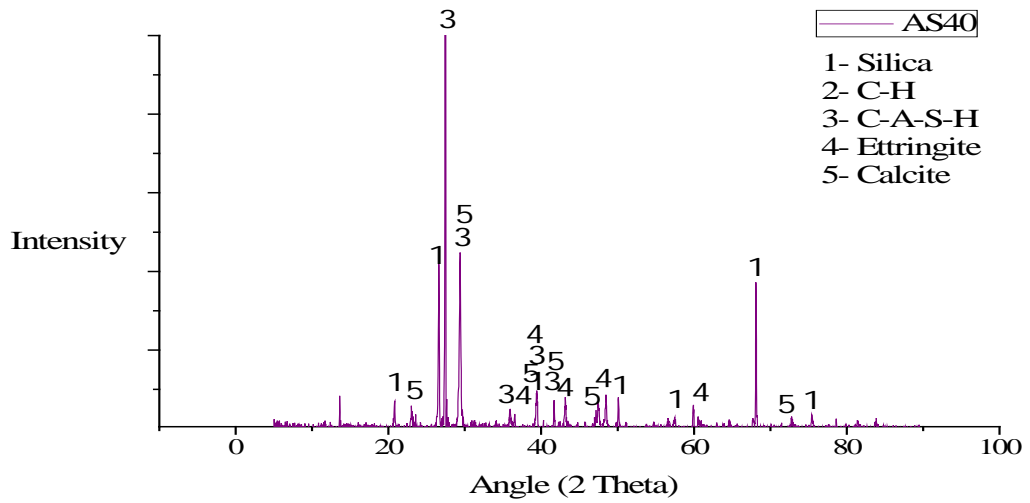


Figure 4.46 XRD pattern of Mix AS40

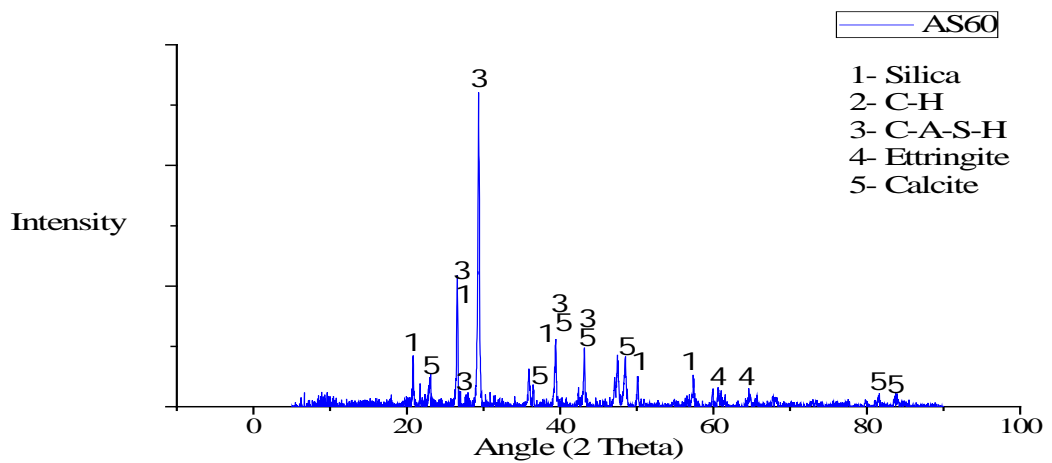


Figure 4.47 XRD pattern of Mix AS60

4.3.11 Acid Attack

Acid attack on mortar samples was evaluated by using 5 % sulfuric acid solution (H₂SO₄) for different immersion period of 1, 7, 14, 28 and 90 days. The effect of sulfuric acid on mortar mixes was judged by calculating variation in compressive strength and weight, using expressions 10 and 11 (section 3.5.14). Also, internal phase transformation during sulphuric acid exposure was analyzed for selected mortar mixes (series A) by FTIR technique.

The variation in compressive strength of mortar mixes has been presented in Figures 4.48-4.51. It was observed that the compressive strength loss was progressively increased with the increase of immersion period for all mortar series. This was attributed to production of soluble salts (gypsum) as byproduct of reaction between calcium hydroxide (portlandite or CH) and acid. Gypsum was deposited into pores present in the mortar and developed internal stresses which lead to loss in compressive strength.



Acid exposure period between 1 and 28 days, compressive strength loss in KSS and KSCS containing mortar was less than that of their control mortar. However at 90 days acid exposure, strength loss in mortar mix containing 40% KSS and KSCS for series A, B and D were more as compared to other mortar mixes. The minimum strength loss was found in mix AS20, BC20, CS30 and DC20 which is about 32.1, 33.3, 38 and 37.6% respectively. Whereas maximum strength loss was observed by mix AS40, BC40, control (series C) and DC40, that is about 41.31, 41.10, 57.42 and 60.30%. Results were revealed that mortar mixes containing 20-30 % KSS and KSCS were observed with significantly reduced compressive strength loss.

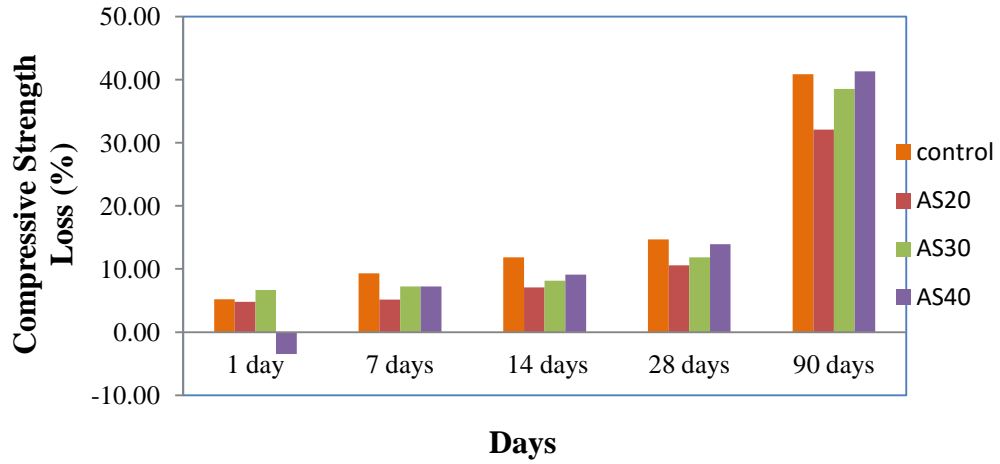


Figure 4.48 Compressive Strength Loss in Mortar Mixes of Series A

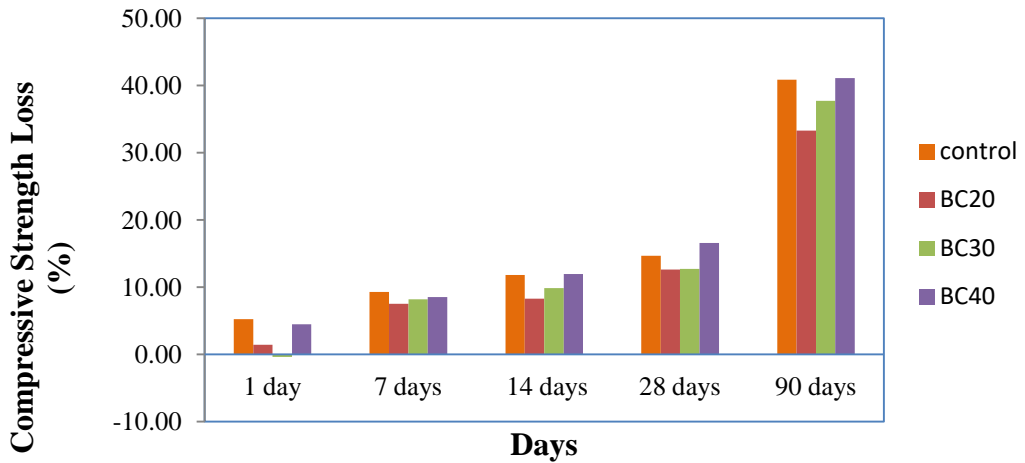


Figure 4.49 Compressive Strength Loss in Mortar Mixes of Series B

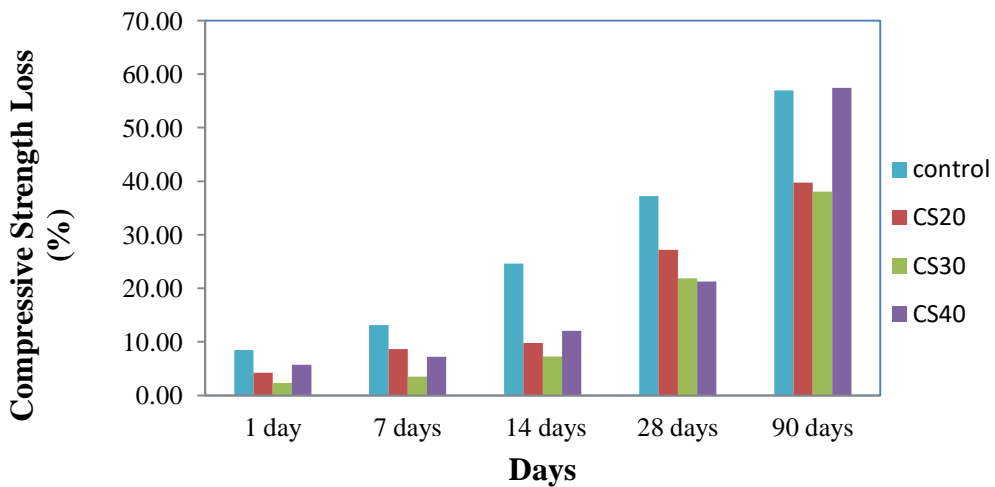


Figure 4.50 Compressive Strength Loss in Mortar Mixes of Series C

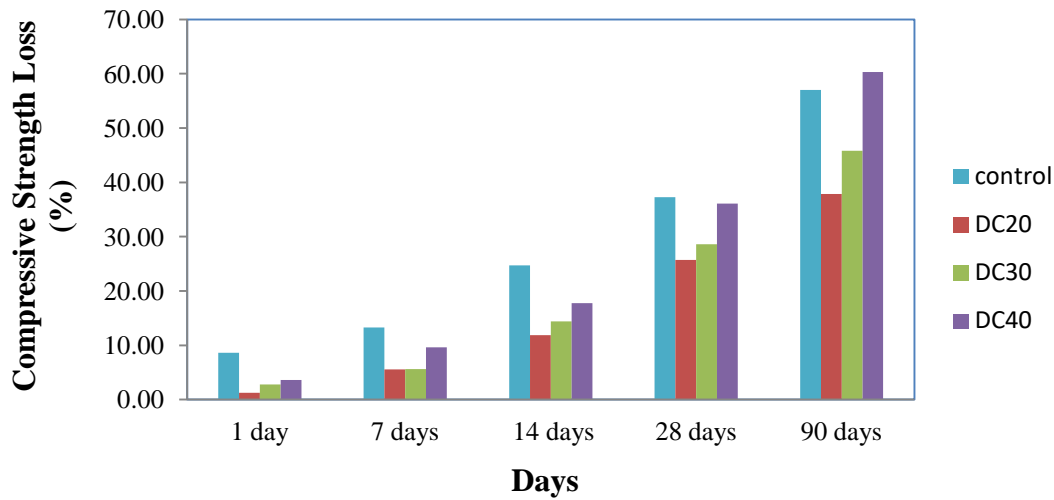


Figure 4.51 Compressive Strength Loss in Mortar Mixes of Series D

The variation in weight of mortar mixes for all series is presented Figures 4.52-4.55. In first day observation, weight of the mortar mixes containing KSS and KSCS of series A and B (except BC30) was increased may be due to absorption of solution. However this change was very low or insignificant. Acid exposure period between 7 and 28 days, considerable weight loss observed in all mortar mixes. It was noted that the mortar mix with 40% KSS and KSCS has maximum weight loss in their respective series. Whereas, minimum weight loss found in mortar with 20% KSS and KSCS in all mortar series. Nevertheless mortar with 30% KSS and KSCS (except BC30) has less weight loss when it compared to their respective control mortar.

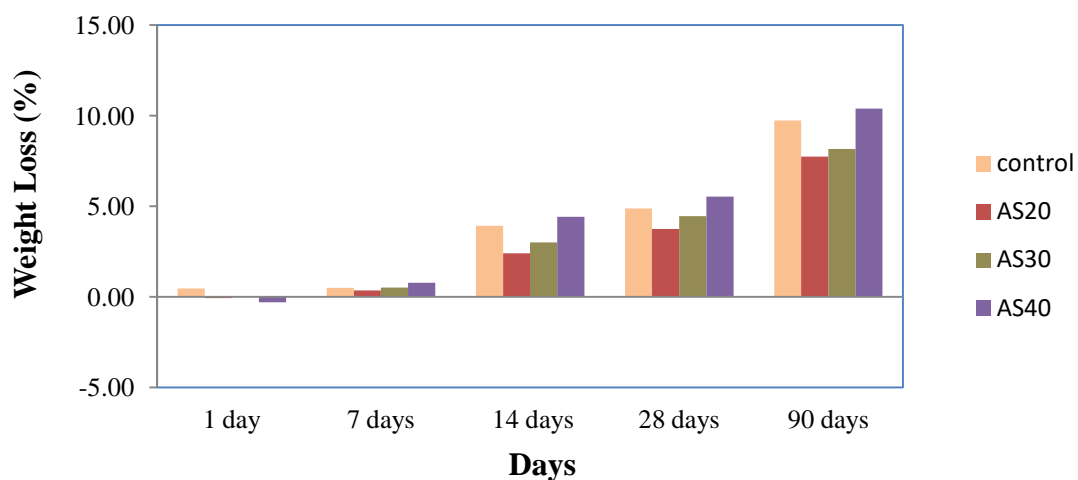


Figure 4.52 Weight Loss in Mortar Mixes of Series A

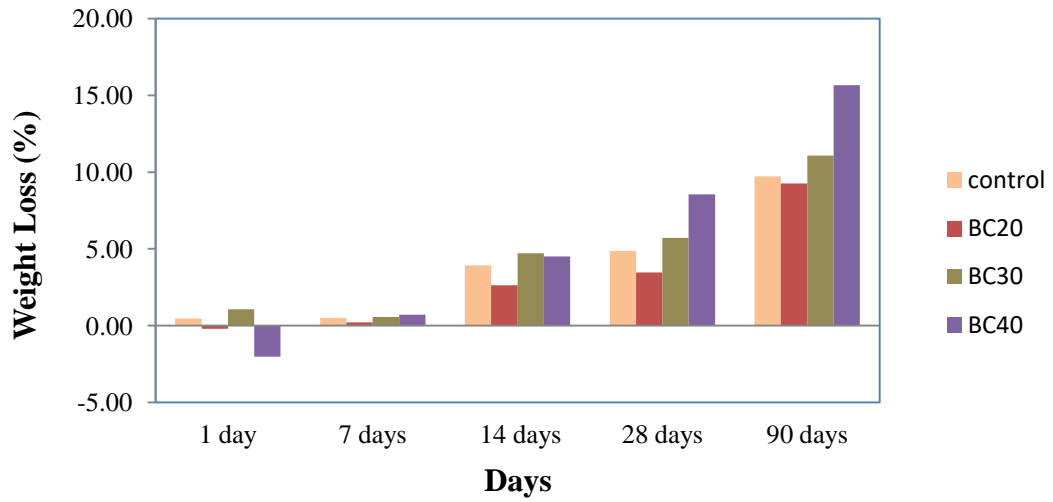


Figure 4.53 Weight Loss in Mortar Mixes of Series B

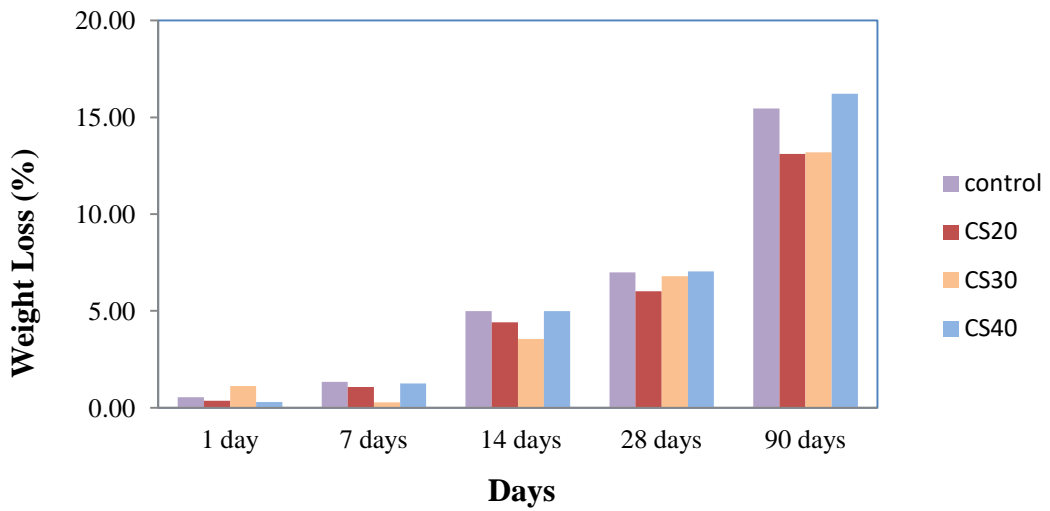


Figure 4.54 Weight Loss in Mortar Mixes of Series C

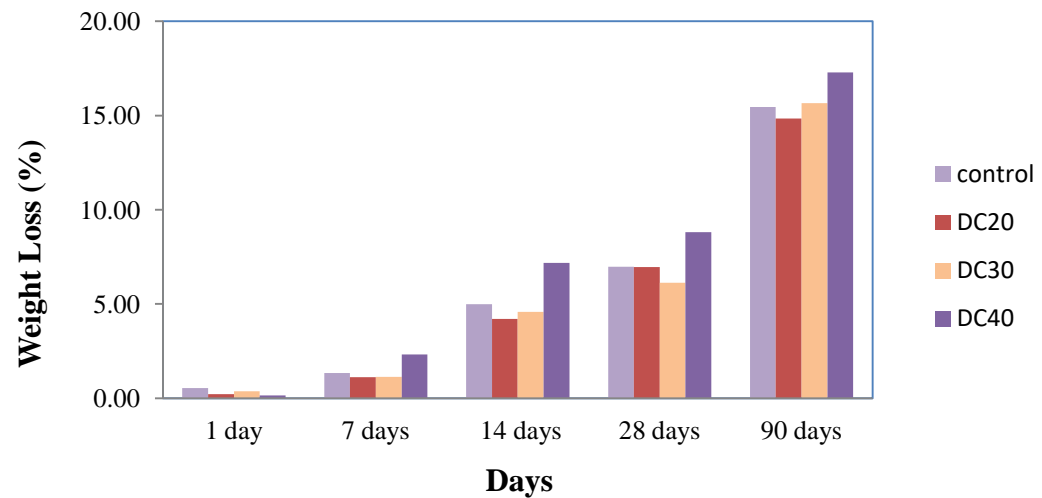


Figure 4.55 Weight Loss in Mortar Mixes of Series D

The above behaviour of mortar containing KSS and KSCS can be attributed to three main reasons; first, low water-cement ratio of these mixes, second was pore filling effect by dense C-S-H formation which reduced pores in mortar matrix and third was higher amount of calcite content compared to control mortar. By pore filling effect, amount of gypsum deposited in to mortar matrix was reduced. This resulted into minimum internal stress causing reduction in compressive strength loss in mortar mixes containing KSS and KSCS. Similar behaviour was noticed by (Bederina et al., 2013; Ghrici and Kenai, 2007) where they claimed limestone containing mortar showed good performance against aggression of hydrochloric and sulfuric acid.

Additionally, the above behaviour was also understood by FTIR analysis on mortar mixes of series A. The FTIR spectra of mortar mixes exposed at 28 and 90 days sulfuric acid solution presented in Figure 4.56-4.63. In these spectra, sharp deep band at 876 cm^{-1} was noted for C-O bond which was responsible for calcite present in the mix. It was observed that the KSS containing mortar intensity of C-O bond was high than that of control mortar which indicates presence of significant amount calcite in such mixes.

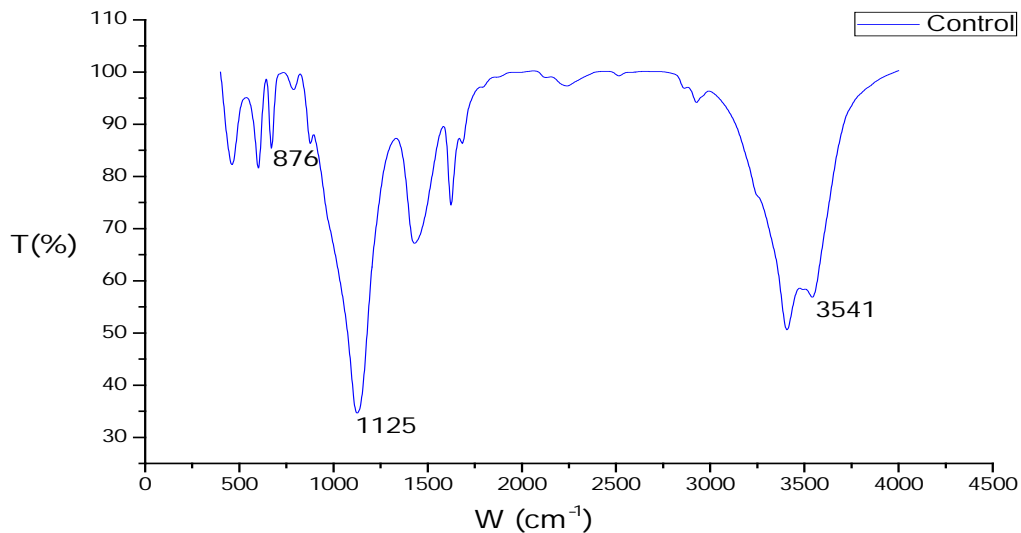


Figure 4.56 FTIR Spectra for Control Mix of Series A at 28 Days Acid Immersion Period

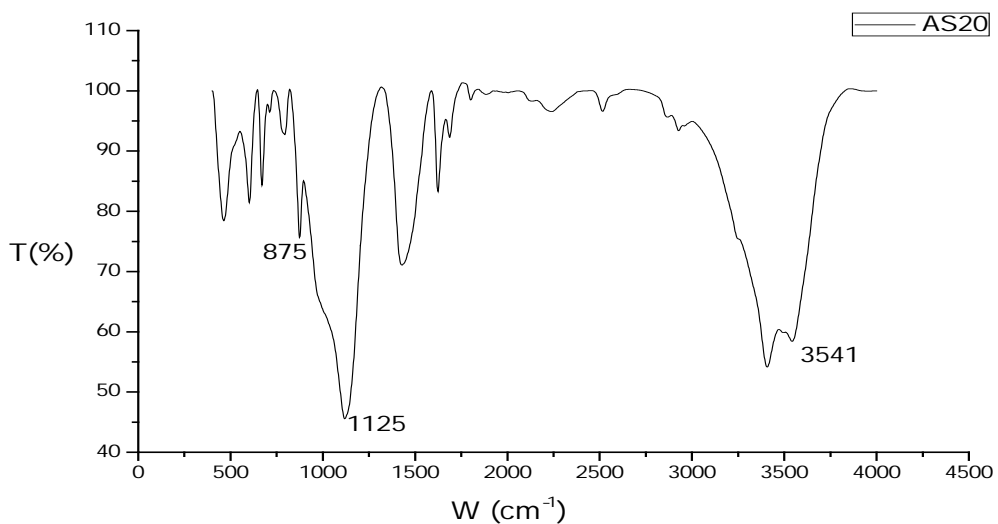


Figure 4.57 FTIR Spectra for Mix AS20 at 28 Days Acid Immersion Period

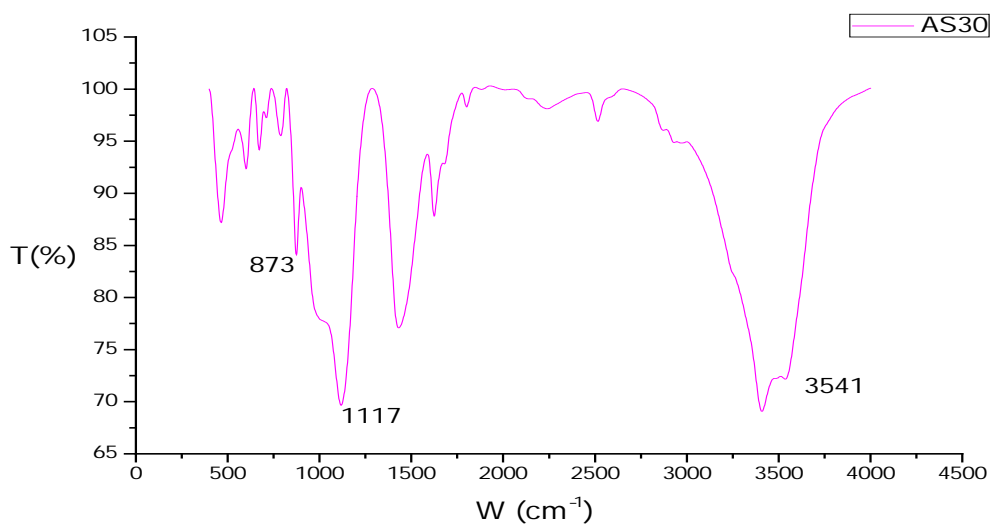


Figure 4.58 FTIR Spectra for Mix AS30 at 28 Days Acid Immersion Period

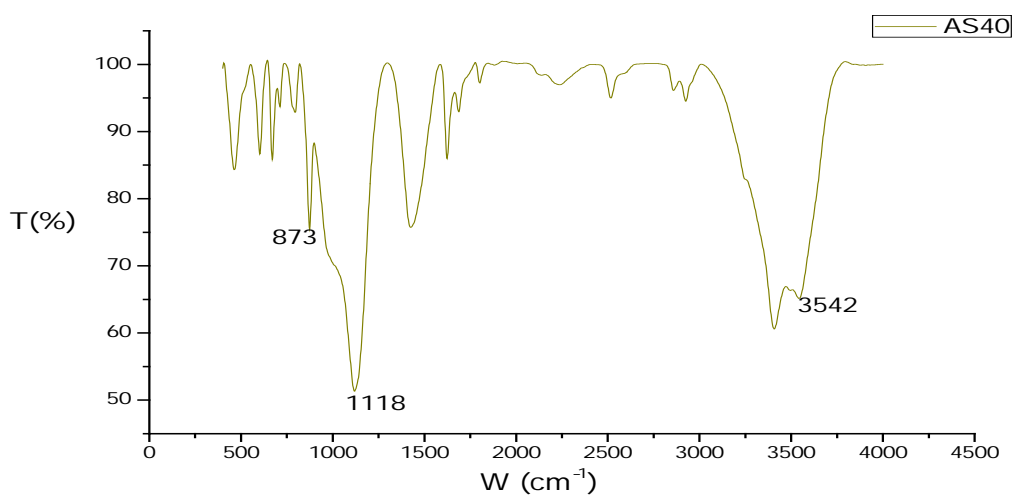


Figure 4.59 FTIR Spectra for Mix AS40 at 28 Days Acid Immersion Period

The band near about 3600 cm^{-1} (C-H bond) was missing in all spectra that indicate complete consumption of calcium hydroxide due to the primary reaction between CH and acid. This resulted in to formation of gypsum and traced at wavenumber 1100 cm^{-1} and 3500 cm^{-1} . In 28 days acid exposure samples, intensity of these bands in control mortar was more as compared to KSS containing mortar, causing high strength and weight loss. However, at 90 days acid exposure period, the maximum intensity of gypsum was observed with 40 % KSS which attributed to maximum strength and weight loss in this mix.

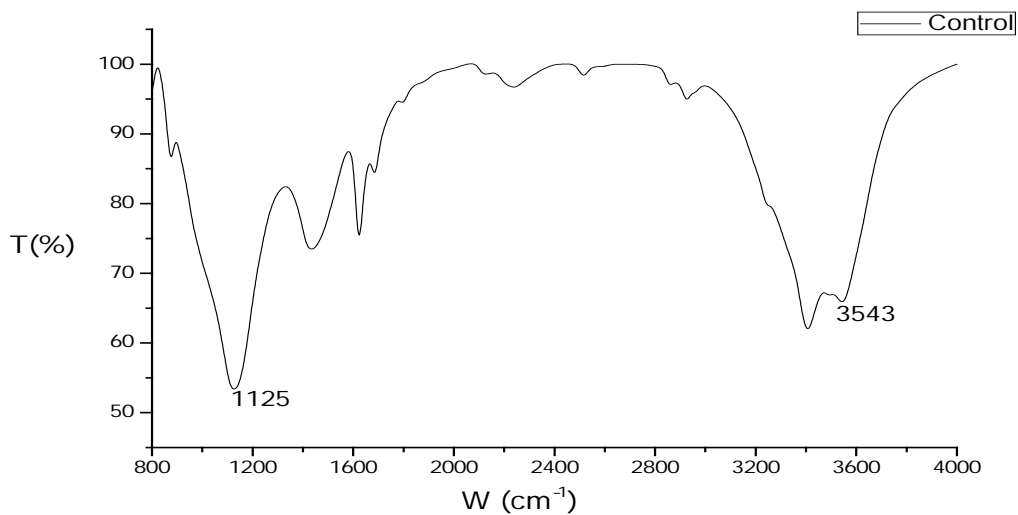


Figure 4.60 FTIR Spectra for Control Mix of Series A at 90 Days Acid Immersion Period

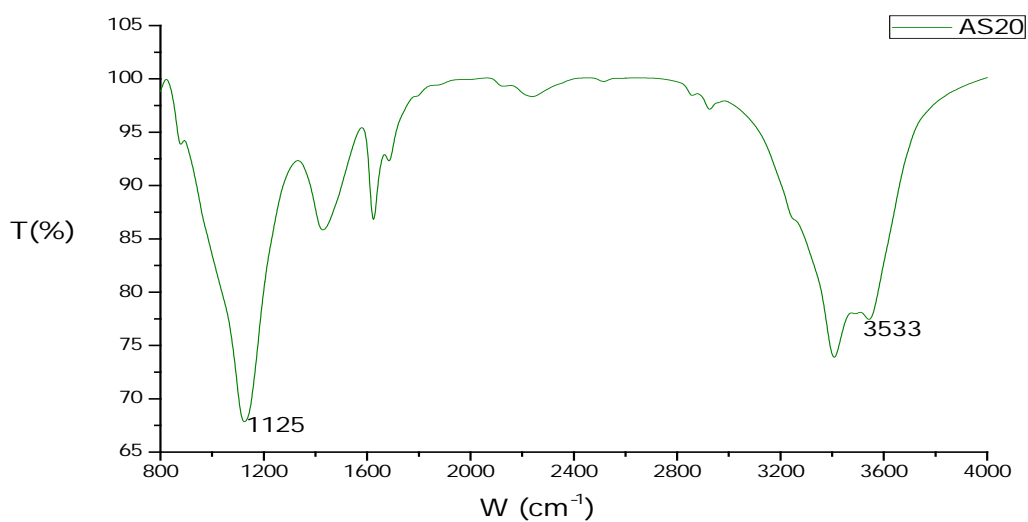


Figure 4.61 FTIR Spectra for Mix AS20 at 90 Days Acid Immersion Period

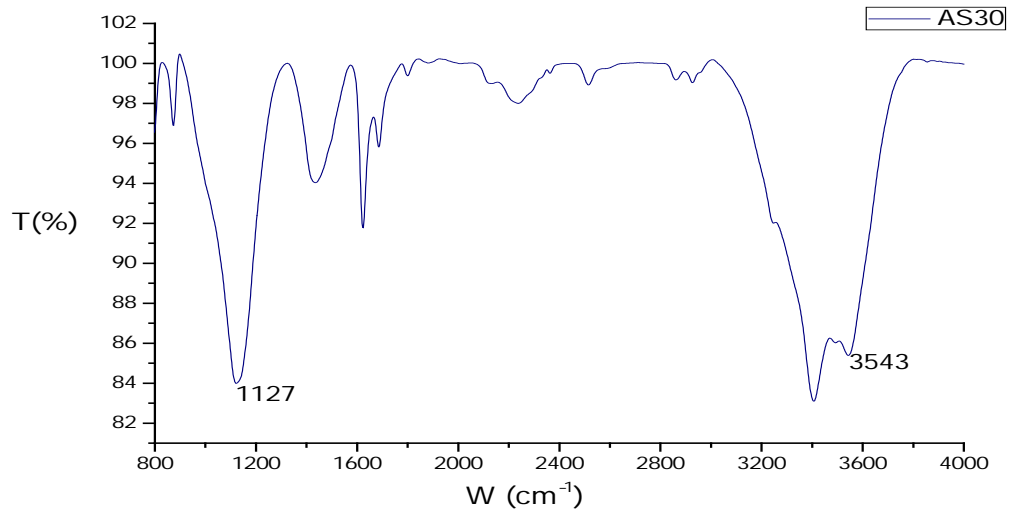


Figure 4.62 FTIR Spectra for Mix AS30 at 90 Days Acid Immersion Period

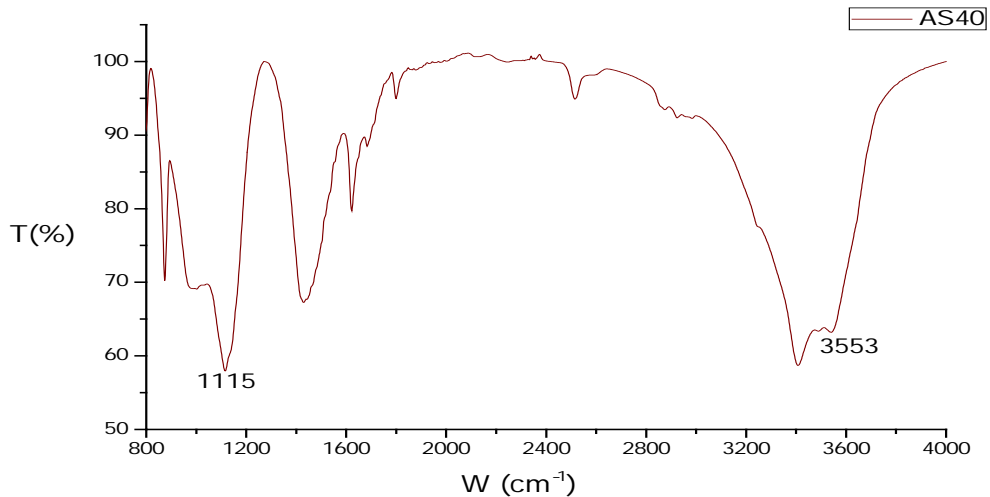
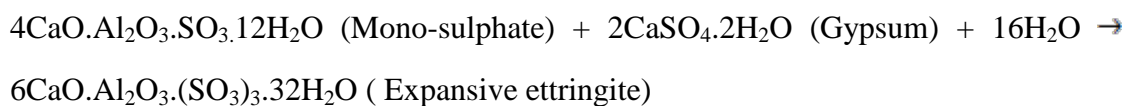


Figure 4.63 FTIR Spectra for Mix AS40 at 90 Days Acid Immersion Period

4.3.12 Sulphate Attack

Sulphate attack in mortar occurs due to reaction between sulphates presents in groundwater, drainage solutions and hydrated products ($\text{Ca}(\text{OH})_2$). This reaction leads to generate gypsum, expansive ettringite and thaumasite as byproduct responsible for deterioration of mortar. Following reactions are undertaken during the sulphate attack.



Sulphate attack effect on different mortar mixes of series A-D is evaluated in terms of change in compressive strength and weight as presented in Figure 4.64-4.71. In Figure 4.64-4.67, there are no significant changes observed in compressive strength of mortar mixes when immersed in to sulphate solution between 1 to 7 days. After this, as the sulphate exposure period increased till 90 days, compressive strength of mortar mixes also increased. Improvement in compressive strength was found between 20.5 and 57.4% with KSS and KSCS containing mortar, whereas in control mortars were between 44.5 and 62.5%. Strength enhancement was attributed to formation of expansive ettringite as shown in above equation. Expansive ettringite fills the pores resulting into reduced porosity of mortar mixes. KSS and KSCS containing mortar performed better against sulphate attack because their presence formed dense CSH/CASH which delayed above reaction of sulphate attack; due to this, the consumption of portlandite in to gypsum was reduced.

For longer immersion period, compressive strength was observed reducing. This loss in strength was maximum in control mortar of all series which was about 42.5% for series A&B and 71.3% for series C&D, whereas minimum strength loss was observed at 40% replacement level in all series.

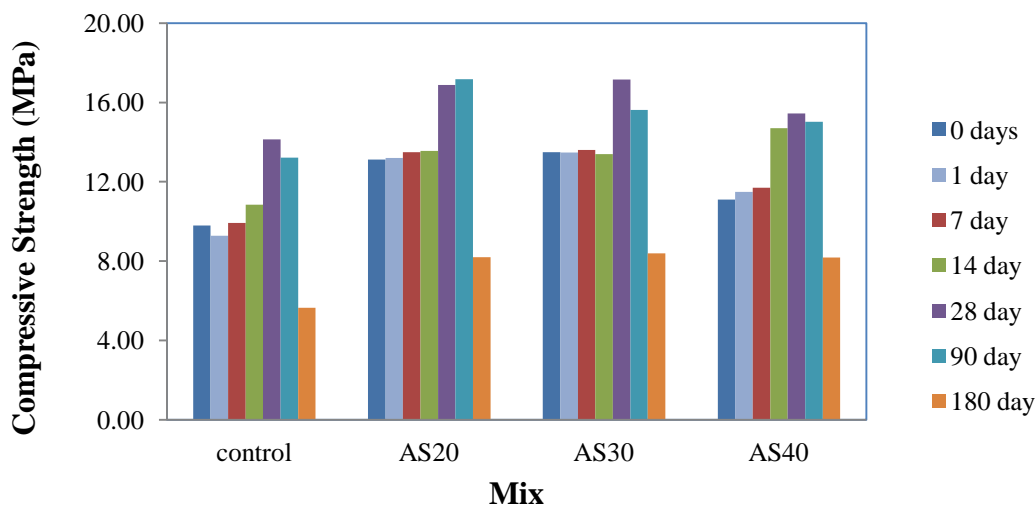


Figure 4.64 Changes in Compressive Strength of Mortar Mixes of Series A

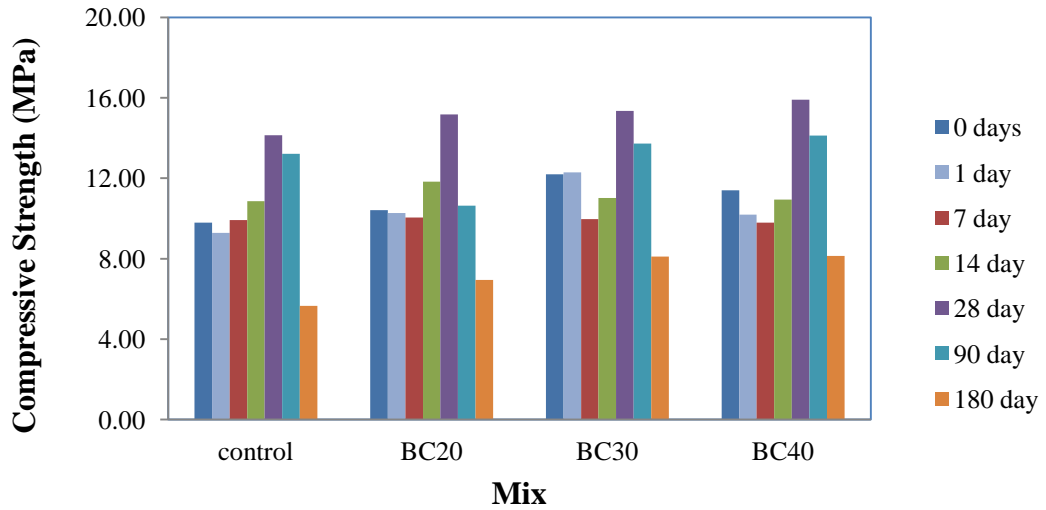


Figure 4.65 Changes in Compressive Strength of Mortar Mixes of Series B

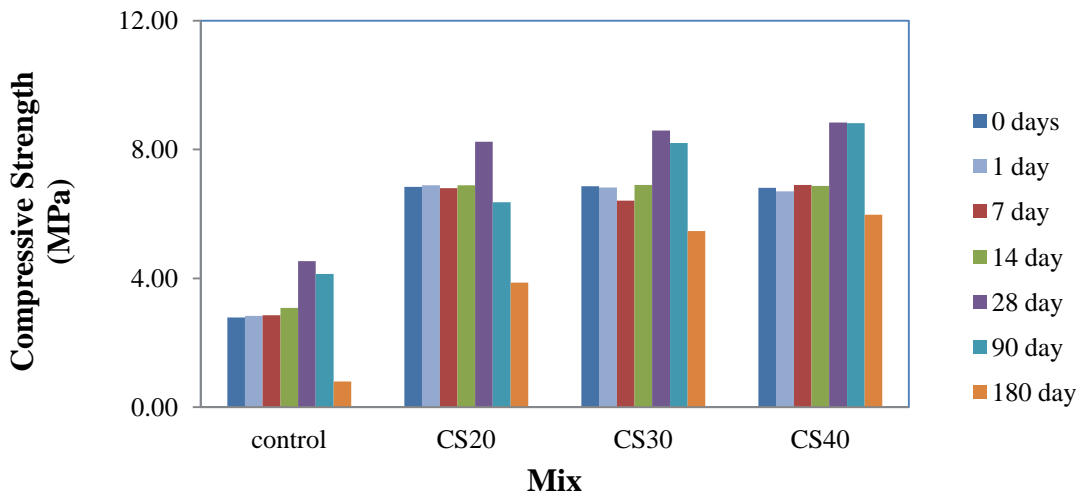


Figure 4.66 Changes in Compressive Strength of Mortar Mixes of Series C

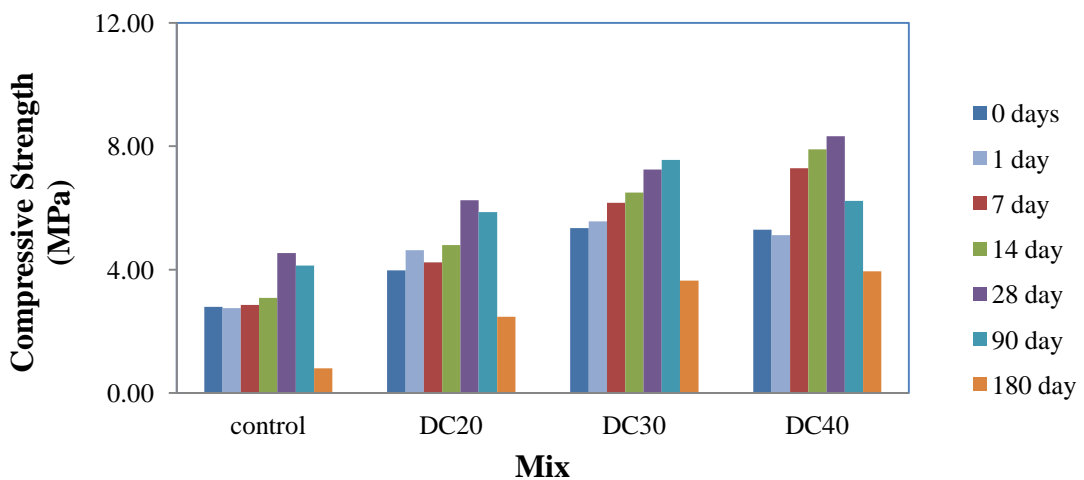


Figure 4.67 Changes in Compressive Strength of Mortar Mixes of Series D

Variation in weight of the mortar mixes due to exposure into sulphate solution was shown in Figure 4.68-4.71. It was observed that initially up to 28 days sulphate exposure period, weight of the mortar mixes were increased because of formation of expansive ettringite or gypsum, which reduce the pore volume of the mortar. However, in later ages weight loss happens due to excess amount of gypsum and ettringite. Nevertheless, mortar mixes containing KSS and KSCS have lesser weight loss as compared to their control mortar. In 180 days sulphate exposed mixes of series A and C have minimum weight loss in mix AS40 and CS40. Whereas in series B and D, mix BC30 and DC20 performed superior to that of another mortar mix of respective series.

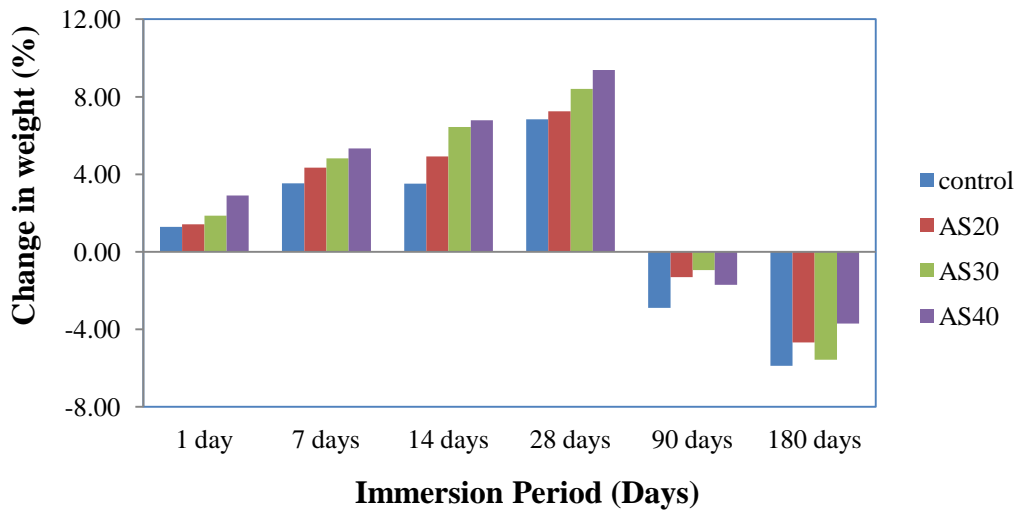


Figure 4.68 Weight Change in Sulphate Exposed Mortar Mixes of Series A

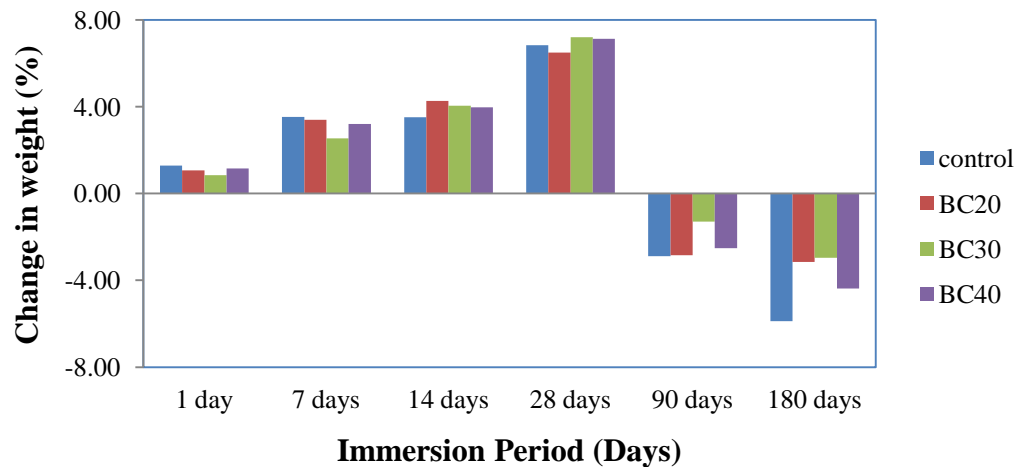


Figure 4.69 Weight Change in Sulphate Exposed Mortar Mixes of Series B

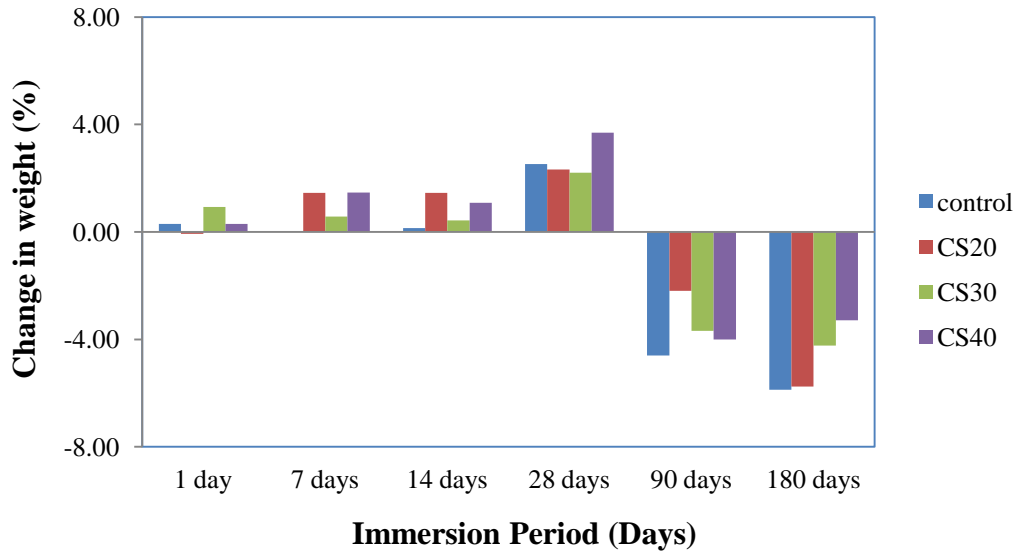


Figure 4.70 Weight Change in Sulphate Exposed Mortar Mixes of Series C

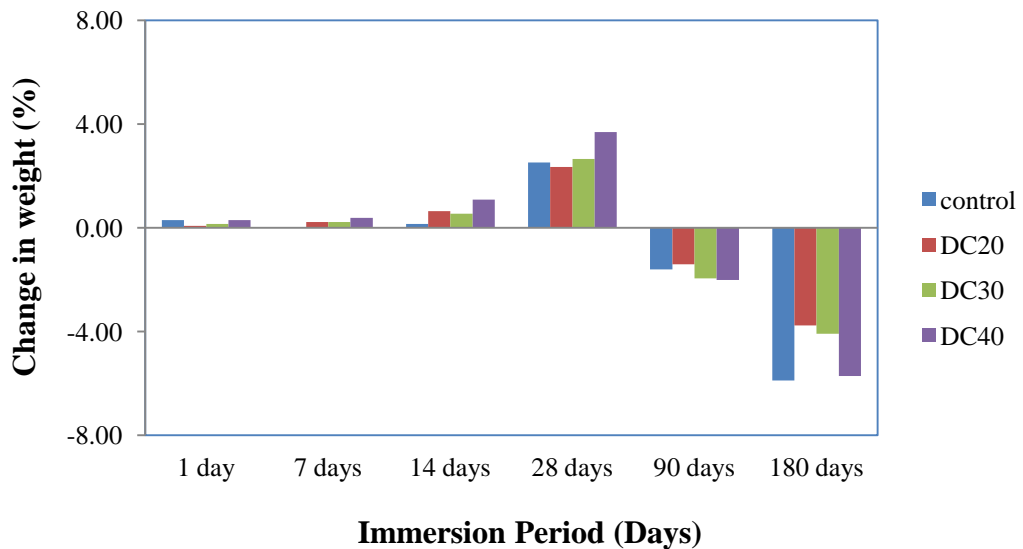


Figure 4.71 Weight Change in Sulphate Exposed Mortar Mixes of Series D

Additionally, this behaviour was also predicted by FTIR spectra as shown in Figure 4.72-4.79. In spectra, CSH/CASH was traced at around wavenumber 978 cm^{-1} . The intensity of peak at this wavenumber in 90 days sulphate exposed mixes (series A) was in the order of $AS40 > \text{Control} > AS20 > AS30$ as shown in Figure 4.72-4.75. These results validate the maximum (AS40; 35.25%) and minimum (AS30; 15.75%) improvement in compressive strength at 90 days sulphate immersion period.

After 180 days sulphate exposure mixes spectra (Figure 4.76-4.79), the intensity of C-S-H band was observed high in mixes containing KSS as compared to control mix. Also, gypsum was traced at 1093 cm^{-1} wavenumber with lower intensity,

may be due to its consumption during reaction between calcium silicate hydrates (CSH) and sulphates in the presence of carbonates to form thaumasite, as given below.



Formation of thaumasite resulted in to loss of binding material and hence the maximum strength and mass loss observed for control mix. An earlier study by (Baldermann et al., 2018) (Baldermann et al., 2018) found similar observation when cement blended with 35 to 50% limestone.

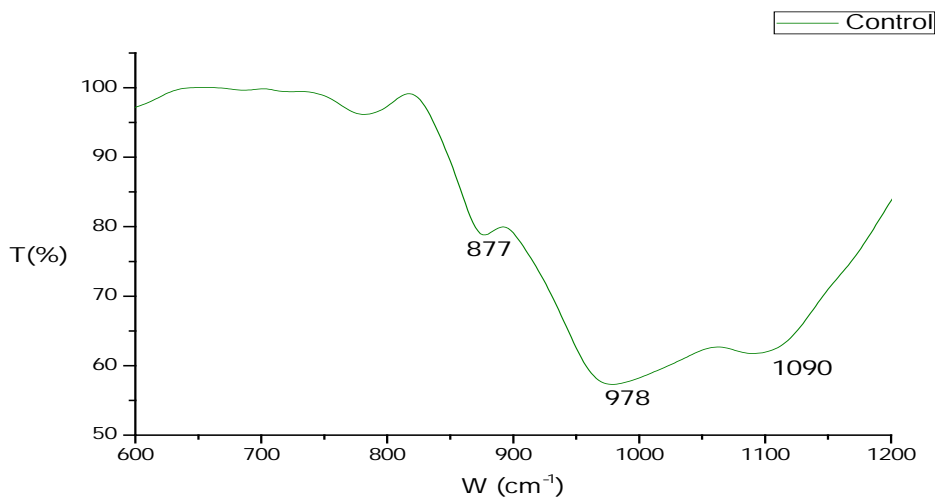


Figure 4.72 FTIR Spectra for Control Mix of Series A at 90 Days Sulphate Immersion Period

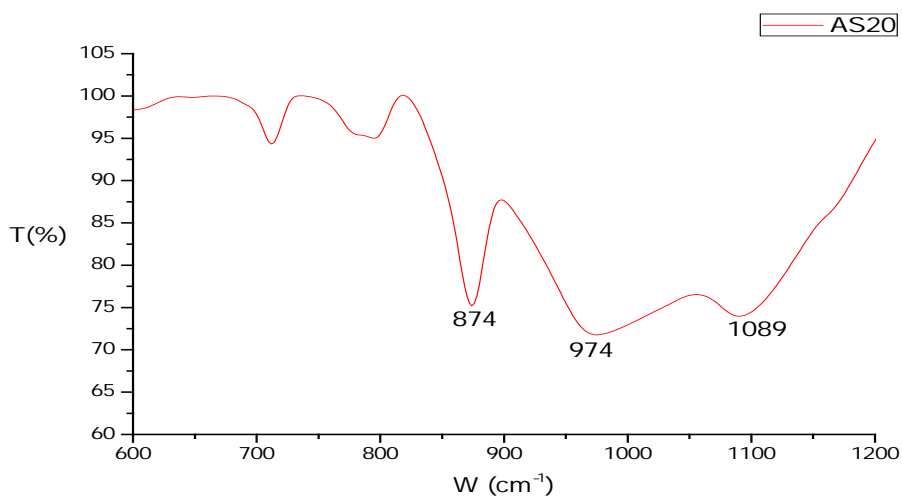


Figure 4.73 FTIR Spectra for Mix AS20 at 90 Days Sulphate Immersion Period

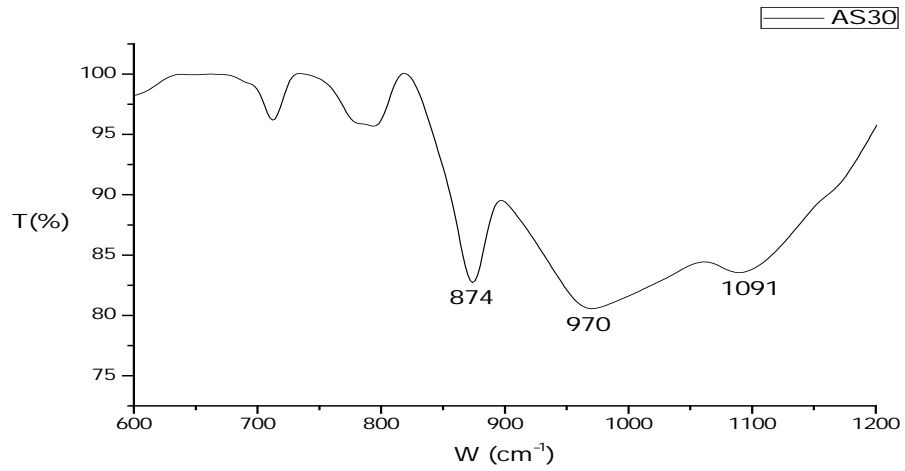


Figure 4.74 FTIR Spectra for Mix AS30 at 90 Days Sulphate Immersion Period

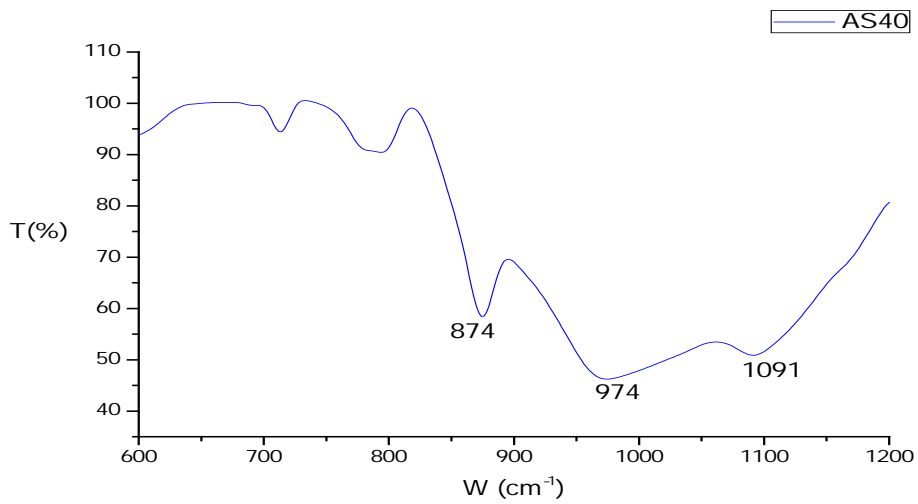


Figure 4.75 FTIR Spectra for Mix AS40 at 90 Days Sulphate Immersion Period

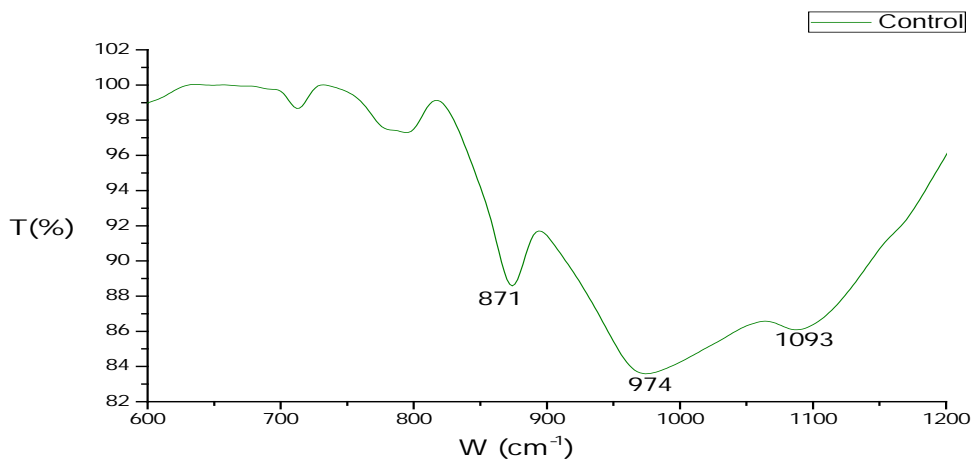


Figure 4.76 FTIR Spectra for Control Mix of Series A at 180 Days Sulphate Immersion Period

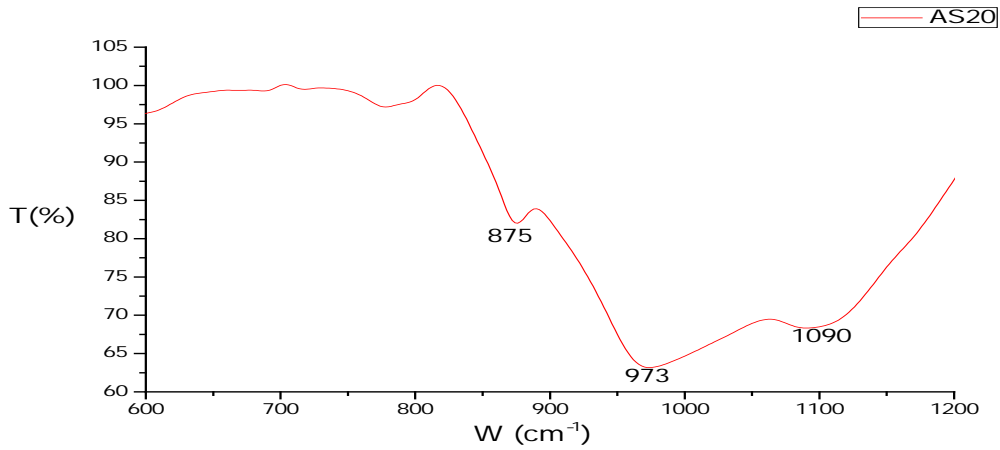


Figure 4.77 FTIR Spectra for Mix AS20 at 180 Days Sulphate Immersion Period

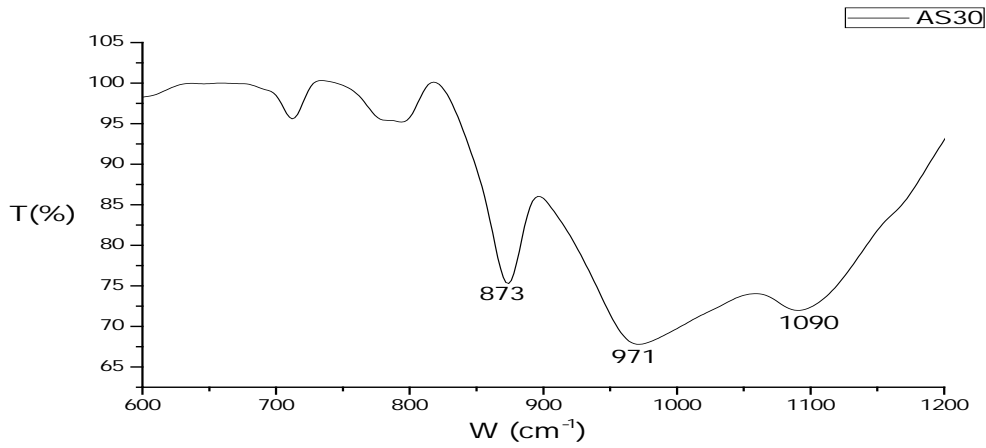


Figure 4.78 FTIR Spectra for Mix AS30 at 180 Days Sulphate Immersion Period

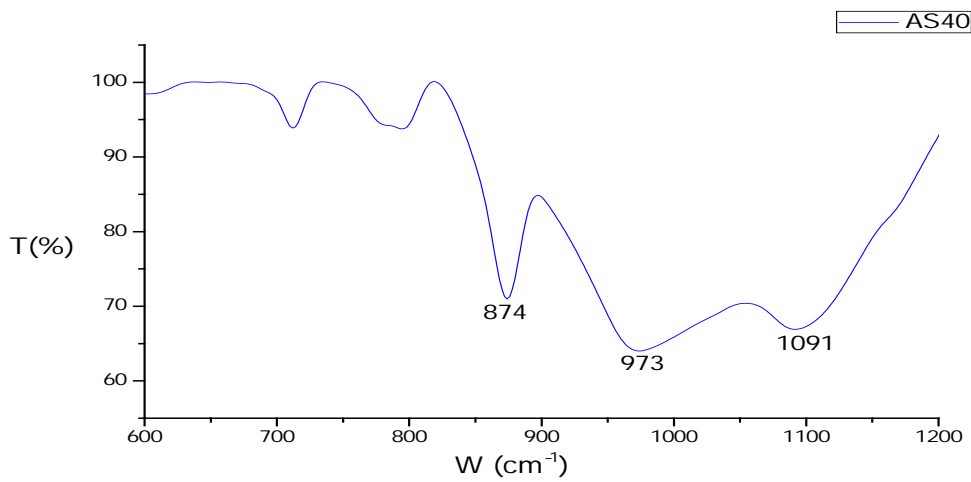


Figure 4.79 FTIR Spectra for Mix AS40 at 180 Days Sulphate Immersion Period

4.3.13 Fire Resistance

Influence of fire or elevated temperature on mortar mixes was evaluated on different temperature between 200°C and 800°C. It is necessary because of mortar is the first element of building that is directly affected during fire action. To know the fire effect, mortar samples were exposed to the fire furnace at 200, 400, 600, and 800 °C. Effects of fire on these samples were evaluated by calculating compressive strength and weight of mortar mixes at particular fired temperature. The variation in compressive strength and weight of fired exposed mortar samples are presented in Figure 4.80-4.87.

In Figure 4.80-4.83, the compressive strength of mortar mixes was found increasing with increase in temperature up to 400°C for series C, D, and 600°C for series A, B when compared to their control mortar. In mortar mixes of series A and B, maximum compressive strength was achieved at 400°C which was about 47 to 64% more as compared to their normal temperature compressive strength, whereas in series C and D, it was maximum at 200°C temperature, which is about 16.5 and 30% more than that of their normal temperature strength. Although, KSS and KSCS contained mortar had superior performance than control mortars at such temperature range. Better performance in compressive strength at 200°C and 400°C was attributed to van der Waals effect. According to this, presence of free moisture in mortar sample creates pore pressure in internal mortar surface, by which attraction due to van der Waals forces reduce. When samples were heated up to 400°C, available free water evaporated and this resulted into increase in van der Waals forces of attraction caused improvement in compressive strength (Mehta and Monteiro, n.d.).

Additionally, hydration of un-hydrated grains during heating process may be responsible to high compressive strength up to 400°C. In this process, consumption of portlandite increase to form additional CSH product with low Ca/Si ratio (Morsy et al., 2012). This hydrated product provides additional strength to the mortar mixes. Although KSS and KSCS have dense CSH gel and lower CH content as compared their control mortar, which reduces the thermal stresses on mortar pores resulting in to enhanced thermal resistant capacity of mortar mixes.

Moreover, compressive strength was observed decreasing with further increase in temperature up to 800°C. However in series A and B this loss was observed only at

800⁰C. Maximum strength loss observed for mix AS40, control, CS40 and, of series A, B, C and D respectively, whereas minimum strength loss observed for mix AS30, BC20, CS20 and DC20. At 600⁰C, calcium carbonate is dissociated into CaO and CO₂, which further reduces strength of mortar mixes. Furthermore, at 800⁰C, hydrated product gets degraded resulting into maximum strength loss.

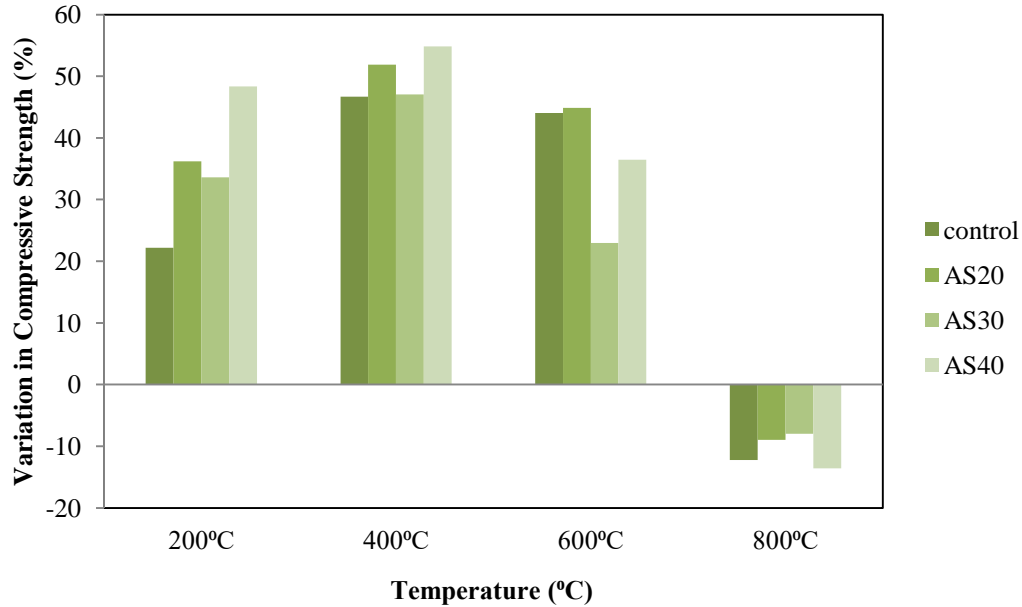


Figure 4.80 Variation in Compressive Strength of Fire Exposed Mortar Mixes of Series A

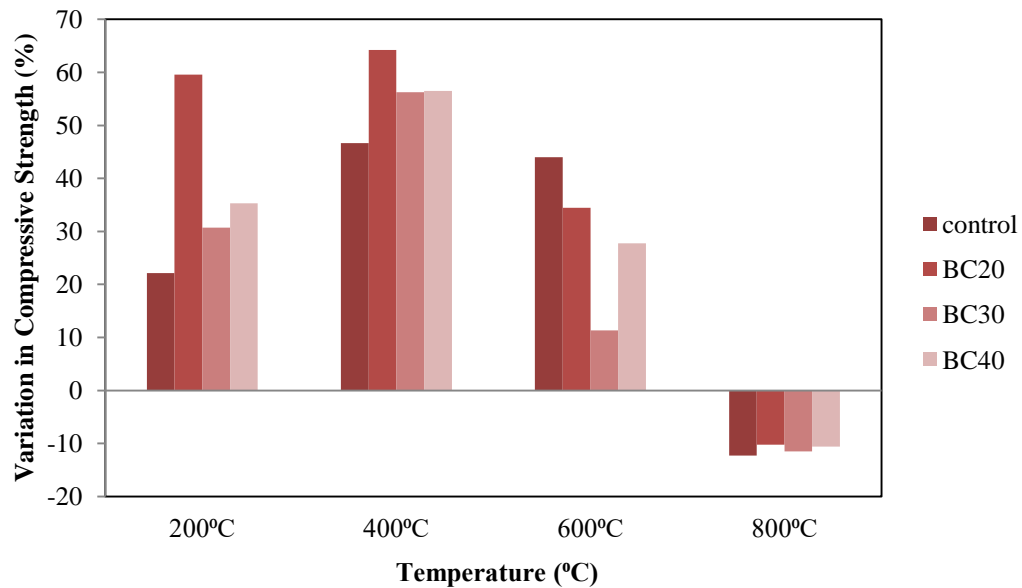


Figure 4.81 Variation in Compressive Strength of Fire Exposed Mortar Mixes of Series B

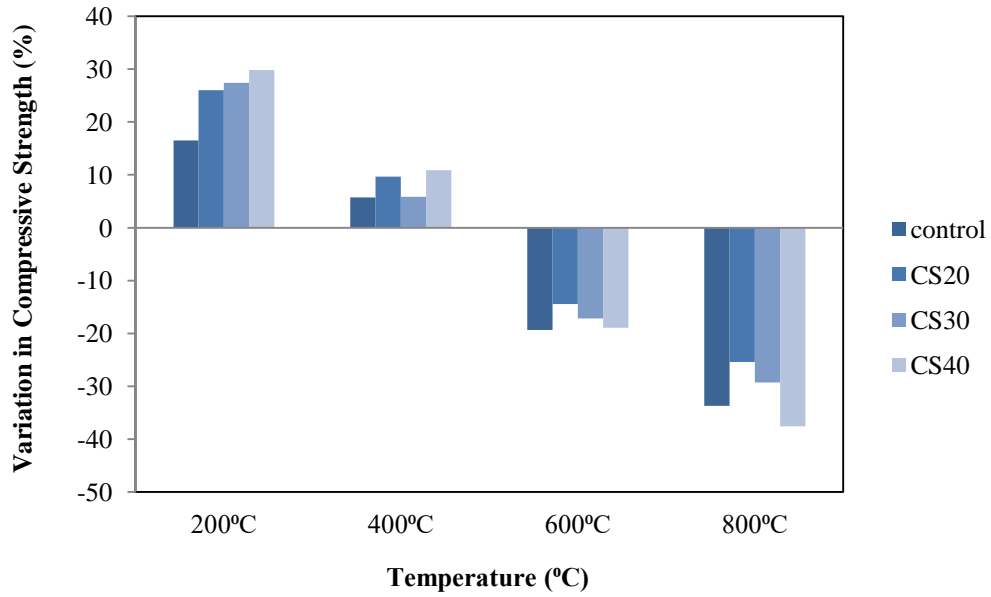


Figure 4.82 Variation in Compressive Strength of Fire Exposed Mortar Mixes of Series C

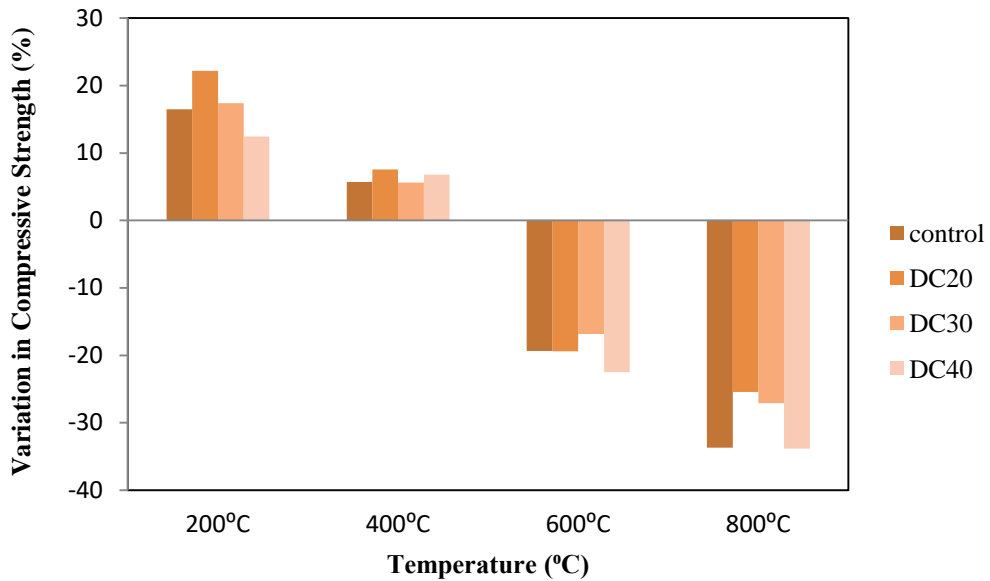


Figure 4.83 Variation in Compressive Strength of Fire Exposed Mortar Mixes of Series D

Weight of the mortar mixes reduced with an increase in temperature up to 800⁰C as shown in Figure 4.84-4.87. When mortar mixes exposed to fire between 200⁰C and 400⁰C, gradual decrement in weight observed. This was because of evaporation of free water available in mortar pores and decomposition of portlandite

(Kumer et al., 2019; Morsy et al., 2012). Furthermore, significant weight loss observed at 600°C and 800°C temperature for all mortar mixes. In this range, minimum weight loss observed in mixes AS20, BC20, CS20 and DC20, because of more dense structure produced with 20% KSS and KSCS. At higher replacement level, the quantity of calcite increase with incorporation of KSS and KSCS, which further decalcified into calcium oxide and water at 600°C temperature. This could be the reason of maximum weight loss in KSS and KSCS containing mortar at 30 and 40% replacement levels. Similar trend observed at 800°C in all series, due to degradation of hydrated products.

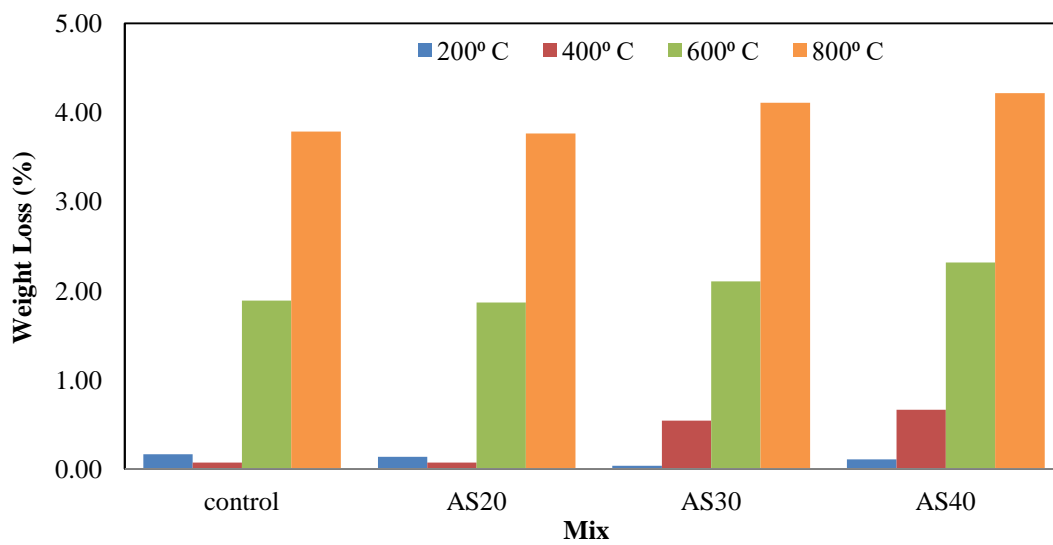


Figure 4.84 Weight Loss in Fire Exposed Mortar Mixes of Series A

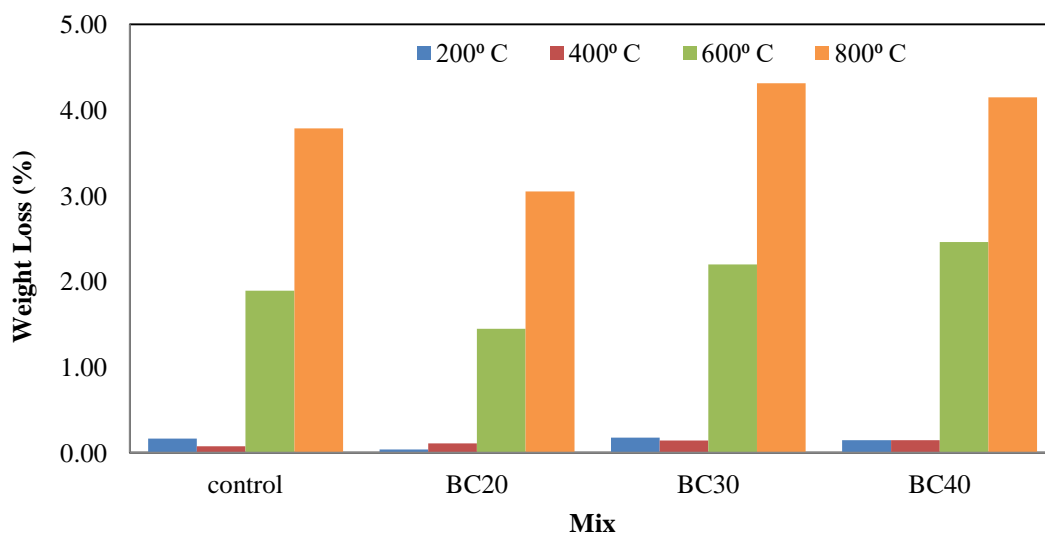


Figure 4.85 Weight Loss in Fire Exposed Mortar Mixes of Series B

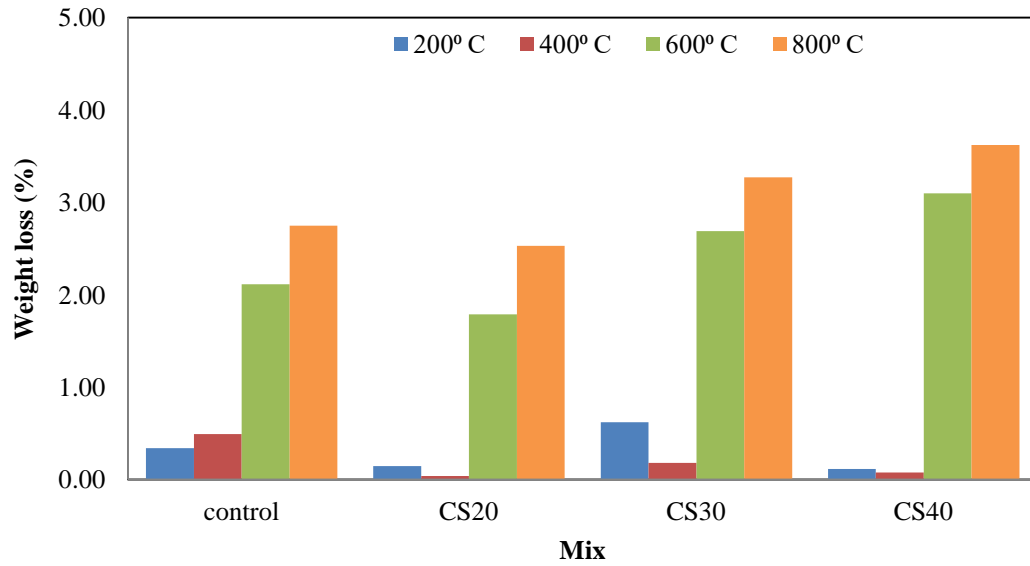


Figure 4.86 Weight Loss in Fire Exposed Mortar Mixes of Series C

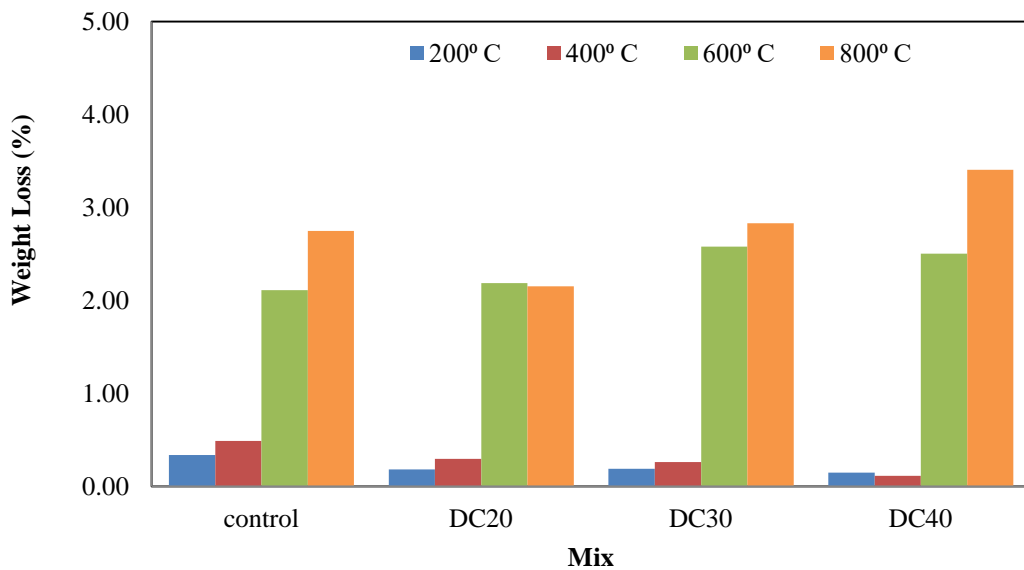


Figure 4.87 Weight Loss in Fire Exposed Mortar Mixes of Series D

4.3.14 Carbonation

Carbonation test on mortar samples was preceded according to (RILEM CPC 18, 1988). The results of carbonation test on mortar samples of series A-D on 1, 7, 14, 28, 56 and 90 days CO₂ exposure period are presented in Figure 4.88-4.91. After 1 and 7 days CO₂ exposure period, depth of carbonation in mortar samples of series A-B (Figure 4.88-4.89) was in the range of 4-12 mm, which indicates lesser amount of CO₂ penetration in to the mortar samples. However, after 7 days considerable carbonation

depth observed in all mortar mixes. Maximum carbonation depth observed after 90 days exposure period in all mortar mixes which was about 40 to 59 mm in series A and B. However, 20% KSS and KSCS contained mortar mixes (AS20 and BC20) has minimum carbonation depth in their respective series. This is because of minimum water-cement ratio and porosity of these mixes, which reduces the rate of CO₂ inclusion in to the mortar samples (Li et al., 2018). Further, the carbonation depth was increased with increase in KSS and KSCS but was observed comparable to that of control mix.

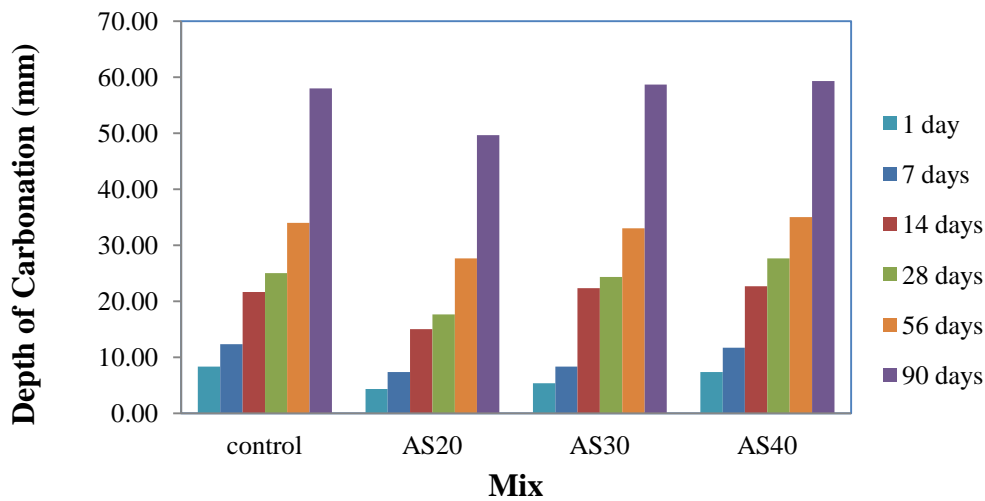


Figure 4.88 Carbonation depth in Mortar Mixes of Series A

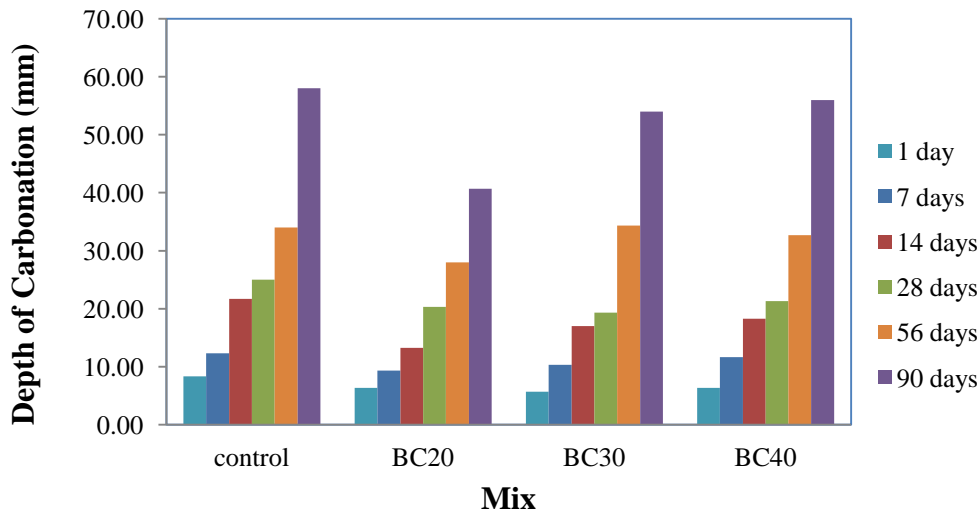


Figure 4.89 Carbonation depth in Mortar Mixes of Series B

The trend of carbonation depth in series C and D (Figure 4.90 and 4.91) was similar as observed in series A and B. However in series C and D, the carbonation depth of mortar mixes was more when it compared to rich mortar mixes of series A and B because of high water to cement ratio of these mixes. Nevertheless, KSS and

KSCS containing mortar reduced the carbonation depth at all CO₂ exposure periods. At 90 days CO₂ exposure period, carbonation depth was observed minimum for mix CS30 and DC40.

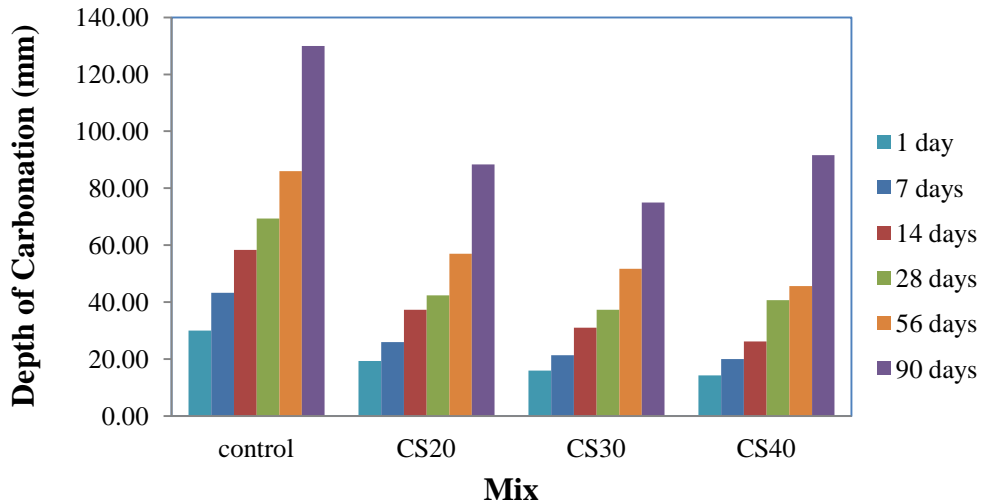


Figure 4.90 Carbonation depth in Mortar Mixes of Series C

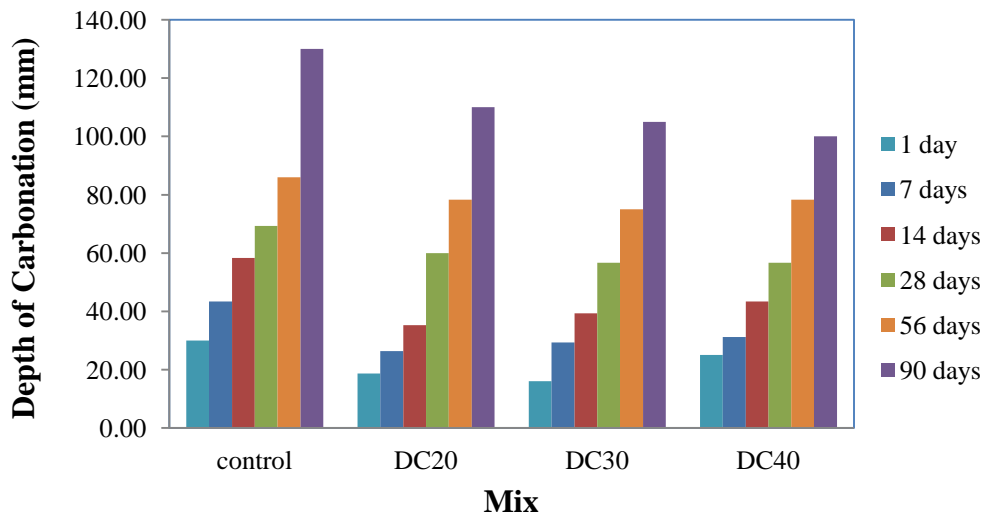


Figure 4.91 Carbonation depth in Mortar Mixes of Series D

This behaviour of mortar was attributed to improvement in density of mortar with inclusion of KSS and KSCS. Additionally, the porosity of these mixes was also responsible for above results, which was less or comparable to their control mortar as discussed in porosity (section 4.3.4). Carbonation depends on the availability of calcite, which densifies the microstructure of mortar mixes. KSS and KSCS contained mortars have more calcite content as observed in microstructure analysis by XRD; this

resulted in to better performance against carbonation action. These results were in agreement with the previous study by (Rana, 2017), where they observed that the concrete prepared using 25% Kota stone manufactured had displayed better performed against carbonation action.

4.3.15 Chloride ion penetration

Chloride ion penetration depth of the mortar samples was recorded at the end of 1, 7, 14, 28, 56 and 90 days NaCl immersion period. Similar to carbonation, depth of chloride ion depth was progressively increased with increase in NaCl immersion period as shown in Figure 4.92-4.95. However, in first observation, it was negligible for all mortar mixes, which indicates no sign of Cl^+ ions intrusions in to the mortar samples. In all series, mortar containing KSS and KSCS has less chloride ion penetration depth as compared to their respective control mortar. The minimum Cl^+ ion penetration depth after 90 days NaCl immersion period was observed in mix AS30, BC30, CS20 and DC20 of series A, B, C and D respectively. This behaviour was attributed to dense microstructure with less microcracks as observed in SEM images (Figure 4.36-4.39) and lower water-cement ratio, which effectively inhibited the ingress of chloride ions.

This behaviour of KSS and KSCS containing mortars were in agreement with results of (Rana, 2017) and (Li et al., 2018), where it was asserted that the inclusion of Kota stone manufactured sand and limestone fines in concrete reduced Cl^+ ion penetration significantly.

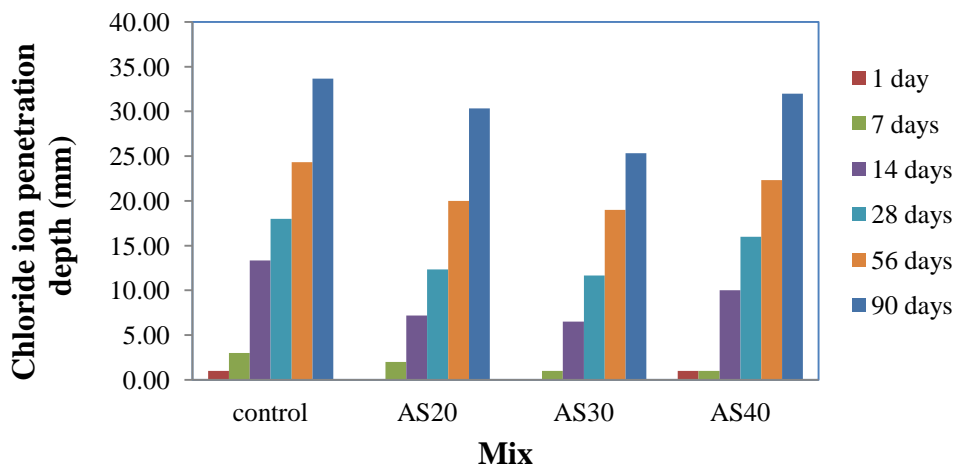


Figure 4.92 Chloride Ion Penetration depth in Mortar Mixes of Series A

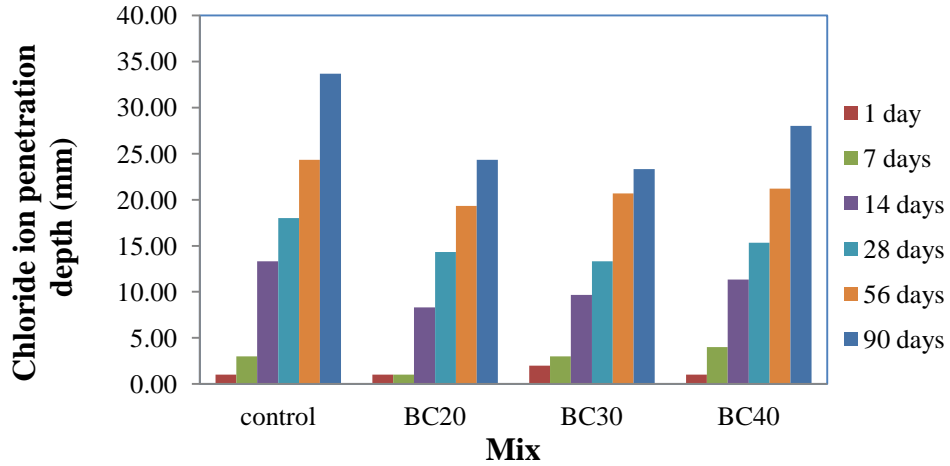


Figure 4.93 Chloride Ion Penetration depth in Mortar Mixes of Series B

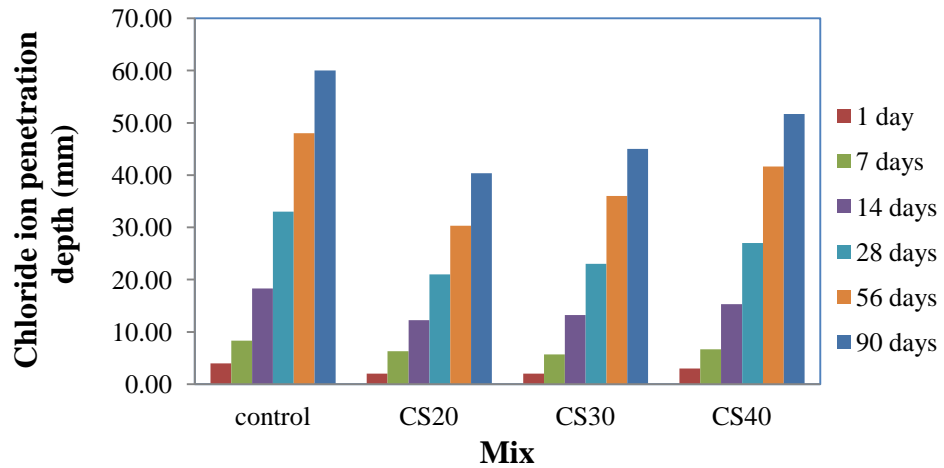


Figure 4.94 Chloride Ion Penetration depth in Mortar Mixes of Series C

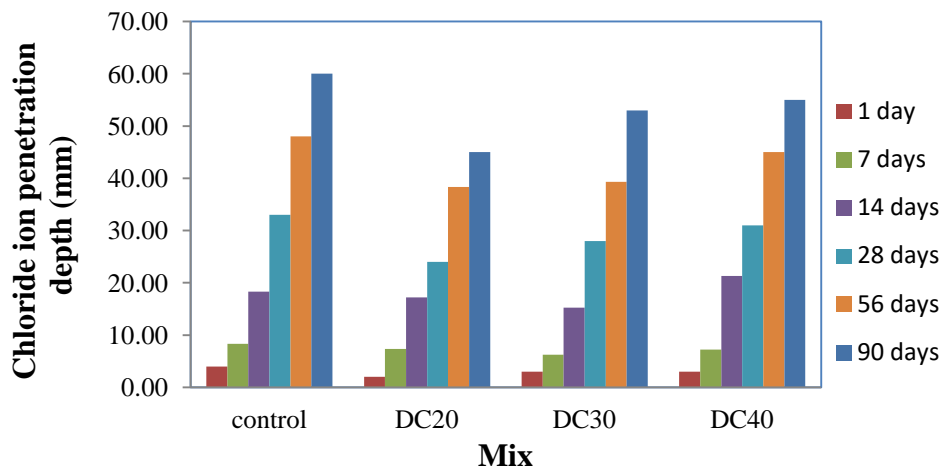


Figure 4.95 Chloride Ion Penetration depth in Mortar Mixes of Series D

4.3.16 Wetting and drying cycles

Wetting and drying cycles test was performed on mortar samples accordance to (BS EN 14066, 2013). The test samples were exposed to 20 wetting and drying cycles and their effect on mortar samples were evaluated on the basis of physical appearance and variation in weight after completing cycles.

Variation in weight of mortar mixes after 20 wetting and drying cycles for series A-B and series C-D are presented in Figure 4.96 and 4.97, respectively. In Figure 4.96, there is no significant change observed in weight of the mortar mixes for series A and B. This variation was observed in the range between -0.14 to 1.13%. Whereas in series C and D, weight of the mortar mixes was considerably reduced. The loss in weight was observed into the range of 0.37 to 2.63%. This loss in weight was attributed to small cracks which were generated during heating and cooling process. However, KSS and KSCS containing mortars had lesser weight loss observed as compared to the control mortar mix.

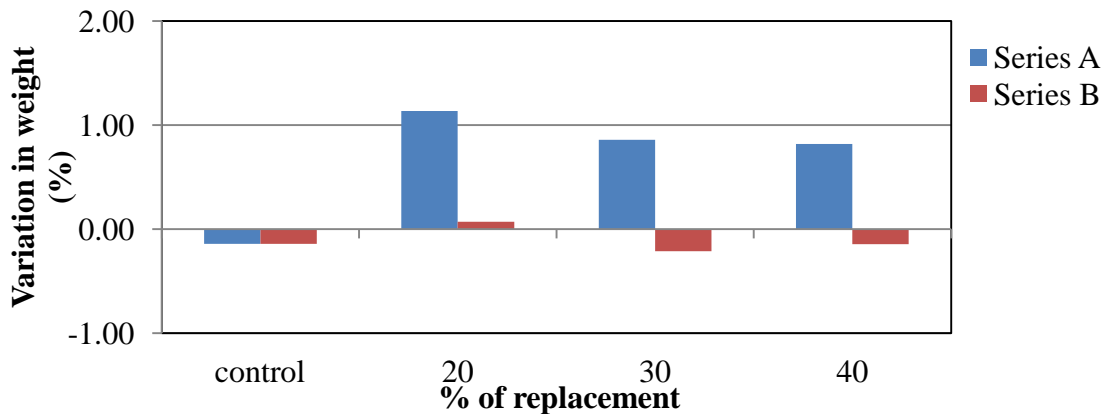


Figure 4.96 Variations in Weight of the Mortar Mixes after 20 Wetting and Drying Cycles for Series A and B

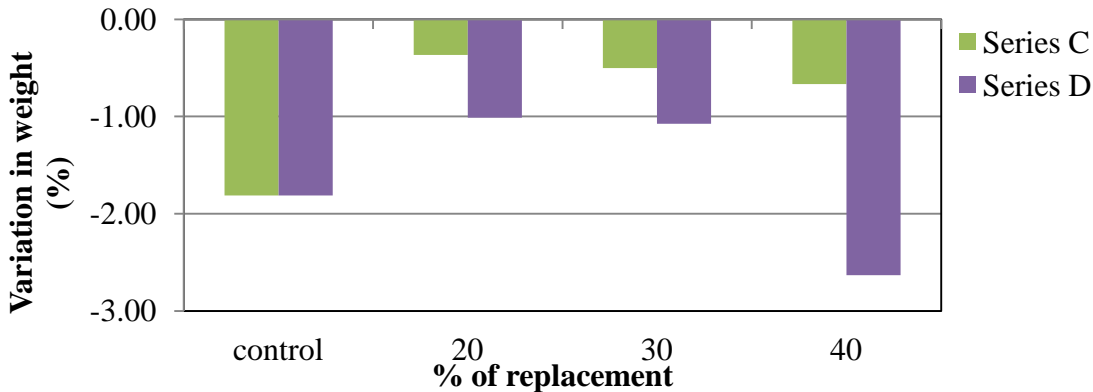


Figure 4.97 Variations in Weight of the Mortar Mixes after 20 Wetting and Drying Cycles for Series C and D

Physical appearance of wetting and drying cycle exposed mortar mixes was shown in Figure 4.98-4.99. In Figure 4.98 for series A and B, no cracks and damages observed in mortar mixes whereas in lean mortar mixes of series C and D, edges were slightly roughed and damaged. Also it seems that the control mortar of series C and D was more affected as compared to KSS and KSCS containing mortars. Improvement in density of mortar was exhibited to better performance of KSS and KSCS containing mortar against alternate wetting and drying action.

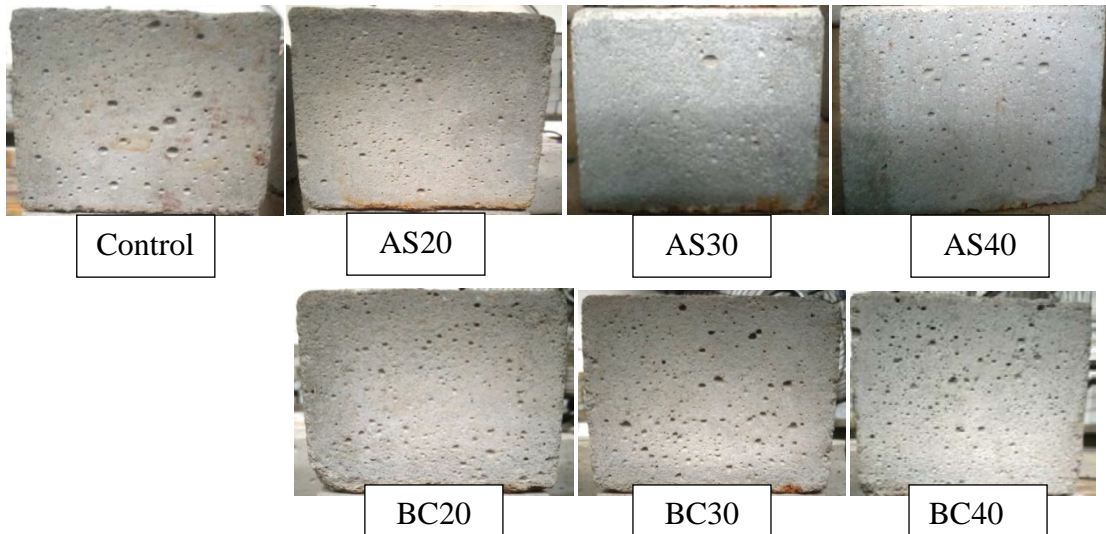


Figure 4.98 Physical Appearance of Wetting and Drying Cycle Exposed Mortar Mixes of Series A and B

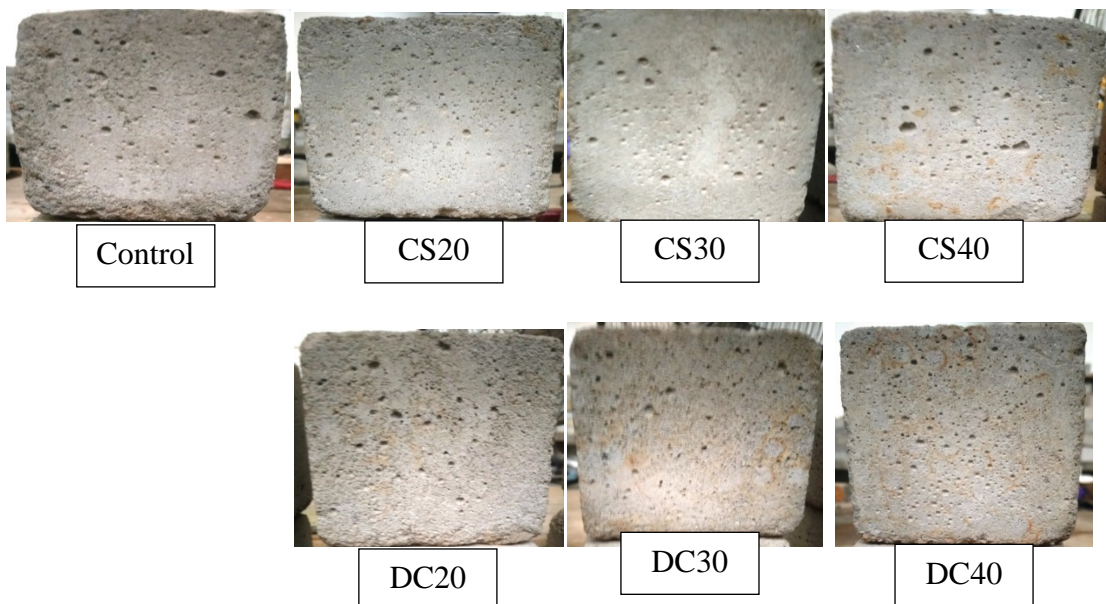


Figure 4.99 Physical Appearance of Wetting and Drying Cycle Exposed Mortar Mixes of Series C and D

CHAPTER 5:

CONCLUSIONS AND RECOMMENDATIONS

5.1 Conclusions

Aim of this study was to find out suitability of Kota stone cutting and polishing waste as fine aggregate in cement mortar mixes. For this, detailed investigations including mechanical, durability and microstructure analysis have been conducted on cement mortar mixes prepared with Kota stone waste (KSS and KSCS).

Based on test results, following conclusions were drawn:

Workability of mortar mixes was observed improving with decrease in w/c ratio at each replacement level of KSS and KSCS. However it was observed reducing beyond 40% replacement in series A.

Strength properties of mortar mixes including compressive, flexural, adhesive and tensile bond strength were observed improved with inclusion of KSS and KSCS as river sand replacement between 20 to 60%. This enhancement was attributed to the pore filling effect and improvement in workability (lower w/c ratio) of mortar mixes with addition of KSS and KSCS. Also, UPV and dynamic modulus of elasticity were found increasing with increase in KSS and KSCS up to 20% and 60% replacement level for Series A&B and Series C&D respectively.

Drying shrinkage, water absorption, porosity and density of mortar mixes containing KSS and KSCS were observed with satisfactory results when compared with control mix up to 20 and 40% replacement.

Enhancement in durability parameters of mortar mixes containing KSS and KSCS were observed up to 30 and 40% replacement, as indicated by results of acid attack, sulphate attack, Carbonation and chloride ion penetration, wetting and drying cycle and fire resistance test (up to 400° C). However, beyond 400° C more weight loss was observed due to decalcification of calcite in all mixes containing KSS and KSCS.

Microstructure study of mortar mixes with SEM analysis reveals that the mortar with KSS had more dense and compact internal structure as compared

to control mixes. Also, FTIR and XRD analysis of mortar mixes with KSS substantiate better performance of these mixes.

5.2 Recommendations

Based on test results, it is recommended to use 30-40% Kota stone slurry and Kota stone crushed sand for making masonry and plaster mortars. For exterior plaster work, it is recommended to use up to 20%. Additionally, research on mortar mixes with OPC cement needs to be explored. Also, the effect of Kota stone waste inclusion on salt crystallization and freeze/thaw action should be studied.

REFERENCES

- Ana Rita Santos, Veiga, M. do R., Silva, A.S., Brito, J. de, Álvarez, J.I., 2018. Evolution of the microstructure of lime based mortars and influence on the mechanical behaviour : The role of the aggregates. *Construction and Building Materials* 187, 907–922. doi:10.1016/j.conbuildmat.2018.07.223
- Arif, M., Gupta, V., Choudhary, H., Kumar, S., Basu, P., 2018. Performance evaluation of cement concrete containing sandstone slurry. *Construction and Building Materials* 184, 432–439. doi:10.1016/j.conbuildmat.2018.07.007
- ASTM C 642-06, 2008. Standard Test Method for Density , Absorption , and Voids in Hardened Concrete, United States: American Society for Testing and Material. doi:10.1520/C0642-13.5.
- ASTM C1148-92, 2014. Standard Test Method for Measuring the Drying Shrinkage of Masonry Mortar. ASTM Standard Book i, 2–4. doi:10.1520/C1148-92AR14.2
- ASTM C230, 2010. Standard Specification for Flow Table for Use in Tests of Hydraulic Cement, Annual Book of ASTM Standards. doi:10.1520/C0230
- ASTM C348, 1998. Standard Test Method for Flexural Strength of Hydraulic-Cement Mortars ASTM C348, Annual Book of ASTM Standards. doi:10.1520/C0348-14.2
- ASTM C597, 2016. Standard Test Method for Pulse Velocity Through Concrete, ASTM International. doi:10.1520/C0597-16.2
- ASTM C952-02, 2003. Standard Test Method for Bond Strength of Mortar to Masonry Units 1 1–8.
- Balasubramanian, J., Gopal, E., Periakaruppan, P., Nadu, T., Balasubramanian, J., Gopal, E., Periakaruppan, P., Gopal, E., Nadu, T., Nadu, T., Balasubramanian, J., Gopal, E., Periakaruppan, P., 2016. Strength and microstructure of mortar with sand substitutes 68, 29–37. doi:10.14256/JCE.1245.2015
- Baldermann, A., Rezvani, M., Proske, T., Grengg, C., Steindl, F., Sakoparnig, M., Baldermann, C., Galan, I., Emmerich, F., Mittermayr, F., 2018. Effect of very

- high limestone content and quality on the sulfate resistance of blended cements. *Construction and Building Materials* 188, 1065–1076.
doi:10.1016/j.conbuildmat.2018.08.169
- Ballester, P., Mármol, I., Morales, J., Sánchez, L., 2007. Use of limestone obtained from waste of the mussel cannery industry for the production of mortars. *Cement and Concrete Research* 37, 559–564. doi:10.1016/j.cemconres.2007.01.004
- Bederina, M., Makhloufi, Z., Bounoua, A., Bouziani, T., Quéneudec, M., 2013. Effect of partial and total replacement of siliceous river sand with limestone crushed sand on the durability of mortars exposed to chemical solutions. *Construction and Building Materials* 47, 146–158. doi:10.1016/j.conbuildmat.2013.05.037
- Benabed, B., Kadri, E.H., Azzouz, L., Kenai, S., 2012. Properties of self-compacting mortar made with various types of sand. *Cement and Concrete Composites* 34, 1167–1173. doi:10.1016/j.cemconcomp.2012.07.007
- Bensted, J., 1999. *Cement & Concrete Composites Thaumassite background and nature in deterioration mortars and concretes*. *Cement and Concrete Composites* 21, 117–121.
- Bilir, T., Gencil, O., Topcu, I.B., 2015. Properties of mortars with fly ash as fine aggregate. *Construction and Building Materials* 93, 782–789.
doi:10.1016/j.conbuildmat.2015.05.095
- Bonavetti, V.L., Irassar, E.F., 1994. The effect of stone dust content in sand. *Cement and Concrete Research* 24, 580–590.
- Braga, M., De Brito, J., Veiga, R., 2012. Incorporation of fine concrete aggregates in mortars. *Construction and Building Materials* 36, 960–968.
doi:10.1016/j.conbuildmat.2012.06.031
- BS EN 14066, 2013. BSI Standards Publication Natural stone test methods — Determination of resistance to ageing by thermal shock.
- Chouhan, H. singh, Kalla, P., Nagar, R., Gautam, P.K., 2017. Recent Trends in Civil Engineering & Technology Partial Replacement of Cement by Kota Stone Slurry in Mortar. *STM Journals* 7, 8–13.

- Chouhan, H.S., Kalla, P., Nagar, R., Gautam, P.K., Arora, A.N., 2018. Investigating use of dimensional limestone slurry waste as fine aggregate in mortar. *Environment, Development and Sustainability*. doi:10.1007/s10668-018-0286-9
- Colleparidi, M., 1999. Thaumasite formation and deterioration. *Cement and Concrete Composites* 21, 147–154.
- Corinaldesi, V., Mazzoli, A., Moriconi, G., 2011. Mechanical behaviour and thermal conductivity of mortars containing waste rubber particles. *Materials and Design* 32, 1646–1650. doi:10.1016/j.matdes.2010.10.013
- Corinaldesi, V., Moriconi, G., 2009. Behaviour of cementitious mortars containing different kinds of recycled aggregate. *Construction and Building Materials* 23, 289–294. doi:10.1016/j.conbuildmat.2007.12.006
- Corinaldesi, V., Moriconi, G., Naik, T.R., 2010. Characterization of marble powder for its use in mortar and concrete. *Construction and Building Materials* 24, 113–117. doi:10.1016/j.conbuildmat.2009.08.013
- EN 1015-12, 2000. Methods of test for mortar for masonry - Part 12: Determination of adhesive strength of hardened rendering and plastering mortars on substrates.
- ERMCO, 2005. The European Guidelines for Self-Compacting Concrete.
- Farinha, C., de Brito, J., Veiga, R., 2015. Incorporation of fine sanitary ware aggregates in coating mortars. *Construction and Building Materials* 83, 194–206. doi:10.1016/j.conbuildmat.2015.03.028
- Felekoğlu, B., Tosun, K., Baradan, B., Altun, A., Uyulgan, B., 2006. The effect of fly ash and limestone fillers on the viscosity and compressive strength of self-compacting repair mortars. *Cement and Concrete Research* 36, 1719–1726. doi:10.1016/j.cemconres.2006.04.002
- Germano, R., Molin, D., Daniel, F., Longhi, A., Clemente, R., Souza, T. De, Meneghetti, M., Dias, R., Paulo, V., Paraíso, R., Mário, L., Jorge, D.M., 2018. Self - compacting mortar with sugarcane bagasse ash : development of a sustainable alternative for Brazilian civil construction. *Environment, Development and Sustainability*. doi:10.1007/s10668-018-0127-x

- Ghrici, M., Kenai, S., 2007. Mechanical properties and durability of mortar and concrete containing natural pozzolana and limestone blended cements. *Cement and Concrete Composites* 29, 542–549. doi:10.1016/j.cemconcomp.2007.04.009
- Gupta, L.K., Vyas, A.K., 2018. Impact on mechanical properties of cement sand mortar containing waste granite powder. *Construction and Building Materials* 191, 155–164. doi:10.1016/j.conbuildmat.2018.09.203
- Haach, V.G., Vasconcelos, G., Loureno, P.B., 2011. Influence of aggregates grading and water/cement ratio in workability and hardened properties of mortars. *Construction and Building Materials* 25, 2980–2987. doi:10.1016/j.conbuildmat.2010.11.011
- Hooton, R.D., Thomas, M.D.A., 2002. The Use of Limestone in Portland Cements : Effect on Thaumasite Form of Sulfate Attack.
- Irassar, E.F., 2009. Cement and Concrete Research Sulfate attack on cementitious materials containing limestone filler — A review. *Cement and Concrete Research* 39, 241–254. doi:10.1016/j.cemconres.2008.11.007
- IS: 2250-1981, 1981. Preparation and Use of Masonry Mortar IS: 2250-1981.
- IS 1489, 1991. म □ नक.
- IS 1542: 1992, 1999. SAND FOR PLASTER - SECIFICATION.
- IS 2116: 1980, 1999. Specification for sand for masonry mortars , IS 2116: 1980.
- IS 2116, 1980. Specification for Sand for Masonry Mortars.
- Jain, A., Majumder, R., 2016. Strength , Permeability and Carbonation properties of Concrete containing Kota Stone Slurry. *SSRG International Journal of Civil Engineering* 3, 1–8.
- Jiménez, J.R., Ayuso, J., López, M., Fernández, J.M., Brito, J. De, 2013. Use of fine recycled aggregates from ceramic waste in masonry mortar manufacturing. *Construction and Building Materials* 40, 679–690. doi:10.1016/j.conbuildmat.2012.11.036
- Kabeer, K.I.S.A., Vyas, A.K., 2018. Utilization of marble powder as fine aggregate in

- mortar mixes. *Construction and Building Materials* 165, 321–332.
doi:10.1016/j.conbuildmat.2018.01.061
- Kalla, P., Rana, A., Chad, Y.B., Misra, A., Csetenyi, L., 2015. Durability studies on concrete containing wollastonite. *Journal of Cleaner Production* 87, 726–734.
doi:10.1016/j.jclepro.2014.10.038
- Kallel, T., Kallel, A., Samet, B., 2016. Durability of mortars made with sand washing waste. *Construction and Building Materials* 122, 728–735.
doi:10.1016/j.conbuildmat.2016.06.086
- Khyaliya, R.K., Kabeer, K.I.S.A., Vyas, A.K., 2017. Evaluation of strength and durability of lean mortar mixes containing marble waste. *Construction and Building Materials* 147, 598–607. doi:10.1016/j.conbuildmat.2017.04.199
- Kumar, R., Lakhani, R., 2017. A simple novel mix design method and properties assessment of foamed concretes with limestone slurry waste, *Journal of Cleaner Production*. Elsevier B.V. doi:10.1016/j.jclepro.2017.10.073
- Kumar, S., Skariah, B., Gupta, V., Basu, P., 2018. Sandstone wastes as aggregate and its usefulness in cement concrete – A comprehensive review *Sandstone wastes as aggregate and its usefulness in cement concrete – A comprehensive review*. *Renewable and Sustainable Energy Reviews* 81, 1147–1153.
doi:10.1016/j.rser.2017.08.044
- Kumer, A., Kumar, P., Golovanevskiy, V., 2019. Thermal properties and residual strength after high temperature exposure of cement mortar using ferronickel slag aggregate. *Construction and Building Materials* 199, 601–612.
doi:10.1016/j.conbuildmat.2018.12.068
- Kwan, A.K.H., McKinley, M., 2014. Effects of limestone fines on water film thickness, paste film thickness and performance of mortar. *Powder Technology* 261, 33–41. doi:10.1016/j.powtec.2014.04.027
- Lakhani, R., Kumar, R., Tomar, P., 2014. Utilization of stone waste in the development of value added products: A state of the art review. *Journal of Engineering Science and Technology Review* 7, 180–187.

- Larrard, F. de, 1999. *Concrete Mixture Proportioning A scientific approach*, 9th ed, Modern Concrete Technology Series. Taylor & Francis.
- Lenart, M., 2013. Impact assessment of lime additive and chemical admixtures on selected properties of mortars. *Procedia Engineering* 57, 687–696.
doi:10.1016/j.proeng.2013.04.087
- Li, L.G., Huang, Z.H., Tan, Y.P., Kwan, A.K.H., Liu, F., 2018. Use of marble dust as paste replacement for recycling waste and improving durability and dimensional stability of mortar. *Construction and Building Materials* 166, 423–432.
doi:10.1016/j.conbuildmat.2018.01.154
- Lu, B., Shi, C., Zhang, J., Wang, J., 2018. Effects of carbonated hardened cement paste powder on hydration and microstructure of Portland cement. *Construction and Building Materials* 186, 699–708. doi:10.1016/j.conbuildmat.2018.07.159
- Makhloufi, Z., Aggoun, S., Benabed, B., Kadri, E.H., Bederina, M., 2016. Effect of magnesium sulfate on the durability of limestone mortars based on quaternary blended cements. *Cement and Concrete Composites* 65, 186–199.
doi:10.1016/j.cemconcomp.2015.10.020
- Makhloufi, Z., Bouziani, T., Hadjoudja, M., Bederina, M., 2014. Durability of limestone mortars based on quaternary binders subjected to sulfuric acid using drying-immersion cycles. *Computers and Chemical Engineering* 71, 579–588.
doi:10.1016/j.conbuildmat.2014.08.086
- Martínez, I., Etxeberria, M., Pavón, E., Díaz, N., 2013. A comparative analysis of the properties of recycled and natural aggregate in masonry mortars. *Construction and Building Materials* 49, 384–392. doi:10.1016/j.conbuildmat.2013.08.049
- Mashaly, A.O., Shalaby, B.N., Rashwan, M.A., 2018. Performance of mortar and concrete incorporating granite sludge as cement replacement. *Construction and Building Materials* 169, 800–818. doi:10.1016/j.conbuildmat.2018.03.046
- Mehta, P.K., Monteiro, P.J.M., n.d. *Concrete Microstructure, Properties, and Materials*.
- Moriconi, G., Corinaldesi, V., Antonucci, R., 2003. *Environmentally-friendly*

- mortars : a way to improve bond between mortar and brick. *Materials and Structures* 36, 702–708. doi:10.1617/13872
- Moropoulou, A., Bakolas, A., Anagnostopoulou, S., 2005. Composite materials in ancient structures. *Cement and Concrete Composites* 27, 295–300. doi:10.1016/j.cemconcomp.2004.02.018
- Morsy, M.S., Abbas, H., Alsayed, S.H., 2012. Behavior of blended cement mortars containing nano-metakaolin at elevated temperatures. *Construction and Building Materials* 35, 900–905.
- Okamura, H., Ouchi, M., 2003. Self-Compacting Concrete. *Journal of Advanced Concrete Technology* 1, 5–15.
- Pliya, P., Cree, D., 2015. Limestone derived eggshell powder as a replacement in Portland cement mortar. *Construction and Building Materials* 95, 1–9. doi:10.1016/j.conbuildmat.2015.07.103
- POWERS, T.C., 1958. Structure and Physical Properties of Hardened Portland Cement Paste. *Journal of the American Ceramic Society* 41, 1–6. doi:10.1111/j.1151-2916.1958.tb13494.x
- Pozo-Antonio, J.S., 2015. Evolution of mechanical properties and drying shrinkage in lime-based and lime cement-based mortars with pure limestone aggregate. *Construction and Building Materials* 77, 472–478. doi:10.1016/j.conbuildmat.2014.12.115
- Pozo-Antonio, J.S., Dionísio, A., 2017. Physical-mechanical properties of mortars with addition of TiO₂ nanoparticles. *Construction and Building Materials* 148, 261–272. doi:10.1016/j.conbuildmat.2017.05.040
- Ramezani-pour, A.M., Hooton, R.D., 2013. Thaumassite sulfate attack in Portland and Portland-limestone cement mortars exposed to sulfate solution. *Construction and Building Materials* 40, 162–173. doi:10.1016/j.conbuildmat.2012.09.104
- Rana, A., Kalla, P., Csetenyi, L.J., 2016. Recycling of dimension limestone industry waste in concrete. *International Journal of Mining, Reclamation and Environment* 0930, 1–20. doi:10.1080/17480930.2016.1138571

- Rana, A., Kalla, P., Csetenyi, L.J., 2015. Sustainable use of marble slurry in concrete. *Journal of Cleaner Production* 94, 304–311. doi:10.1016/j.jclepro.2015.01.053
- RILEM CPC 18, 1988. Measurement of hardened concrete carbonation depth Mesure de la profondeur de carbonatation du b6ton durci 435–440.
- Rodrigues, F., Teresa, M., Evangelista, L., Brito, J. De, 2013. Physical e chemical and mineralogical characterization of fi ne aggregates from construction and demolition waste recycling plants. *Journal of Cleaner Production* 52, 438–445. doi:10.1016/j.jclepro.2013.02.023
- Saiz Martínez, P., Gonz alez Cortina, M., Fern andez Martínez, F., Rodríguez S anchez, A., 2016. Comparative study of three types of fine recycled aggregates from construction and demolition waste (CDW), and their use in masonry mortar fabrications. *Journal of Cleaner Production* 118, 162–169. doi:10.1016/j.jclepro.2016.01.059
- Senhadji, Y., Escadeillas, G., Mouli, M., Khela, H., 2014. Influence of natural pozzolan, silica fume and limestone fine on strength, acid resistance and microstructure of mortar. *Powder Technology* 254, 314–323. doi:10.1016/j.powtec.2014.01.046
- Shi-cong, K., Chi-sun, P., 2009. Properties of concrete prepared with crushed fine stone , furnace bottom ash and fine recycled aggregate as fine aggregates. *Construction and Building Materials* 23, 2877–2886. doi:10.1016/j.conbuildmat.2009.02.009
- Silva, J., Brito, J. de, Veiga, R., 2009. Incorporation of fine ceramics in mortars. *Construction and Building Materials* 23, 556–564. doi:10.1016/j.conbuildmat.2007.10.014
- Sims, I., Huntley, S.A., 2004. The thaumasite form of sulfate attack-breaking the rules. *Cement and Concrete Composites* 26, 837–844. doi:10.1016/j.cemconcomp.2004.01.002
- Singh, S., 2016. Strength and Durability Studies on Concrete Containing Granite Cutting Waste as Partial Replacement of Sand Strength and Durability Studies on Concrete Containing Granite Cutting Waste as Partial Replacement of Sand.

- Singh, S., Khan, S., Khandelwal, R., Chugh, A., Nagar, R., 2015. Performance of sustainable concrete containing granite cutting waste. *Journal of Cleaner Production* 119, 86–98. doi:10.1016/j.jclepro.2016.02.008
- Singh, S., Nagar, R., Agrawal, V., Rana, A., Tiwari, A., 2016. Sustainable utilization of granite cutting waste in high strength concrete. *Journal of Cleaner Production* 116, 223–235. doi:10.1016/j.jclepro.2015.12.110
- Skariah, B., Kumar, S., Sahan, H., 2017. Sustainable concrete containing palm oil fuel ash as a supplementary cementitious material. *Renewable and Sustainable Energy Reviews* 80, 550–561. doi:10.1016/j.rser.2017.05.128
- Soroka, I., Setter, N., 1977. The effect of fillers on strength of cement mortars. *Cement and Concrete Research* 7, 449–456. doi:10.1016/0008-8846(77)90073-4
- Thamboo, J., Jayarathne, N., Bandara, A., 2019. Characterisation and mix specification of commonly used masonry mortars. *SN Applied Sciences*. doi:10.1007/s42452-019-0312-z
- Turgut, P., Murat Algin, H., 2007. Limestone dust and wood sawdust as brick material. *Building and Environment* 42, 3399–3403. doi:10.1016/j.buildenv.2006.08.012
- Türkel, S., Altuntaş, Y., 2009. The effect of limestone powder, fly ash and silica fume on the properties of self-compacting repair mortars. *Sadhana - Academy Proceedings in Engineering Sciences* 34, 331–343. doi:10.1007/s12046-009-0011-3
- Weerdt, K. De, Haha, M. Ben, Saout, G. Le, Kjellsen, K.O., Justnes, H., Lothenbach, B., 2011. Cement and Concrete Research Hydration mechanisms of ternary Portland cements containing limestone powder and fly ash. *Cement and Concrete Research* 41, 279–291. doi:10.1016/j.cemconres.2010.11.014
- Yilmaz, B., Olgun, A., 2008. Studies on cement and mortar containing low-calcium fly ash, limestone, and dolomitic limestone. *Cement and Concrete Composites* 30, 194–201. doi:10.1016/j.cemconcomp.2007.07.002

LIST OF PUBLICATION FROM THESIS

JOURNALS

H.S. Chouhan, P. Kalla, R. Nagar, P.K. Gautam, “Influence of dimensional stone waste on mechanical and durability properties of mortar: A Review,” *Construction and Building Material*. (**Published**) (*Sci*)

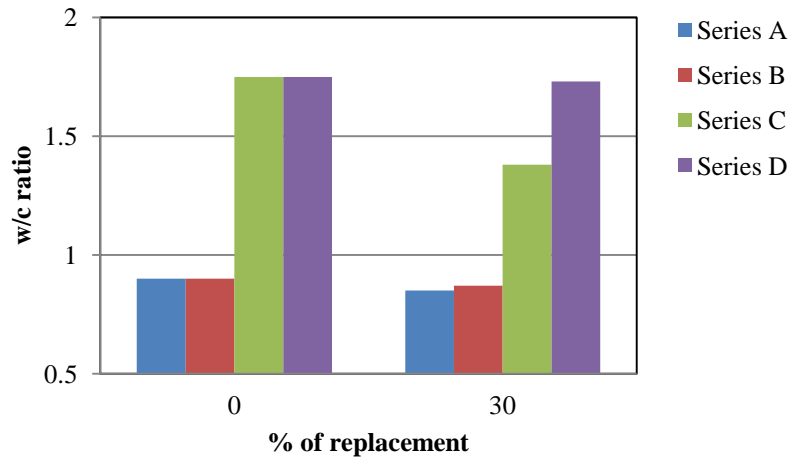
H.S. Chouhan, P. Kalla, R. Nagar, P.K. Gautam, “Gainful utilization of dimensional limestone waste as fine aggregate in cement mortar mixes,” *Construction and Building Material* (2019). (**Published**) (*Sci*)

H.S. Chouhan, P. Kalla, R. Nagar, P.K. Gautam, A.N. Arora, “Investigating use of dimensional limestone as fine aggregate in mortar,” *Environment, Development and Sustainability* (2018). (**Published**) (*Sci*)

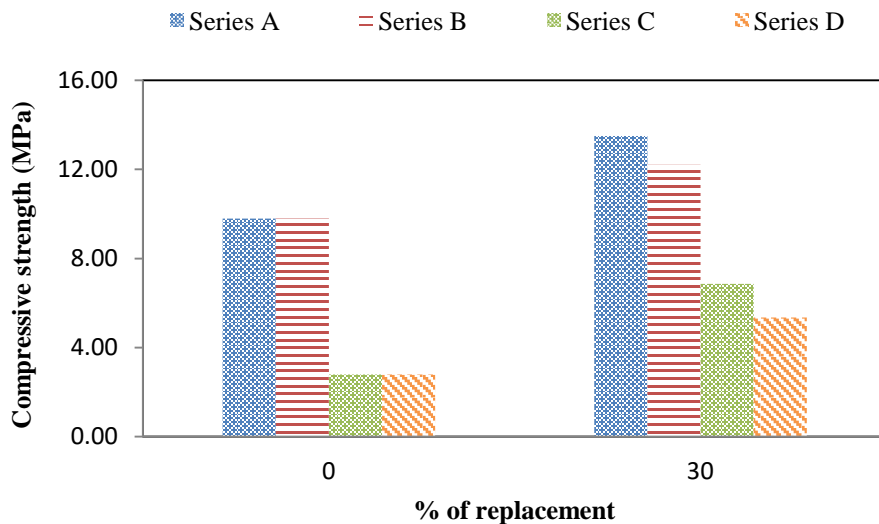
H.S. Chouhan, P. Kalla, R. Nagar, “Evaluation of mechanical properties of cement mortar containing kotastone slurry waste,” *Advanced Science, Engineering and Medicine* (2018). (**Published**) (*Scopus*)

APPENDIX

(a) Water-cement ratio comparison between 0% (control) and 30% KSS and KSCS containing mortar



(b) Compressive strength comparison between 0% (control) and 30% KSS and KSCS containing mortar



(c) Cost Analysis

Based on present study, a lump sum cost estimation of 1:3 mortar mix proportion for control, AS40 and AB40 mix is shown in below Tables. Assuming all parameters like labor cost, contractor profit, sundries etc. same. It is observed that use of DLSW will prove to be 15.5% economical with respect to control mix whereas

DLCS will add around 6.5% extra cost due to crushing charges. However using this material will preserve non-renewable resource (river sand), provide efficient use of accumulated waste, ease out landfill pressure and preserve local environment. Considering all the long term positive impact DLCS can be used where DLW produced as solid waste and there is restrictions in the use of river sand

For control mix:

Material Incl. Transport Charges	Qty.	Units	Rs. /Unit	Amount (Rs.)	Sub-Total (Rs.)
CEMENT BAGS	7	Bags	300	2100	2100.0
SAND	1.481	Tone	900	1332.9	1332.9
TOTAL COST					3432.9

For mortar mix AS40 (containing 40% DLSW):

Material Incl. Transport Charges	Qty.	Units	Rs. /Unit	Amount (Rs.)	Sub-Total (Rs.)
CEMENT BAGS	7	Bags	300	2100	2100.0
SAND	0.8892	Tone	900	800.28	800.3
DLSW	0.365	Tone	0	0	0
TOTAL COST					2900.28

For mortar mix AS40 (containing 40% DLCW):

Material Incl. Transport Charges	Qty.	Units	Rs. /Unit	Amount (Rs.)	Sub-Total (Rs.)
CEMENT BAGS	7	Bags	300	2100	2100
SAND	0.8892	Tone	900	800.28	800.28
DLCS	0.4929	Tone	0	0	0
CRUSHING COST	0.4929	Tone	1500	739.35	739.35
TOTAL COST					3639.63

AUTHOR'S BIO-DATA



1. **Name** : **Harshwardhan Singh Chouhan**
2. **Date of Birth** : July 23, 1990
3. **Address** : Opposite 2-B-7 Housing Board, Banswara-327001
(Raj) Email: harsh.civil.rec@gmail.com
Phone: +919461170745
4. **Education** : **B.Tech.** (Civil Engineering): Kautilya Institute of
Technology and Engineering, Jaipur
M.Tech. (Structural Engineering): Kautilya
Institute of Technology and Engineering, Jaipur

5. **List of Publications:**

H.S. Chouhan, P. Kalla, R. Nagar, P.K. Gautam, “Gainful utilization of dimensional limestone waste as fine aggregate in cement mortar mixes,” *Construction and Building Material* (2019). (**Published**) (*Sci*)

H.S. Chouhan, P. Kalla, R. Nagar, P.K. Gautam, A.N. Arora, “Investigating use of dimensional limestone as fine aggregate in mortar,” *Environment, Development and Sustainability* (2018). (**Published**) (*Sci*)

H.S. Chouhan, P. Kalla, R. Nagar, “Evaluation of mechanical properties of cement mortar containing kotastone slurry waste,” *Advanced Science, Engineering and Medicine* (2018). (**Published**) (*Scopus*)

H.S. Chouhan, P. Kalla, R. Nagar, P.K. Gautam, “Influence of dimensional stone waste on mechanical and durability properties of mortar: A Review,” *Construction and Building Material*. (**Published**) (*Sci*)

P.K. Gautam, P. Kalla, A.S. Jathoo, R. Agrawal, **H.S. Chouhan**, “Sustainable use of waste in flexible pavement: A review,” *Construction & Building Materials* (2018). (**Published**) (*Sci*)

